Characterization of the autophagy machinery in *Schistosoma mansoni,* a parasite of public health relevance

Inaugural Dissertation
submitted to the
Faculty of Veterinary Medicine
in partial fulfillment of the requirements
for the PhD-Degree
of the Faculties of Veterinary Medicine and Medicine
of the Justus Liebig University Giessen

by
Mughal, Mudassar Niaz
of
Multan, Pakistan

Giessen (2022)

From the Institute of Parasitology of the Justus Liebig University Giessen
Director / Chairman: Prof. Dr. med. vet. Anja Taubert
of the Faculty of Veterinary Medicine of the Justus Liebig University Giessen

First Supervisor and Committee Member: Prof. Dr. Christoph G. Grevelding
Second Supervisor and Committee Member: Prof. Dr. Andreas Meinhardt
Committee Members: Prof. Dr. Nobert Weißmann
PD. Dr. Martina Sombetzki

Date of Doctoral Defense: 15.06.2022

TABLE OF CONTENTS

1 INTRODUCTION

1.1 Schistosomiasis

1.1.1 Epidemiology

Schistosomiasis (bilharzia) is a neglected tropical disease caused by blood dwelling flukes (schistosomes) of the genus *Schistosoma*. In tropical and sub-tropical countries, this debilitating illness remains a significant veterinary and public health problem (McManus et al. 2018). *Schistosoma mansoni, S. japonicum,* and *S. haematobium* are the three most important species affecting humans. Besides these three, other species exist that occur geographically more restricted including *S. mekongi*, *S. intercalatum,* and *S. guineensis*. In most endemic countries, the documented annual mortality rate for schistosomiasis is ~ 200,000 (Verjee 2020). According to global burden of disease (GBD) estimates, ~ 680 million people are at risk of schistosomiasis and > 200 million people are infected with schistosomes, with an impact of about 1.6 million disability adjusted life years (DALY) annually (GBD 2016 DALYs and HALE Collaborators 2017; French et al. 2018; WHO 2020). For example, in the People's Republic of China alone, surveillance data reported 115,614 cases of *S. japonicum* in year 2014 (Song et al. 2016), and recorded > 68.6 million people at risk of schistosomiasis.

Nowadays, schistosomiasis is not only limited to people living in endemic areas, but surveillance studies have indicated that travellers and immigrants are also infected (Hatz 2006; Gautret et al. 2015). In Europe, a sudden autochthonous transmission of urinary schistosomiasis was noted, because of infected travellers in southern Corsica (France) and in Almeria (Spain). Significant changes in climate during the recent years support environmental conditions for the development of *Bulinus* snails, which are the intermediate hosts of *S. haematobium*, in the Mediterranean area from where reports of infected travellers but also of local population were noted (de Laval et al. 2014; Salas-Coronas et al. 2021). However, the manifestation of disease is multi-factorial and depends on host genotype (Dessein et al. 1999; Rodrigues et al. 1999; Henri et al. 2002), sex (Booth et al. 2004), age (Chan et al. 1996), immune status (Hoffmann et al. 2002), co-infection status (Mwinzi et al. 2001; Mwatha et al. 2003; Naus et al. 2003), and the duration of schistosome infection (Mohamed-Ali et al. 1999). Apart from humans, schistosomes can also infect other vertebrate mammalian hosts and thus pose significant socio-economic threat to livestock industry. Prevalence studies indicate that about 530 million cattle are present in endemic areas of Africa and Asia, where infection rates vary from 31% to 81% (De Bont and Vercruysse 1998). Especially in Asia, water buffaloes

play an important role because they can be infected by *S. japonicum* (Huang and Manderson 2005; Wang et al. 2009; Gray et al. 2009; Olveda et al. 2014).

1.1.2 Life cycle

Schistosomiasis is transmitted via snail intermediate hosts. Within the definitive mammalian host (human host for *S. mansoni* and *S. haematobium*, and human as well as animal hosts for *S. japonicum*), the adult male and female worms live as couples in the blood stream, and migrate to portal veins of liver (*S. mansoni* and *S. japonicum*) or the venous plexus of the urinary bladder (*S. haematobium*). At this predilection site, they reproduce sexually, and the female worms produce eggs that make their way out of the definitive host in excreta (feces or urine). After reaching fresh water, miracidia (first larval stage) hatch from the eggs and invade particular species of intermediate snail hosts (depending on schistosome species), leaving behind a ciliated ectoderm. Within the intermediate host, the miracidia undergo asexual reproduction (replication) and differentiation via mother and daughter sporocyst stages to generate numerous cercariae. Infected snails can shed thousands of infectious cercariae into the fresh-water environment. By swimming and chemotaxis, cercariae find their final hosts (Figure 1.1). Thus, the different developmental stages of schistosomes experience distinct environmental conditions during their life cycles, ranging from fresh water, via molluscan intermediate host tissues, to blood and tissues within the definitive host (McManus et al. 2018).

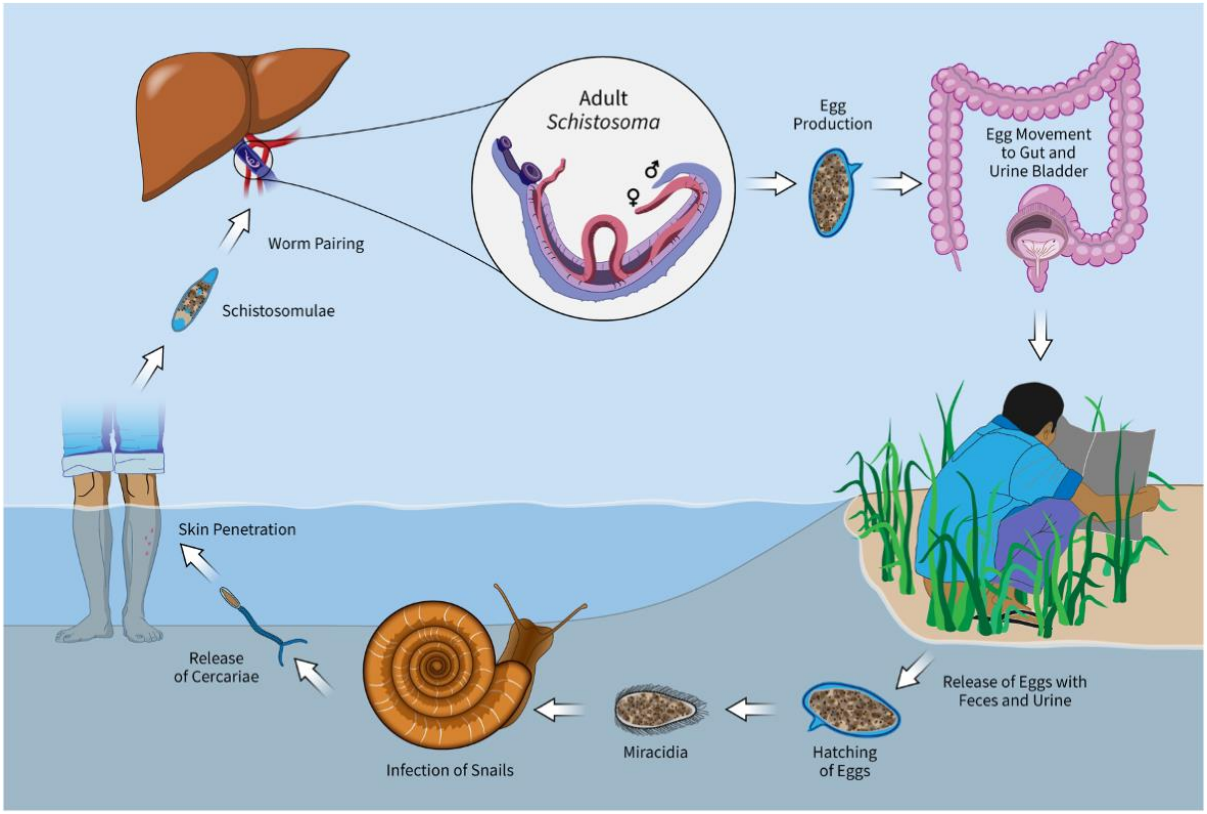

Figure 1.1: Life cycle of *S. mansoni*. After the infection of snails with miracidia, the latter complete mother- and daughter sporocyst stages within the snails to generate and release cercariae in the water. Cercariae move with their bifurcated tails and are attracted towards their mammalian host (humans or animals) by chemokinesis (Haeberlein and Haas 2008). Following skin penetration, the cercariae lose their tails to transform into schistosomula, which then develop into adults in 5-7 weeks and migrate towards their predilection site (hepatic portal vein for *S. mansoni*, bladder veins for *S. haematobium*) and pairing occurs. Adult couples feed themselves on the host blood and produce eggs, which are then excreted outside either with feces (*S. mansoni*) or urine (*S. haematobium*). Miracidia hatch from the released eggs and penetrate the intermediate host (snails) to continue the life cycle (Modified from Illustration: **www.hegasy.de**).

1.1.3 Pathology

Parasitic worms have no significant pathogenic potential; however, the eggs are the main source of disease burden. After eggs have been laid by female worms, half of the eggs reaches the environment by leaving the host body through urine or feces in order to continue the life cycle. The other half remains inside the host body within the blood circulation and gets trapped in the blood vessels near liver and spleen (in case of *S. mansoni* and *S. japonicum*) or in the blood vessels of bladder and ureter (in case of *S. haematobium*), where they initiate

severe pathological processes (Ross et al. 2002). The body's inflammatory reaction is a cellular, granulomatous response around entrapped eggs, which leads to inflammation and fibrosis (Ross et al. 2002).

1.1.4 Treatment and control

Environmental attempts to fight schistosomiasis include provision of clean water, adequate sanitation, and elimination of snail reservoirs in order to break the life cycle of the parasite (McManus et al. 2018). However, the major goal against the disease is to reduce the egg production via minimizing the worm load during infection, which ultimately leads to the reversal of detrimental effects of disease like periportal fibrosis and portal hypertension (Gryseels et al. 2006). Praziquantel (PZQ) is known as the only drug of choice, due to high efficiency against all schistosome species and low cost of treatment. PZQ induces significant damages to the tegument of the parasite and exposes antigens to the host immune system (Doenhoff et al. 2008; Reimers et al. 2015). Despite being the recommended drug, PZQ is not effective against the juvenile worms and larval stages of schistosomes (El Ridi and Tallima 2013; McManus et al. 2020). Due to mass administration of PZQ in many countries and it's low efficacy (Barakat and Morshedy 2011), the possibility of schistosome resistance towards PZQ has been discussed (Doenhoff et al. 2008; Wang et al. 2012; Fukushige et al. 2021). In order to work towards a vaccine, the World Health Organization (WHO) recommended six possible vaccine candidates (triose phosphate isomerase, glutathione-S-transferase, myosine heavy chain, 14 kDa fatty acid binding protein, 23 kDa transmembrane surface protein and paramyosin), but none of them has achieved adequate protective efficacy in experimental animal models yet (Pearce 2003; Morel et al. 2014; Inobaya et al. 2014). Thus, there is an increasing demand to find new therapeutics and to develop improved intervention strategies to assist the control and treatment of schistosomiasis.

Currently, minimization of morbidity and elimination of infection are the focal points of schistosomiasis research, which mainly relies on the single drug – PZQ. Due to serious threats of evolving drug resistant strains of schistosomes as a consequence of ongoing mass drug administration, the identification of new chemical compounds and druggable targets represents the only most feasible approach to combat schistosomiasis. In line with this, maintenance of *in vitro* culture and establishment of functional genomics tools provided strong standpoints to discover new therapeutics or combination of therapeutics and new drug targets as well as inspired this study to contribute in exploring the significance of autophagy in homeostasis and reproduction of *S. mansoni*.

1.2 Reproductive biology of schistosomes

1.2.1 Sex determination and development of schistosomes

The three main schistosome species, *S. haematobium*, *S. japonicum,* and *S. mansoni*, have 2n = 8 chromosomes. The sex chromosomes W and Z determine the sex (Atkinson 1980). Male schistosomes have a homozygous ZZ chromosome pair, whereas female schistosomes have a heterozygous ZW karyotype. The other seven autosomal chromosome pairs control various biological processes as well as gender-specific, species-specific, strain-specific, stage-specific, and maturation-specific development (Liberatos and Short 1983; Hoffmann et al. 2002; Fitzpatrick et al. 2004; Dillon et al. 2006; Braschi and Wilson 2006; Vermeire et al. 2006; Fitzpatrick and Hoffmann 2006; Gobert et al. 2006).

1.2.2 Male-dependent maturation of the female

A unique biological feature of schistosomes is that the female has to pair with a male partner in order to develop and mature sexually. In the absence of a male, the female remains sexually immature, with undifferentiated oogonia within the ovaries, and with vitellaria exclusively containing stem cell-like precursor cells. Once a female pairs with a male partner, essential mitogenic cascades of development are induced in the female gonads. As a result of this sexual maturation, the length of the female significantly increases as it develops the vitellarium (largest reproductive organ of the female). Furthermore, the size of the ovary also increases as the differentiation of primary oocytes occurs. Development of both ovary and vitellarium are required for egg formation (Popiel and Basch 1984; Kunz 2001). The effect of this pairing-dependent maturation stimulus in females remains present as long as there is physical contact with males, even if the male is anorchid (Armstrong 1965; Popiel and Basch 1984; Jourdane et al. 1995).

Interestingly, the male-dependent pairing effect on the female is reversible. Females separated from male partners stop producing eggs and gradually degenerate back to the sexually immature state. If separated females are given the chance to re-pair with male partners, cell differentiation in females resumes towards sexual maturation, and they start to produce eggs again (Popiel and Basch 1984; Kunz et al. 1995; Grevelding 2004). At the bio-molecular level, this influence of having paired with a male partner also modulates the transcription of many male- and female-specific genes that play roles in the reproduction of schistosomes (Grevelding et al. 1997; Lu et al. 2016). Recently, it has been observed that also in the male gene expression is modified by the presence of a female partner (Lu et al. 2016).

The latter led to the hypothesis of bidirectional molecular communication between male and female schistosomes in copula (Lu et al. 2019).

1.3 Involvement of kinase signaling in *S. mansoni*

It is generally accepted that the main pathogenic cause of schistosomiasis is egg production. Therefore, it is crucial to understand the mechanisms of reproductive maturation of schistosomes, which have evolved dioecy during evolution (Platt and Brooks 1997) and a biological interplay between males and females that regulate male- and female-specific gene expression via one or more stimuli. During the past two decades, protein kinase (PK) pathways have been identified and their involvement in reproductive processes in *S. mansoni* analysed (Knobloch et al. 2007; LoVerde et al. 2007, 2009; Beckmann et al. 2010b; Andrade et al. 2011; Avelar et al. 2011; Beckmann and Grevelding 2012; Wilson 2012). For example, three members of the tyrosine kinase (TK) family of *S. mansoni*, the Syk kinase SmTK4 (Knobloch et al. 2002; Beckmann et al. 2010b), the Src kinase SmTK3 (Kapp et al. 2001) and the hybrid Src/Abl kinase SmTK6 (Beckmann et al. 2011) have been postulated to form a trimeric complex that interacts with integrin and venus kinase receptors in oocytes of paired females. As a confirmational approach, knock-down of SmTK4, Smß-Int1, SmILK, and SmVKRs as well as treatments of *S. mansoni* couples with kinase-specific inhibitors such as TRIKI, Piceatannol, Herbimycin A, BI2536, and QLT-0267 have shown drastic impairments of male and female reproduction but also negative effects on worm vitality (Beckmann et al. 2010a; Gelmedin et al. 2017).

1.3.1 Tyrosine kinase signaling

Cytoplasmic tyrosine kinases (CTKs) are known to be involved in pathways linked to cell differentiation and proliferation via the transcriptional regulation of mitotic genes and cytokinesis as well as cytoskeletal rearrangement (Barone and Courtneidge 1995; Thomas and Brugge 1997; Hubbard and Till 2000; Tatosyan and Mizenina 2000; Frame 2002; Ishizawar and Parsons 2004).

In schistosomes, several CTKs, such as Src kinases SmTK3 (Kapp et al. 2004), a hybrid Src/Abl kinase SmTK6 (Beckmann et al. 2011), Fes kinase (Bahia et al. 2007), and also the Syk kinase SmTK4 (Knobloch et al. 2002) and SmTK5 (Kapp et al. 2001) of the Fyn-type Src kinase, have been identified and characterized. All of these kinases have been localized to the gonads of males and females and postulated to play roles in cellular differentiation processes, except for the Fes kinases which are predominantly found in the cercarial and schistosomule

stages. SmTK4 and SmTK6 have been localized to ovary and testes, but not the vitellarium. SmTK4 was more abundantly transcribed in males as compared to females, and was localized in the ovary and the testes. Although SmTK4 has no influence on regulating vitelline cell mitosis and egg production, this protein is known to be expressed in oocytes and spermatocytes (Knobloch et al. 2002, 2007). Later, SmTK6 was also identified as a SmTK4 partner acting in a kinase complex in the ovary of female *S. mansoni*. Direct interaction of these kinases was confirmed by co-immunoprecipitation experiments (Beckmann et al. 2010a). Similarly, SmTK3 and SmTK5 were found in testes, ovary as well as in vitellarium and observed to play crucial roles in the development of the reproductive system and egg production in female schistosomes (Kapp et al. 2001, 2004; Knobloch et al. 2002).

Herbimycin A, a Src kinase inhibitor, was able to block vitellocyte mitotic activity in females coupled with males in *in vitro* cultured conditions (Knobloch et al. 2006). Moreover, females treated with herbimycin A also suffered a dose-dependent, 40-60% reduction in egg production. Herbimycin A-treated females had significant changes in the vitellarium that appeared porous and contained a lower number of vitelline cells as compared to control females. In treated males, a significantly lower number of spermatocytes was observed in the testicular lobes (Beckmann et al. 2010b).

A study explored the inhibitory role of co-drug treatment using herbimycin A with/without TRIKI, and qRT-PCR-based analyses showed that both TβR1 and Src-TK participate in a signaling pathway influencing eggshell formation in female schistosomes (Buro et al. 2013).

More recently, an alliance of Smß-Int1 and SmVKR1 was found in *S. mansoni* with its interacting partners SmILK, SmPINCH, SmNck2 to form a complex (Gelmedin et al. 2017). Furthermore, RNAi knock-down of Smß-Int1 and SmVKRs indicated their potential roles in oogenesis and egg production of females (Beckmann et al. 2012; Vanderstraete et al. 2014). As SmILK played a central role in this interacting complex, therapeutic inhibition targeting ILK by QTL-0267 was achieved by using varying concentration of 50-200 µM and a dose-dependent effect was observed. Phenotypically, QTL-0267 caused negative *in vitro* effects on pairing stability and egg production. In addition, CLSM showed reduction in number of oocytes, differentiation defects and oocyte degeneration in ovaries. Following QTL-0267 treatment, BCL-2 family members for regulating apoptosis, like BAK and BAX, were transcribed at higher levels as well as caspase 3 activity was increased in the treated worms as compared to DMSO-treated control worms (Gelmedin et al. 2017). These results in *S. mansoni*

have supported the notation that apoptosis plays a significant role in oocyte differentiation under the influence of constant male pairing. However, apart from apoptotic cell death there is a lack of knowledge about the involvement of other types of cell death in schistosomes, such as autophagic cell death.

1.3.2 Abelson-related (Abl) kinase signaling

In eukaryotes, Abl kinases are known to be involved in cytoskeletal reorganization, stress responses, and in cell proliferation, and therefore in the survival of cells (Pendergast 2002). Abl kinases have been identified in schistosomes (Beckmann and Grevelding 2010) and interactions with other signaling pathways have been postulated (Berriman et al. 2009), such as epidermal growth factor, the platelet-derived growth factor, insulin-like growth factors and integrins that can activate Abl kinases.

Two Abl-TKs, SmAbl1 and SmAbl2, have been identified by our group. Transcripts of their genes were detected in the gonads and weakly in the gastrodermis of adult worms (Beckmann and Grevelding 2010). Furthermore, Imatinib is a therapeutic agent against chronic myeloid leukemia (CML) and gastrointestinal stromal tumors in humans (Gleevec; STI-571) (Manley et al. 2002; Larson et al. 2008), and it inhibits Abl kinase function. Imatinib caused drastic effects on *S. mansoni* and *S. japonicum* morphology and gonad development *in vitro* (Beckmann and Grevelding 2010; Li et al. 2019). After observing their significant homology with the human Abl kinases, an *in vitro* study was conducted to assess the effect of imatinib on gene transcription of the parasite; a number of genes that regulate surface, gonad, gut and muscle-associated processes were shown to be differentially transcribed between treated and untreated worms. In addition, employing varying concentrations and exposure times suppressed the enzymatic activity of SmAbl1 and SmAbl2 by 70-90% in GVBD assays (Buro et al. 2014).

Although treatment of worms with PZQ *in vivo* resulted in the up-regulation of genes controlling lipid regulation, muscle function, detoxification, calcium regulation, and drug resistance (Hines-Kay et al. 2012; You et al. 2013), the use of imatinib led to a down-regulation of genes associated with lipoproteins, drug efflux proteins, and calcium/calmodulin binding proteins (Buro et al. 2014). Interestingly, genes contributing to egg formation were up-regulated following imatinib treatment (Buro et al. 2014). However, the extent of up-regulation of these egg-forming genes were the same as observed in a microarray study assessing the effects of a TRIKI inhibitor in adult worms compared with herbimycin A treatment, which down-regulated the transcript level of these genes. Furthermore, *in situ* hybridization

experiments also revealed a higher abundance of SmAbl1 and SmAbl2 in gonads, which is the same as with localization of TGFβR1 transcripts (Beckmann et al. 2010b). Based on these observations, it was postulated that there is an association between these two signaling pathways. Also microarray analysis showed a significant down-regulation of multi-drug resistance (MDR) genes following the exposure of worms to imatinib (Buro et al. 2014).

1.4 Autophagy

Autophagy [auto (self)- phagy (eating)] is an intracellular programmed degradation process that recycles damaged proteins and damaged organelles. Autophagy (usually referred as macroautophagy) enables recycling of intracellular components, and it serves as an alternative source of energy supply during metabolic stress to maintain cellular homeostasis and to ensure cell survival (Figure 1.2) (Levine and Klionsky 2004). Autophagy can also be activated in response to other stress factors such as inflammation, hypoxia, and oxidative stress (Skendros et al. 2018). A molecular understanding of autophagy regulation has been gained only in the past two decades, and this dynamic process is mainly divided into three discrete stages modulated by autophagy-related (Atg) proteins: i) initiation of autophagy, ii) autophagosome formation and elongation, iii) autophagosome maturation and degradation.

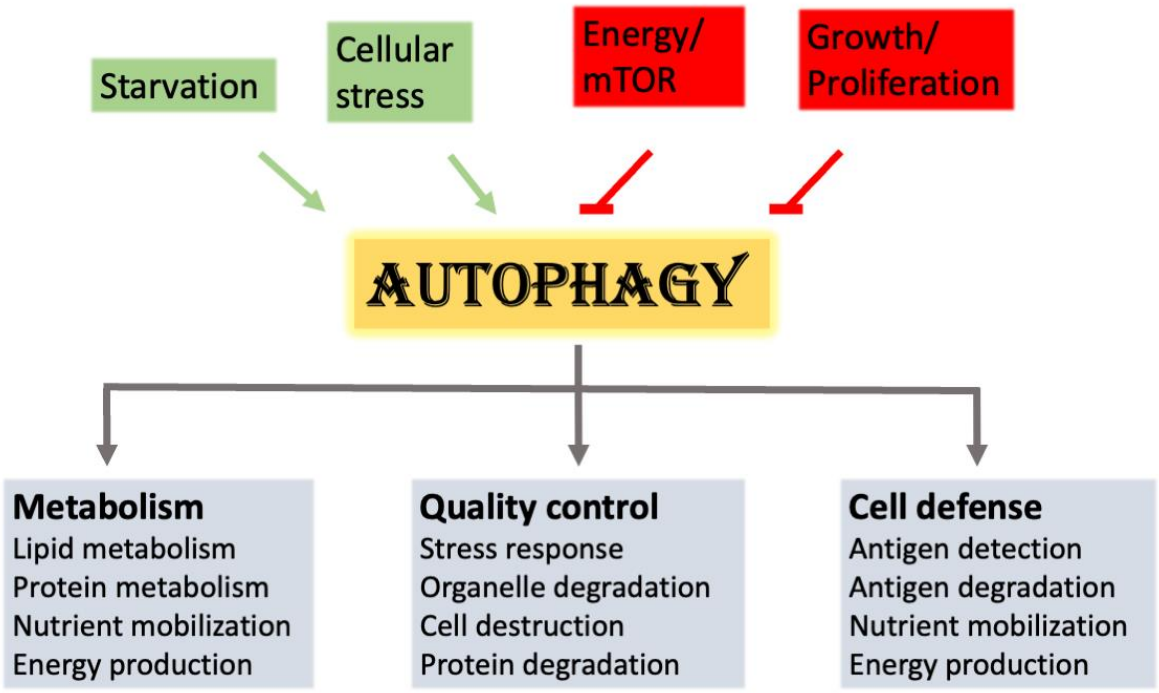

Figure 1.2: Flowchart of autophagy regulators and autophagy functions. Flowchart of autophagy regulators and autophagy functions. Green boxes represent the activators of autophagy. Red boxes represent the inhibitors of autophagy. Grey boxes represent the functional roles of autophagy.

1.4.1 Initiation of autophagy

The lack of essential nutrients is called nutrient starvation and is the most common trigger of autophagy. For example, lack of amino acids, carbon, and/or nucleic acids can induce autophagy in yeast (Takeshige et al. 1992). Similarly, nitrogen and carbon starvation can induce autophagy in plant cells (Moriyasu and Ohsumi 1996; Yoshimoto et al. 2004). In mammals, modulation of autophagy seems to be highly interlinked and complicated. Withdrawal of total amino acids strongly induces autophagy in many cell cultures, but the consequence of individual amino acid loss differs and depends amongst others on the cell type (Mizushima 2007).

The initiation of autophagy starts with the stimulation of a protein complex comprising the Unc-51-like kinase family members ULK1 and 2 (yeast Atg1), ATG13 and FIP200, usually called induction complex (Jung et al. 2009). During starvation, AMP-activated protein kinase (AMPK) phosphorylates ULK1 thus inducing autophagy. In contrast, when nutrients are accessible, the target of rapamycin complex 1 (MTORC1) blocks this activation. MTORC1

dissociates from the induction complex, resulting in dephosphorylation and induction of macroautophagy (Hosokawa et al. 2009; Jung et al. 2009).

1.4.2 Autophagosome formation

The autophagosome, a hallmark of autophagy, is a double-membrane organelle formed by the elongation of an isolation membrane (phagophore), which separates the sequestered unnecessary content from the cytoplasm. At this step, the class III phosphatidylinositol 3-kinase (PI3K-III) complex plays a critical role. This complex comprises of VPS34 with VPS15 and BECLIN1 (yeast Atg6) (Mizushima 2007). BCL-2, as an anti-apoptotic protein, can interact with BH3 domain of BECLIN1 thus inhibiting autophagy (Maiuri et al. 2007). During starvation, the interaction of BCL-2 with BECLIN1 decreases, rendering more BECLIN1 free in cytosol to induce autophagy (Pattingre et al. 2005). UVRAG (UV irradiation resistance-associated gene) and AMBRA1 (Activating molecule in BECLIN1-regulated autophagy protein 1) are among other binding partner proteins that are also known to positively interact with BECLIN1 and induce autophagy (Liang et al. 2006).

In mammals, autophagosome elongation is regulated by two ubiquitin-like conjugation systems that are both essential for autophagy modulation: (i) the Atg12/Atg5, and the (ii) Atg8-phosphatidylethanolamine (Atg8-PE) conjugation systems, (Ohsumi 2001). Atg8 is also known as microtubule-associated protein 1 light chain 3 (LC3). The LC3-PE process is controlled by lipid modification of LC3 mediated by Atg4, Atg7 (E1 activating enzyme) and Atg3 (E2 conjugating enzyme) (Figure 1.3).

The Atg12/Atg5 process starts with conjugation of Atg12 to Atg5, with Atg10 (acting as an E2 enzyme). This Atg12/Atg5 conjugate then binds with ATG16 noncovalently to form a larger complex (Atg12/Atg5/Atg16), which exerts an E3 enzyme-like function and regulates the LC3-PE binding to the autophagosomal membrane (Kuma et al. 2002). Activation of LC3 completes with the reversible conjugation of LC3-I to PE (by Atg7 and Atg3) to form LC3-II on the surface of autophagosomes (Kabeya et al. 2000). LC3–PE is membrane-associated, but can be released from membranes as a result of a second Atg4-mediated cleavage (Geng and Klionsky 2008). This conversion of LC3-I into LC3-II has been widely used to monitor autophagy in various assays.

1.4.3 Autophagosome maturation and degradation

The fusion of the outer membrane of an autophagosome with lysosomes to form an autophagolysosome is called maturation process. It has been shown that RAB7, small GTPase,

LAMP1/2 (lysosomal-associated membrane proteins) and cathepsins L/B/D are involved in the maturation and facilitate autophagosome and lysosome fusion (Eskelinen 2005). Autophagosomes move towards lysosomes with the help of microtubules (Monastyrska et al. 2009). During fusion, URAG is also known to be involved and activates RAB7 GTPase activity (Liang et al. 2008). It has been postulated that different members of soluble N-ethylmaleimide-sensitive factor attachment protein receptor (SNARE) proteins, such as VAM7 and VAM9, play roles during fusion of autophagosomes with lysosomes (Fader et al. 2009; Furuta et al. 2010). Some recent studies have evidenced the involvement of another significant SNARE protein, syntaxin 17, which also regulates the fusion of autophagosome and lysosome through an interaction with SNAP29 and VAMP8 (Itakura et al. 2012). Following fusion, degradation of the inner components is dependent on lysosomal acid hydrolases, including proteinases- A, -B and the lipase Atg15 in yeast (Teter et al. 2001; Epple et al. 2001) and cathepsins B/D/L in mammalian cells (Tanida et al. 2005). As a result, degraded molecules, particularly amino acids, are transported back to the cytosol for protein synthesis and to maintain cellular metabolism as well as other functions under nutrient-starved conditions.

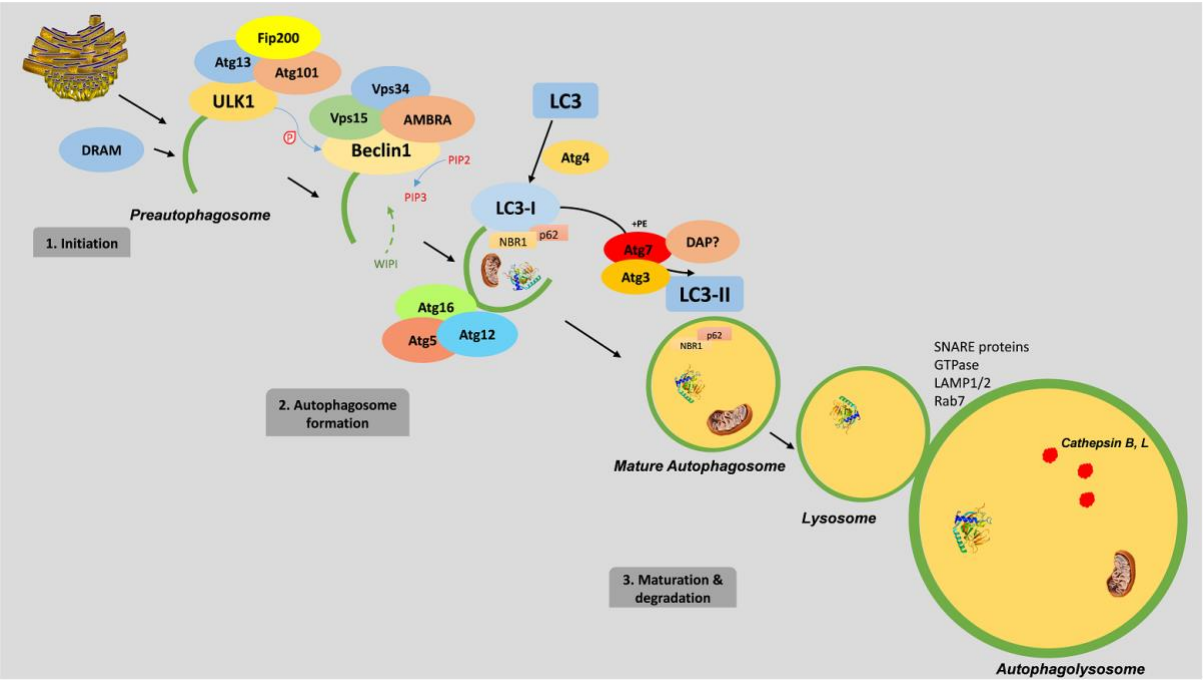

Figure 1.3: Schematic overview of the autophagy pathway. Autophagy is a multistep pathway, which involves at least three main steps of initiation, formation, maturation or degradation. Autophagy is regulated by more than 30 Atg (autophagy-related) proteins and two ubiquitin-like conjugation systems.

1.5 Autophagy regulation

Modulation of autophagy helps cells reacting to a wide range of extra- and/or intracellular stresses, which includes the presence or absence of nutrients, growth factors, endoplasmic or oxidative stress as well as hypoxia (He and Klionsky 2009). Generally, there are two pathways involved in induction of autophagy, the cAMP-dependent protein kinase A (PKA) pathway and the TOR pathway, which are primarily sensitive to carbon and nitrogen deprivation, respectively (Stephan et al. 2010). Under nutrient-rich conditions, PKA is an inhibitor of autophagy in yeast and MTORC1 is a major regulator of autophagy in mammals. The presence of amino acids/nutrients regulates the RAG proteins and small GTPases that mediate the activation of MTORC1 (Kim et al. 2008; Sancak et al. 2008). PKA has also been shown to indirectly modulate the activation of MTORC1 through the inactivation of AMP-activated protein kinase (AMPK) (Djouder et al. 2010). Under nutrient-deprived conditions, AMPK either activates TSC1/2 complex, which then inhibits the MTORC1 activity (Inoki et al. 2003), or directly inhibits MTORC1 (Gwinn et al. 2008; Lee et al. 2010). In addition, several studies have shown that AMPK can phosphorylate and activate ULK1 to initiate autophagy (Lee et al. 2010; Egan et al. 2011; Kim et al. 2011; Shang et al. 2011).

1.6 Pharmacologic manipulation of autophagy

Various compounds described to modulate the autophagy process are available and frequently used to study the role of autophagy in different metabolic and pathological scenarios. Inhibitors of MTOR such as rapamycin, CCI-779 and RAD001 are known to induce autophagy in yeast (Noda and Ohsumi 1998) as well as in animals (Ravikumar et al. 2004). Autophagy inhibitors are usually divided into two categories based on the target molecules to be inhibited: early-stage inhibitors and late-stage inhibitors. Pan-PI3K, Vps34 and ULK inhibitors have been classified as early-stage inhibitors of autophagy (Table 1). Protease-, V-ATPase and lysosome inhibitors are late-stage inhibitors (Pasquier 2016).

Wortmannin (pan-PI3K inhibitor) has also been used to inhibit autophagy at its early stage (Wiesinger et al. 1974) by transiently inhibiting the classes I, II and III of PI3K (Powis et al. 1994; Thelen et al. 1994). Spautin-1, a specific and potent inhibitor of autophagy, is also known to inhibit autophagy at its early stage by promoting the degradation of Vps34 and by deubiquination of Beclin1 via inhibition of USP10 and USP13 (Liu et al. 2011).

In contrast, bafilomycin A1 (BA1), chloroquine (CQ), hydroxychloroquine (HCQ), and NH_4Cl are known to inhibit autophagy at a later stage by limiting the fusion of autophagosomes with

lysosomes (Yamamoto et al. 1998). BA1 is a specific inhibitor of vacuolar H-ATPase, whereas CQ, HCQ and NH_4Cl are lysosome inhibitors that increase intracellular pH and, therefore, limit autophagosome and lysosome fusion, and thus autophagy.

Among all the autophagy modulators studied so far, some of these compounds have effects on other pathways either as off-target effects or additional effects to autophagy inhibition. But nevertheless, they have proven very useful in studying and inhibiting autophagy in laboratory conditions. A more specific and relatively new approach to inhibit autophagy *in vitro* is via shRNA, siRNA, or dsRNA-mediated knock-down of essential autophagy regulating genes, such as Beclin1, Vps34 and LC3 (Helgason et al. 2011). However, various complexities and considerations need to be resolved because knock-down of essential targets of autophagy does not necessarily lead to good inhibition of autophagy as well as functional phenotypic evidences (Staskiewicz et al. 2013).

1.7 Objectives of the study

Since maintenance of cellular homeostasis and body reshaping is crucial for schistosomes, I hypothesized an important role of autophagy in schistosome vitality and reproduction. Despite the well-known significance of autophagy in maintaining cellular survival and homeostasis, until now autophagy has been a neglected topic in schistosome research. The modulation of autophagy as a potential effect of kinase inhibitors in human cancer studies has also raised my research interest. By addressing the following questions and objectives, I explored the autophagy machinery and its involvement in tissue maintenance, pairing-dependent processes and reproduction of *S. mansoni* as well as its implication for the antischistosomal activities of a kinase inhibitor.

In this study, I addressed the following questions:

a) Whether orthologs of autophagy genes are present in *S. mansoni* similar to other multicellular organisms?
b) Whether autophagy gene expression differs among two sexes of *S. mansoni*?
c) What role(s) autophagy may play in *S. mansoni*?
d) Whether or not the role of autophagy in *S. mansoni* is linked to pairing-dependent processes and reproduction?
e) What effect the TK-inhibitor imatinib has on autophagy in *S. mansoni*?

To this end, I investigated:

(i) the gene repertoire of the autophagy machinery in schistosomes compared to other multicellular organisms including humans by an *in silico* screening approach using BLASTN, SMART, and multiple sequence analyses.
(ii) differential patterns of autophagy gene expression between the two sexes of schistosomes by qRT-PCR analyses.
(iii) effects of the *in vitro* culture on the expression levels of autophagy-related genes by qRT-PCR and western blot (WB) analyses.
(iv) effects of the early phase (wortmannin and spautin-1) and late phase (BA1) autophagy inhibitors by studying worm viability, gonadal morphology, and egg production using bright-field and confocal microscopy and western blot analyses of BA1-treated worms.

(v) the cumulative effects of the TK-inhibitor imatinib and the autophagy inhibitor (BA1) by studying worm viability and gastrodermis using bright-field and confocal microscopy.

(vi) the possible mechanism of action of the co-treatment (imatinib + BA1) through modulation of LC3 by western blot analyses and cathepsins by qRT-PCR analyses.

Table 1.1: List of chemical compounds used in this study and their target protein as well as the modulated mechanisms.

Name	**Target protein**	**Target/ Mechanism**	**Reference**
Wortmannin	PI3K	Autophagosome formation	(Powis et al. 1994; Thelen et al. 1994)
Spautin-1	Vps34	Autophagosome formation	(Liu et al. 2011)
Bafilomycin A1	Unknown	Lysosome	(Bowman et al. 1988; Yamamoto et al. 1998)
Imatinib	Abl, c-kit, PDGF-R	Tyrosine kinase	(Druker et al. 1996)
Rapamycin	mTOR	Autophagosome formation	(Ravikumar et al. 2004)

2 MATERIALS AND METHODS

2.1 Materials

2.1.1 Online databases and software tools

Database / software	Hyperlink address	Application
PubMed - U.S. National Library of Medicine National Institutes of Health	http://www.ncbi.nlm.nih.gov/pubmed/	Literature search
NCBI – national center for biotechnology information	http://www.ncbi.nlm.nih.gov/pubmed/	Homology search
WormBase ParaSite (Version 15)	https://parasite.wormbase.org/index.html	Homology search
WormBase ParaSite Blast (Version 15)	https://parasite.wormbase.org/Multi/Tools/Blast	Protein blast
NCBI-blast	http://blast.ncbi.nlm.nih.gov/Blast.cgi	Nucleotide / protein blast
Reverse Complement	https://www.bioinformatics.org/sms/rev_comp.html	Reverse complement
SMART - simple modular architecture research tool	http://smart.embl-heidelberg.de/	Protein domain analyses
MAFFT – mutliple alignment using fast fourier transform	https://www.ebi.ac.uk/Tools/msa/mafft/	Multiple sequence alignment
Clustal Omega	https://www.ebi.ac.uk/Tools/msa/clustalo/	Multiple sequence alignment

Meta RNAseq in *S. mansoni*	https://v7test.schisto.xyz/	Gene transcripts of *S. mansoni*
SchistoCyte Atlas	http://collinslab.org/schistocyte/	Single-cell transcriptiomic of *S. mansoni*
Primer3Plus	https://www.bioinformatics.nl/cgi-bin/primer3plus/primer3plus.cgi/	Primer design
Oligo Calc - Oligonucleotide Properties Calculator	http://biotools.nubic.northwestern.edu/OligoCalc.html	Melting temperature adjustment
Oligo Analyzer Tool	https://eu.idtdna.com/pages/tools/oligoanalyzer	Primer analyses
ImageJ	https://imagej.nih.gov/ij/	Densitometry analyses
Prism (Version 8.0)	https://www.graphpad.com/scientific-software/prism/	Statistical analyses

2.1.2 Primers

2.1.2.1 qRT-PCR primers

Gene name	**Smp number**	**Primers (5'→ 3')**	**$A_{(T)}$ ^{o}C**	**Product (bp)**
Sm*ambra1*	Smp_156350.1	TGTTGGATCCTGTCTCGTCAA	59.5	152
		AGTACCGTAAAGAATGCTGCCA	60.1	
Sm*beclin*	Smp_048990.1	GGTCGTTTGCCTAATCGTCC	60.5	142
		TTGACTGGCTACCCATTGGC	60.5	
Sm*vps34*	Smp_128130.1	TCCAACCGAATGGCGATACG	60.5	168
		CGAGACGGTTACTTGTAGCC	60.5	

Sm*dram*	Smp_006750.2	TGGGAGTCGTATTTTCAGCG TT TTTTCTAGGGAATGGACCGT G	60.1 59.5	173
Sm*dap*	Smp_023840.1	CAGTTAAAGCCGGAAAGAT GAGA GTTTAGTAACTGTTGGCATT GGC	60.9 60.9	171
Sm*lc3.1*	Smp_073790.1	TCGGACCTAACTGTCGGACA GCAATGTAGAGGAAGAGAT CAC	60.5 60.1	167
Sm*lc3.2*	Smp_087940.2	CGTCATCGCCATTCGCAAAT TTGTGGCACTTGTTTGAGGC	58.4 58.4	169
Sm*letm1*	Smp_065110	GAAGGTGATCAAGCTCCATT GT TTGTACTGCATGGATAGGTG GT	60.1 60.1	162
Sm*map3k9*	Smp_176580	CTTCCAAAATGGCCGTGA TGGTGAGGAAACTCGGAGA C	60.5 60.5	132
Sm*psmb7*	Smp_073410	GGTCTGGTGGTTTCTCGTTC GTACCTTCTGTTGCCCGTG	60.5 59.5	160
Sm*ptpa*	Smp_166290	GTAAAACTGGTCCATTTGAA GAAC TACCGAATAGGAAATGTTGA ACGA	60.3 59.2	150
Sm*cath.l-q1*	Smp_343260.1	TGGTGCAGTTACTCCAGTCA A TGTACCACCTTGACATCCAT CA	59.5 60.1	178
Sm*cath.blp_q1*	Smp_067060.1	AGGAAGAAATGGCCTGGTT G	58.4	178

		GAGCTGTTGCGAAAGTTGTG	58.4	
Sm*cath.b_q1*	Smp_085180.1	AATTATGAGTTCCCGCCGTG T	59.5	154
		TGAATGGTCCGGTCATAGCA A	59.5	
Sm*cath.b1_q1*	Smp_103610	TTGACCACAATGATTGGAAT GTG	59.2	161
		CTGTATGCAGCTTCGATCAC TC	59.3	

2.1.2.2 dsRNA primers

The annealing temperatures ($A_{(T)}$) was calculated without T7 primer extension (red).

Gene name	**Smp number**	**Primers (5'→3')**	**$A_{(T)}$ ^{O}C**	**Product (bp)**
Sm*ambra*_ dsRNA_1	Smp_156350.1	TAATACGACTCACTATAGGGAGAT GCTTGCGAGTGGATGTCTT	60	471
		TAATACGACTCACTATAGGGAGAC ACATGAGGCTTCGGGAGTT	60	
Sm*ambra*_ dsRNA_2	Smp_156350.1	TAATACGACTCACTATAGGGAGAA TCGTCTGCAACCGGAACAT	58.4	439
		TAATACGACTCACTATAGGGAGAA ACCGGTGCCAACGATCTAA	58.4	
Sm*ambra*_ dsRNA_3	Smp_156350.1	TAATACGACTCACTATAGGGAGAG CCGGTGGGAACTGAGTTTA	60.5	427
		TAATACGACTCACTATAGGGAGAG AAGGTATGCGTGTGGTTGC	60.5	
Sm*ambra*_ dsRNA_4	Smp_156350.1	TAATACGACTCACTATAGGGAGAA GGGTGAAGTTCGTCGAAGC	60.5	400
		TAATACGACTCACTATAGGGAGAA TTACAGCACGAGACTGGGG	60.5	
Sm*beclin*	Smp_048990.1	TAATACGACTCACTATAGGGAGAG CGTACAGAAGAATTAGATCGAGC	63.6	434

		TAATACGACTCACTATAGGGAGAC		
		GAATTTGCCAGCGCTCAAT	58.6	
Sm*vps34*	Smp_128130.1	TAATACGACTCACTATAGGGAGAT	60.5	457
		CCAACCGAATGGCGATACG		
		TAATACGACTCACTATAGGGAGAA		
		CTTCAGGTGCCATCGGTTT	58.5	
Sm*dram*	Smp_006750.2	TAATACGACTCACTATAGGGAGAC	58.5	415
		GCCTGAAAGCTGCGTATTT		
		TAATACGACTCACTATAGGGAGAA		
		ATGGACCGTGGATTTCCCC	60.5	
Sm*dap*	Smp_023840.1	TAATACGACTCACTATAGGGAGAT	58.4	209
		GGACGGAACTTCAGACACT		
		TAATACGACTCACTATAGGGAGAA		
		GTAACTGTTGGCATTGGCT	56.4	
Sm*lc3.1*	Smp_073790.1	TAATACGACTCACTATAGGGAGAC	58.4	256
		GTCCGTTTGAAAAACGCCT		
		TAATACGACTCACTATAGGGAGAG		
		AGCACCCATAGTAGCGCTT	60.5	
Sm*lc3.2*	Smp_087940.2	TAATACGACTCACTATAGGGAGAG	60.5	236
		CAAAGACAGCAGGACTCCT		
		TAATACGACTCACTATAGGGAGAT		
		TGTGGCACTTGTTTGAGGC	58.5	

2.1.3 Buffers and solutions

2.1.3.1 General buffers and solutions

Buffers / solutions	**Composition**	**Use**
DEPC-dH_2O	0.1 % diethylpyrocarbonate in dH_2O; autoclaved	Preparation of solutions
Ethidium bromide	0.5 µg/ml in TAE-buffer	Nucleic acid staining
MOPS-buffer (10x)	200 mM morpholino propanesulfonic acid (MOPS), 50 mM sodium acetate,	RNA gel electrophoresis

	10 mM EDTA, all in DEPC-H_2O; pH 7.0; autoclaved	
1x Reaction buffer B	80 mM Tris-HCl, 20 mM $(NH_4)_2SO_4$, 0.02% w/v Tween20, 2.5 mM $MgCl_2$	PCR DNA amplification
TAE-buffer (50x)	2 M Tris, 1 M acetic acid, 50 mM EDTA; pH 8.0, dH_2O upto 1 L	DNA gel electrophoresis
Orange dye (10x)	50 % sucrose, 0.6 % orange G in 1x TAE buffer	DNA gel electrophoresis
AFA-Fixative	2% acetic acid; 3% formaldehyde; 70% ethanol	Fixation of *S. mansoni*
Carmine red solution	1 mg carmine red (Ceristain, Merck), 1 ml conc. HCl, 1 ml dH_2O, 90 % ethanol upto 40 ml	Staining of *S. mansoni*
Mounting solution	Canada balsam in xylene (2:1) (Merck)	Preparation of CLSM slides

2.1.3.2 Buffers and solutions for western blotting

Buffers / solutions	**Composition**	**Use**
2x SDS sample buffer	0.5 M Tris; pH 6.8, 20% glycerol, 10% 2-Mercaptoethanol, 6% SDS, 1% Proteinase inhibitor cocktail (Sigma Aldrich)	Preparation of protein lysate
20% SDS	20 g in 100 ml dH_2O	Protein experiments
Stacking gel buffer	0.5 mM Tris-Cl, 0.4% SDS; pH = 6.8	Protein gel electrophoresis
Separting gel buffer	1.5 M Tris-Cl, 0.4% SDS; pH = 8.8	Protein gel electrophoresis
SDS-PAGE running buffer	25 mM Tris, 190 mM glycine, 0.1% SDS; pH 8.3	Protein gel electrophoresis
Transfer blot buffer	25 mM Tris, 192 mM glycine, 20% methanol and 0.06% SDS in dH_2O; pH 8.3	Transfer of proteins

Ponceau S Red staining buffer (10x)	2% Ponceau S in 30% trichloroacetic acid and 30% sulfosalicylic acid.	Visualization of proteins on membrane
Coomassie Blue staining buffer	40% dH_2O, 10% acetic acid, 50% methanol and 0.25% Coomassie Brilliant Blue R-250	Visualization of proteins on SDS-gel
Destaining solution	67.5% dH_2O, 7.5% acetic acid, 25% methanol	De-staining of the gel after coomassie blue staining
PBS (1x)	137 mM NaCl, 2.7 mM KCl, 1.5 mM KH_2PO_4, 6.5 mM Na_2HPO_4; pH 7.5	Washing
TBS (1x)	50 mM Tris-Cl, 150 mM NaCl; pH 7.5	Washing
PBST	1x PBS, 0.1% Tween-20	Washing
TBST	1x TBS, 0.1% Tween-20	Washing
Blocking solution	1x TBS, 0.1% Tween-20, 5% non-fat dry milk	Blocking after transfer of proteins to the membrane

2.1.4 Media and supplements

Media	**Composition**	**Use**
Supplemented M199 medium	M199 (Gibco), 10% NCS, 1% HEPES, 1% ABAM,	*In vitro* culture
NCS	Newborn calf serum (Sigma Aldrich)	Supplementation of M199 medium
HEPES	[4-(2-hydroxyethyl)-1-piperazinyl]-ethan-sulfonic acid	Supplementation of M199 medium
ABAM	Antibiotic, antimycotic solution (Sigma Aldrich)	Supplementation of M199 medium
M199 medium	M199 (Gibco, Life technologies)	Gonad isolation
Tegument solubilisation (TS) buffer	100 ml PBS, 0.1 g Brij35 (Roth), 0.1 g Nonidet P40 (Sigma Aldrich), 0.1 g	Gonad isolation

	Tween 80 (Sigma Aldrich), 0.1 g Triton X-405 (Sigma Aldrich)

2.1.5 Kits and antibodies

Kit / Antibody	Company catalog number	Use
PeqGOLD TriFast	# 30-2010; Peqlab	RNA extraction
Monarch™ PCR & DNA cleanup kit	# T1030; New England BioLabs	DNA purification
Monarch™ DNA Gel extraction kit	# T1020; New England BioLabs	DNA extraction
NucleoSpin™ Gel and PCR Clean-up	# 740609; Macherey-Nagel	DNA extraction
Monarch™ Total RNA Miniprep kit	# T2010; New England BioLabs	RNA extraction
Monarch™ T7 High yield RNA synthesis kit	# E2040; New England BioLabs	dsRNA synthesis
QuantiTect reverse transcription kit	# 205311; Qiagen	Reverse transcription
FirePol *Taq*-Polymerase	# 01-01-00500; Solis Biodyne	DNA polymerase
PerfeCTa SYBR Green Super Mix	# 95054; Quanta	qRT-PCR master mix
Hyperladder™ 50 bp	# BIO-33039; Bioline	DNA gel electrophoresis
GelRed™ Nucleic Acid Gel stain	#41003, Biotium	DNA gel electrophoresis
GENE's protein ladder wide range	# 310020; GeneON	SDS gel electrophoresis
Albumin Standard™ (BSA)	# 23209; Thermo Scientific	Quantification of protein
LC3B	# 2775; Cell Signaling Technology	Western Blot
Goat anti-Rabbit IgG	# 31460; Thermo Scientific	Western Blot

Pierce ECL Western Blotting Substrate	# 32132; Thermo Scientific	Detection of Western Blot

2.1.6 Chemicals and inhibitors

Chemical / Inhibitor	**Company catalog number**	**Use**
Tricaine	Ethyl-3-aminobenoat-methansulfonat # E10521; Sigma Aldrich	Narcotization of worms
Elastase	# E0258; Sigma Aldrich	Organ isolation
Trypan Blue	# T8154; Sigma Aldrich	Organ isolation
DMSO	# D4540; Sigma Aldrich	Solvent for chemical compounds
Rapamycin	# 53123-88-9; Cayman Chemicals	Treatment of *S. mansoni*
Bafilomycin A1	# 88899-55-2; Cayman Chemicals	Treatment of *S. mansoni*
Wortmannin	# 19545-26-7; Cayman Chemicals	Treatment of *S. mansoni*
Spautin-1	# 1262888-28-7; Cayman Chemicals	Treatment of *S. mansoni*
Imatinib	# 220127-57-1; Enzo Life Sciences	Treatment of *S. mansoni*

2.2 Methods

2.2.1 Ethics Statement

All animal experiments have been performed in accordance with the European Convention for the Protection of Vertebrate Animals used for experimental and other scientific purposes (ETS No 123; revised Appendix A) and have been approved by the Regional Council (Regierungspraesidium) Giessen (V54-19 c 20/15 c GI 18/10).

2.2.2 *S. mansoni* laboratory life cycle

For the *S. mansoni* life cycle maintenance under the laboratory conditions, *Biomphalaria glabrata* snails were used as intermediate hosts, and Syrian hamsters (*Mesocricetus auratus*) as final hosts. The laboratory-strain of *S. mansoni* was originated from a Liberian isolate from Bayer AG, Monheim (Grevelding 1995). Adult worms were collected by hepatoportal perfusion 46 (bisex; bs) or 67 (single-sex; ss) days post infection (p.i.).

2.2.3 Infection of snails

Snails were maintained in aerated snail-water at 26°C and at a day-night light rhythm of 16/8 h. They were fed every second day with cucumber slices. Snail infection was done overnight (o/n) in 12-well culture plates containing 2 ml snail-water in each well. For polymiracidial infections, snails were exposed to 10-15 miracidia. For monomiracidial infections, only one miracidium per snail was used for infections (Grevelding 1999).

2.2.4 Perfusion of hamsters and *S. mansoni in vitro* culture

Hamsters were first anesthetized with isoflurane in a glass chamber and then euthanized using a combination (2.5 - 3 ml) of anaesthetic and muscle relaxant (Xylariem 3.1 %, Ketamine 0.19 %, in 0.9 % NaCl). Before opening the abdominal cavity to expose heart and intestines, hamsters were cleaned with 70% ethanol for semi-sterilization to avoid possible contaminations of the following *in vitro* culture of the recovered worms.

Perfusion was performed following already established protocol (Smithers and Terry 1965; Duvall and DeWitt 1967) with modifications. After anaesthesia, the hamster body was dissected to access the internal organs. The hepatic portal vein was cut with a canula, connected to a flexible tube and a bottle with 37°C pre-warmed perfusion medium. Subsequently, the canula was introduced into the left heart chamber, and the perfusion medium was pumped through the blood circulation, thus flushing the worms out of the blood circulation. Worms were then collected by a fine brush and transferred to a culture-medium in a petri dish.

Mesenteric veins were also checked for the presence of worms. Following perfusion, worms were then placed in groups of either 20 couples, or 25 males, or 25 females to Petri dishes of 60 mm. Worms were kept in 4 ml supplemented M199 medium and incubated at 37ºC and 5% CO_2 in an incubator. If required, couples from bs infections were manually separated into male and female worms by pipetting after narcotization in 2.6% tricaine (Sigma Aldrich), or using feather-weight tweezers and used for further experiments (gonad isolation, RNA extraction etc).

2.2.5 Isolation and staining of gonads

The isolation of reproductive organs was performed by an established protocol in our laboratory (Hahnel et al. 2013).

2.2.5.1 Isolation of ovaries and testes

In order to isolate the gonads, 60 female or male worms were transferred into 2 ml Eppendorf tubes. The culture-medium was removed, and the worms were washed once with 2 ml non-supplemented M199 medium. After removal of the medium, the tegument was disrupted for 2 x 5 min (females) or 3 x 5 min (males) in 400 µl tegument solubilisation buffer in DEPC-PBS, pH 7.2 - 7.4; 0.2 µm (filtered before use) at 1,200 rpm and 37°C on a thermal shaker. To remove the dissolved tegument, worms were washed three times with 2 ml non-supplemented M199 medium, and the medium was removed completely.

As a next step, enzymatic digestion was done by shaking worms with 300 µl elastase (5 U/ml in non-supplemented M199) for 20 - 40 min at 37°C and 650 rpm. Shaking was stopped when the medium became clouded with small fragments, and when the worms became soft and viscous. The mixture was incubated on the heating block for 1 min. Afterwards, 1 ml non-supplemented M199 medium was added to the tube, and 2 - 4 times gentle pipetting was performed to gradually break up and dissolve the leftover body tissue. The mixture was transferred into a 30 mm dish filled with 1 ml non-supplemented M199, which was observed under an inverted microscope (Leica Labovert, Germany) to check the viability and for collection. Intact gonads were collected by pipetting using 10 µl tips and transferred 2 - 3 times to new dishes for purification from tissue debris. Following collecting, purified organs were transferred into RNase-/DNAse-free vessels on ice. Testes and ovaries were centrifuged for 5 min at 1,000 g and 1 min at 8,000 g, respectively, and were kept frozen at -80°C after removing the supernatant. In order to check the viability of isolated gonads, trypan-blue staining was performed. Besides the morphological analyses by bright-field microscopy, 4 - 6 organs were

stained with 10 µl Trypan Blue (0.4%; Sigma Aldrich). In case dead cells occur, they are stained within one minute.

2.2.6 Isolation of nucleic acids

2.2.6.1 RNA extraction from adult worms and gonads

RNA extraction was performed using 10 - 20 male and female worms (either bs or ss) or 50 - 150 gonads, which were collected into separate RNase-free 1.5 ml tubes. The samples were then subjected to total RNA extraction either by Trizol (PeqGOLD TriFast, Peqlab) or by using the Monarch total RNA Miniprep kit (New England BioLabs) following the manufacturer's protocol.

For sample preparation by Trizol, 200 µl Trizol was added to each tube containing worms that were mechanically homogenized with plastic pistons. 50 µl Trizol was immediately added to the tubes containing gonads (either ovaries or testes), and the complete disruption of cells was done by three snap freeze-thaw cycles using liquid nitrogen. Following sample preparation, further Trizol was added up to 500 µl, and the tubes were kept at RT for 5 min to allow the dissociation of the nucleic acid and protein binding. After that, 100 µl chloroform was added, and the samples were vigorously shaked for 15 sec and incubated at RT for 5 - 10 min to induce the phase separation. The different phases were then separated through centrifugation at 12,000 g and 4°C for 15 min and the aqueous phase was transferred into new RNase-free 1.5 ml tubes. After adding 300 µl isopropanol and a brief vortex, RNA was precipitated at -20°C o/n. The following day, the tubes were centrifuged at 12,000 g and 4°C for 15 min, and the upper liquid was discarded. The pellet was washed with 1 ml pre-cooled 75% ethanol and was again centrifuged. Subsequently, the pellet was dried at RT for 5 min. The total RNA was resuspended in 20 µl of the nuclease-free water.

The Monarch total RNA Miniprep kit also based on the same principle as Trizol method, but the gDNA removal step was more efficient. Using this method, worms or gonads were collected into separate RNase-free 1.5 ml tubes in 100 µl of 1x RNA/DNA protection buffer and stored at -80°C until further processing. Adult worm samples were mechanically homogenized using plastic pistons. For gonads, three freeze-thaw cycles were done in liquid nitrogen for complete disruption of gonad cells in RNA/DNA protection buffer. A mixture of 30 µl Prot K reaction buffer and 15 µl of Prot K (both included in kit) was added to the sample mixture. After a brief vortex, the mixture was incubated at 55°C for 5 min. The mixture was then centrifuged at 16,000 g and RT for 2 min. After the transfer of supernatant to new RNase-

free 1.5 ml tubes, an equal volume of RNA lysis buffer was added. Later, the sample mixture was passed through the gDNA removal column and RNA purification column, each time centrifuged at 16,000 g and RT for 1 min using table-top centrifuge machine. Further enzymatic removal of gDNA was done by incubating the column matrix with a mixture of 5 µl DNAase I and 75 µl of DNAase I reaction buffer 15 min at RT. Following gDNA removal step, column matrix was purified using 500 µl of RNA priming buffer and RNA wash buffer, each time centrifuged at 16,000 g and RT for 1 min. Subsequently, RNA on the column matrix was eluted in new RNase-free 1.5 ml tubes using 20 µl of nuclease-free water. The buffers and solutions used in this procedure were provided by the manufacturer (New England BioLabs). Total RNA was then placed on ice for downstream steps, or they were placed at -20°C for short-term storage, or at -80°C for long-term storage.

2.2.6.2 RNA analyses

After extraction, RNA quality and quantity were checked by electropherogram analyses using the BioAnalyzer 2100 and an Agilent RNA 6000 Pico (for gonads) or Nano (for worms) Chip according to the manufacturer's instructions (Agilent Technologies). For each sample, 1 µl of RNA (50 pg - 25 ng) was loaded onto the chip.

2.2.7 Gel electrophoresis of nucleic acids

Nucleic acids were separated according to size in agarose gels (Maniatis et al. 1988). Due to the negatively charged phosphate backbone, nucleic acids move towards the anode in an electric field. This movement of nucleic acids through the agarose gel depends on the concentration of the gel and molecular weight of the nucleic acids.

2.2.7.1 DNA gel electrophoresis

In this work, 1 - 2 % horizontal agarose gels were used to separate DNA fragments. Gels were made by dissolving agarose in 1x TAE-buffer, and this solution was supplemented with diluted GelRed. GelRed intercalates into the DNA and allows detection of DNA fragments under the exposure of UV-light (320 nm).

Running of DNA gel electrophoresis was monitored by a Hyperladder marker (Bioline) and an orange dye as sample buffer added to each sample before loading on the gel. Sample buffer increases the density of the sample and facilitates sinking into the gel pockets. Gel electrophoresis was performed at 90 - 140 V and 300 mA.

2.2.7.2 DNA gel elution

In order to purify DNA as a template either for standard-curves of real-time PCR or amplification of dsRNA, elution of DNA from cut agarose-gel pieces was performed. Two different commercially available kits were used for cleaning, the Monarch™ DNA Gel extraction kit and NucleoSpin™ Gel and PCR Clean-up. Both kits were used according to the instruction's manual provided by manufacturers.

2.2.8 PCRs

2.2.8.1 Standard PCRs

All PCR reactions for *in vitro* amplification of DNA were performed using the thermal cycler C1000™ (BioRad). The oligonucleotide primers were designed using the Primer3plus online tool, and their metling temperature (Tm) were adjusted to 60°C using the OligoCalc online tool (Howley et al., 2007). After the initial denaturation step, amplification was performed in a three-step process consisting of denaturation, primer hybridization, and synthesis of complementary strand in a 30 - 40 cycles step. Time and temperature were adjusted according to the primers, the polymerase enzyme, and the length of the target product. 'FirePol' Taq polymerase (Solis BioDyne) was used for DNA denaturation at 95°C and 72°C for 1 min was adjusted for polymerization step for approximately 1 kb of DNA (1 min/kb). The standard PCR reaction was adjusted as follows:

DNA-template	10 - 100 ng
10 x Reaction buffer B	2.5 µl
[10 mM] dNTP mix	0.5 µl
[25 mM] $MgCl_2$	2.5 µl
[10 µM] 5' primer	2 µl
[10 µM] 3' primer	2 µl
FirePol Taq-Polymerase (5 U/µl)	0.5 µl
dH_2O	Up to 25 µl

2.2.8.2 Reverse transcription / cDNA synthesis

100 - 500 ng of total RNA per reaction was used for cDNA synthesis using the QuantiTect Reverse Transcription Kit (Qiagen). Residual gDNA was removed by a 'gDNA-wipeout' step, and cDNA was synthesized using a RT-primer mix (included within the kit) consisting of random hexamers and oligo dT-primers at 42°C for 30 min. The enzyme was later

inactivated at 95°C for 3 min. Both steps were performed according to the manufacturer's protocol, and cDNA was stored at -20°C until used as template. Depending on the concentration, a dilution of the respective cDNA (1:5 - 1:40) was used for subsequent PCR reactions.

2.2.8.3 Quantitative real-time PCR

Quantitative real time PCR (qRT-PCR) allows fluorescence-based quantification of specific DNA sequences and found application in my project for the detection of differences of transcript levels. This included the detection of transcript-level reduction following RNAi experiments as well as studies of stage- and organ-specific transcript levels of selected genes. The relative quantification approach is used for comparing the transcription of a gene with that of an endogenous reference gene.

All primers used in qRT-PCR were designed using the software tools "Primer 3Plus" and optimised using "OligoCalc" to a specific Tm of 60°C. The length of the selected amplicon was confined between 140 and 180 bp. First, the efficiency of the qRT-PCR primers was determined via standard curves by using dilutions of the eluted PCR product as template. Only those PCR primers were selected for further qRT-PCR analyses, whose efficiency value was between 90% and 100% and didn't deviate more than 10% from that of the reference gene. In addition, a melting curve analysis was used to exclude amplification of off-target products. Appropriate primers were used on cDNA templates to compare the amplification of the target gene with the reference Sm*letm1* (Haeberlein et al. 2019). The selection of an appropriate reference gene for the qRT-PCR analyses was done as described later. For qRT-PCR assays, a standard curve analyses for Sm*letm1* was carried out to define the threshold of the reaction to determine the Ct-values of individual qRT-PCR run. The threshold defines the level of background fluorescence, while the Ct-value describes the cycle at which a reaction first significantly exceeded this threshold. The evaluation of the relative quantification was performed using the Ct-method according to the given formula (Dorak 2008):

$$\Delta CT = CT\ target\ gene - Ct\ control\ (reference\ gene)$$

$$\Delta\Delta Ct = Ct\ sample - Ct\ calibrator$$

$$n - fold\ expression = 2 - \Delta\Delta Ct$$

In the given formula, ‘sample’ is defined as cDNA from e.g. dsRNA- or inhibitor-treated worms. On the other hand, cDNAs from control groups, either un-treated or treated with DMSO, served as calibrators. All qRT-PCRs were performed using Quanta's "PerfeCTa SYBR Green Super Mix" according to one of the following schemes:

20 µl reactions:

cDNA-template	5 µl
2 x Quanta SYBR Green Super Mix	10 µl
[400 nM] 5’ primer	0.8 µl
[400 nM] 3’ primer	0.8 µl
PCR-H_2O	3.4 µl

10 µl reactions:

cDNA-template	2.5 µl
2 x Quanta SYBR Green Super Mix	5 µl
[400 nM] 5’ primer	0.4 µl
[400 nM] 3’ primer	0.4 µl
PCR-H_2O	1.7 µl

cDNA samples from gonads or adult worms were diluted 1:5 - 1:25 depending upon the concentration to acquire the final concentration of 1 µg in every cDNA sample in each qRT-PCR assay. The reaction profile included an initial denaturation step at 95°C for 3 min, followed by 45 cycles of three temperature steps each: 95°C for 10 sec, 60°C for 15 sec, and 72°C for 20°C.

2.2.9 Protein extraction and analyses

2.2.9.1 Protein extraction and quantification

For preparing whole worm protein lysates, 50 males and 100 females were used. Worms of each gender were collected separately into 2 ml Eppendorf tubes, washed once with non-supplemented M199 medium, and then once with PBS. After that, 200 µl of 2 x SDS

sample buffer and 300 µl of 2 x SDS were added into each sample tube, respectively. Worm samples were subsequently sonicated 3 - 5 times with intermittent cooling on ice until complete disruption. Samples were denatured at 100°C for 10 min, centrifuged for 10 min at 13,000 g, and the supernatant was stored at -20°C. Protein samples were diluted from 1:300 to 1:500 in H_2O, and the average protein amount in each worm sample was analyzed densitometrically on a SDS-PAGE by comparison to different amounts of a BSA-standard. ImageJ was used for densitometric analyses (Schneider et al. 2012).

2.2.9.2 Western blot

For SDS-PAGE, 12 - 15% separating gels were used to separate proteins. The running condition was set as 80 V (25 mA for one gel and 50 mA for two gels) for the stacking gel and 120 V for the separating gel. After that, the gel and PVDF membrane (0.2 mm) were soaked in pre-cooled transfer blot buffer for at least 10 and 3 min, respectively. Tank blotting was performed at RT with ice-pads on the side of the blotting tank, with 120 V and 400 mA for 1 h. After blotting, the membrane was briefly stained with 1 x Ponceau S Red (Sigma Aldrich) staining solution to check blotting efficiency and was used to cut the membrane into pieces according to proteins of different molecular weight (MW) sizes. The transfer membrane was then gently rinsed several times with dH_2O to remove the Ponceau S stain.

For blocking, the PVDF membrane was incubated with 5% non-fat dry milk in 1x TBST as blocking solution at RT for 1 h on a shaker. A SmHSP-70 antibody (Smp_106930; 1:20,000 diluted (Moser et al., 1990)) was used for determining similar amounts of protein in gels thus serving as an internal loading control for the western blot analyses. The membrane was incubated with the primary antibody (LC3B, 1:1,000) in the same blocking solution at 4°C o/n and then washed 3 x 15 min with TBST at RT. As a secondary antibody, membrane was incubated with HRP-conjugated Goat anti-Rabbit IgG antibody (1:10,000) at RT for 1 h with continuous shaking. Afterwards, a second washing step 3 x 15 min with TBST at RT was done, and as a final step, detection of western blot was performed using Enhanced Chemiluminescence. Protein sizes were monitored by a wide range protein ladder (GENE's protein ladder wide range ~ 6.5-270 kDa). Quantification of protein was performed by using Image J ® software (Fiji version 1.53 with gel analyzer plugin).

2.2.10 RNA interference in adult *S. mansoni*

In the present work, RNA interference (RNAi) experiments were performed on adult *S. mansoni* with the double-stranded RNA (dsRNA) using soaking technique (Ndegwa et al.

2007). The aim of the experiments was to reduce transcript levels of selected genes to investigate the consequences of this “transcript knock-down” approach at the molecular and morphological levels.

2.2.10.1 Synthesis of dsRNA

Synthesis of dsRNA for RNAi experiments on adult schistosomes was done using the "HiScribe T7 High Yield RNA Syntheis Kit" (New England BioLabs) according to the manufacturer’s instructions. PCR products with T7 promoter sequences at their 5' and 3' ends were generated by appropriate primer design, and the generated cDNA served as template for *in vitro* transcription. Following synthesis and column purification, dsRNA was precipitated at -20 °C o/n using pre-cooled 1:2 volume of 4 M LiCl and 2.5 x volume of 100% ethanol. Subsequently, the precipitated dsRNA was centrifuged at 12,000 g and 4°C for 15 min and the obtained pellet was washed with 75% ethanol. Following another centrifugation step (12,000 g and 4°C for 15 min), the pellet was dried and resuspended in nuclease-free water. The precipitated dsRNA was then checked for quantity on spectrophotometer and for quality on 1.5% agarose gel electrophoresis. The dsRNA was then stored at -20°C until further use.

2.2.10.2 Soaking of *S. mansoni*

For RNAi, ten couples were incubated in 6-well culture plates with 10 - 30 µg (2 - 6 µg/ml) dsRNA, which was added to 5 ml of M199 supplemented culture medium at 37 °C and 5% CO_2 in an incubator. Every 48 h, the medium and dsRNA were refreshed, and the worms were used after 1 - 3 weeks either for RNA isolation or fixed in AFA for morphological analyses at the microscopic level.

2.2.11 *In vitro*-treatment of *S. mansoni* with chemical compounds

Adult *S. mansoni* couples were transferred to 6-well culture plates containing 5 ml of fresh M199 supplemented medium immediately after perfusion and cultured with different concentrations of inhibitors or inducers at 37°C and 5% CO_2. The culture medium and the chemical compounds were changed after every 24 h. Couples incubated only with the DMSO served as controls.

2.2.12 Phenotypic analyses

Worm motility, pairing stability as well as egg production were monitored daily up to 96 h. Morphological effects on worms and newly laid eggs were assessed every 24 h using an inverted light microscope (Leica, Labovert) and images were obtained by using a digital

camera (SC30, Olympus) (Mughal et al. 2021b). Worm motility score was determined following recommendations by the WHO special programme for research and training in tropical disease (WHO-TDR) (Ramirez et al. 2007) and adapted according to new *in vitro* evaluation protocols (Keiser 2010). A motility score of 4 was assigned for hyperactive movements, score 3 for worms with normal movements, score 2 for reduced movements, score 1 for minimal and sporadic movements and score 0 for dead worms. The inhibitory concentration (IC50) for autophagy inhibitors were calculated from motility scores of treated-*S. mansoni* couples. Subsequently, treated worms (as well as untreated control worms) were fixed in AFA for morphological analyses.

2.2.13 Carmine-red staining of the *S. mansoni*

Adult *S. mansoni* were fixed in AFA at RT for at least 24 h before staining was done with carmine red solution for 30 min. Decolorization was done in acidic ethanol (70% ethanol with 2.5% concentrated HCl) at RT for 20 min on a shaker with changes of the solution every 5 min. This was followed by dehydration of the samples in an ascending alcohol series 70%, 90%, 100%; 5 min each. At the final step, worms were finally fixed and mounted on slides with Canada balsam mixed in xylene (1:1) (Beckmann et al. 2010a).

2.2.14 Confocal Laser Scanning Microscopy (CLSM)

Morphological inspections of carmine-red stained schistosomes were performed with a Leica confocal laser scanning microscope (TSC SP5) in reflection mode with argon laser excitation of 20% at 488 nm and a 470 nm long pass filter for detection. The background and thickness of optical sections were defined by setting the pinhole size to airy unit 1.

2.2.15 Statistical analysis

Statistically significant differences of the obtained data were performed using GraphPad Prism v.5.01 and v.8.01. A two-way ANOVA with Tukey's multiple comparison test was used for monitoring pairing stability, worm motility and egg production of the different groups. One-way ANOVA with Tukey's multiple comparison test was used for other experiments, unless otherwise stated. Values of $P \leq 0.05$ were considered as statistically significant. Error bars are representative of the mean ± SEM of at least three independent experiments.

3 PUBLISHED RESULTS

3.1 First insights into the autophagy machinery

3.1.1 Autophagy scheme in *S. mansoni*

To provide an overview of major autophagy-related genes and their involvement in the various steps of autophagy, the following schematic illustration shows autophagy genes of *S. mansoni* identified and investigated in my study as well as chemical inducer and inhibitors that were used to modulate schistosome autophagy *in vitro* (Figure 3.1).

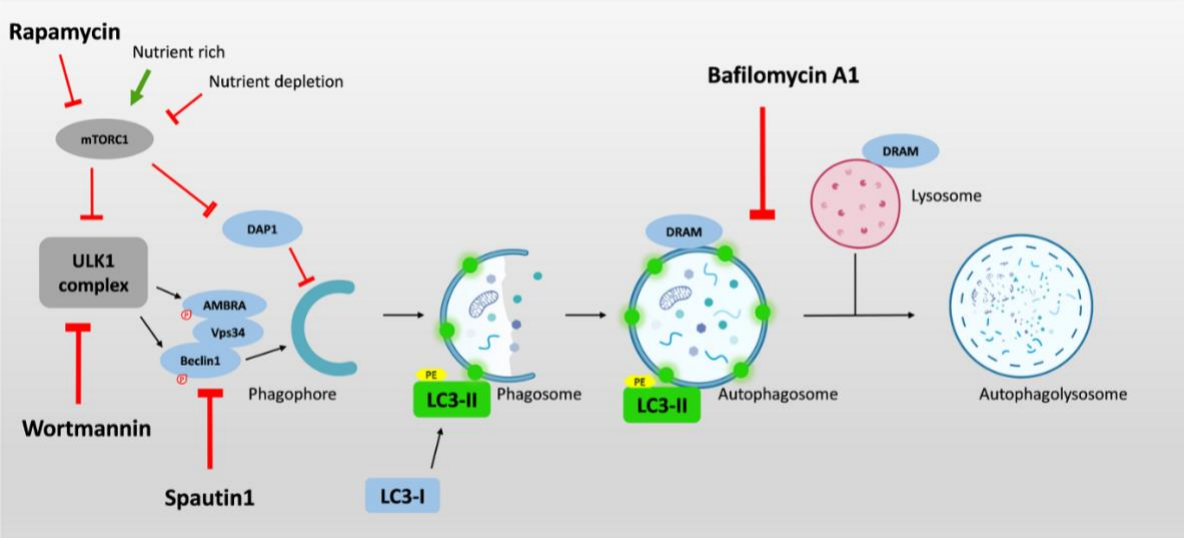

Figure 3.1: Schematic illustration of the autophagy pathway and identified orthologs in *S. mansoni*. The activation of autophagic protein complexes forms the phagophore. Under the action of several protein complexes, the phagophore continues to elongate and mediates the conversion of LC3-I into LC3-II by membrane conjugation of phosphatidylethanolamine (PE). After recruiting of cellular waste, the outer membrane closes to form an autophagosome, which after fusion with a lysosome forms the autophagolysosome. This complete process leads to the degradation of cellular waste and the inner membrane. In my study, orthologs shown in blue were identified and investigated, orthologs shown in grey are still unknown in *S. mansoni*. Autophagy inhibitors employed in this study (wortmannin, spautin-1, and BA1) are indicated as well as their target stages. Green arrows: activation; red lines: inhibition.

3.1.2 Identification of autophagy gene orthologs in *S. mansoni*

To get a first insight for orthologs of autophagy genes in *S. mansoni*, BLASTp search was performed based on known autophagy genes in *H. sapiens* using the schistosome database

WormBase Parasite and GeneDB (Logan-Klumpler et al. 2012; Howe et al. 2017). In *S. mansoni*, I identified: ambra1, beclin, dap1, dram, vps34 and two orthologs of LC3 (named as LC3.1 and LC3.2 in Table 3.1).

Table 3.1: Accession numbers of orthologs of model organisms and autophagy genes identified in *S. mansoni*. E-values obtained for the schistosome orthologs refer to their human counterparts.

Gene	*Schistosoma mansoni*	Homology E-value*	*Homo sapiens*	*Mus musculus*	*Drosophila melanogaster*	*Caenorhabditis elegans*
Beclin	Smp_048990.1	3.3e-40	NP_001300927.1	NP_001346748.1	NP_651209.1	NP_500844.1
Ambra1	Smp_156350.1	4.7e-15	NP_001354397.1	NP_766257.3	NP_001285857.1	NP_001021320.1
Vps34	Smp_128130.1	2.1e-51	NP_001294949.1	NP_852079.2	NP_477133.1	NP_001359780.1
DRAM	Smp_006750.2	2.7e-10	NP_060840.2	NP_082154.2	NP_569979.1	NP_510541.1
DAP	Smp_023840.1	0.032	NP_001017920.2	NP_666169.1	NP_610676.2	NP_492102.1
LC3B.1	Smp_073790.1	0.00049	NP_073729.1	NP_080436.1	NP_727447.1	NP_495277.1
LC3B.2	Smp_087940.2	0.0018	NP_073729.1	NP_080436.1	NP_727447.1	NP_495277.1

* Determined by WormBase Parasite BLASTP

After getting sequences of autophagy orthologs, the presence of conserved protein domains was investigated by SMART analyses (Figure 3.2). The identity and similarity index of the autophagy orthologs were confirmed by analyses of multiple sequence alignment with respective autophagy protein orthologs of other model species (Supplementary Figure S1).

Beclin

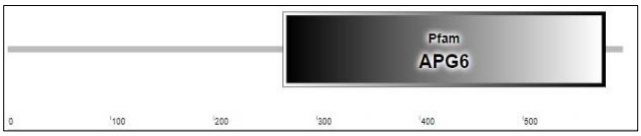

Vps34

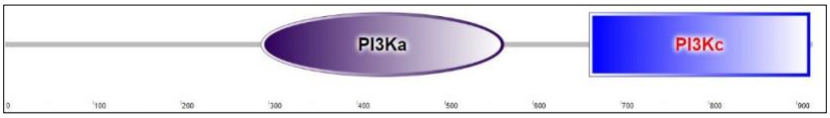

Ambra1

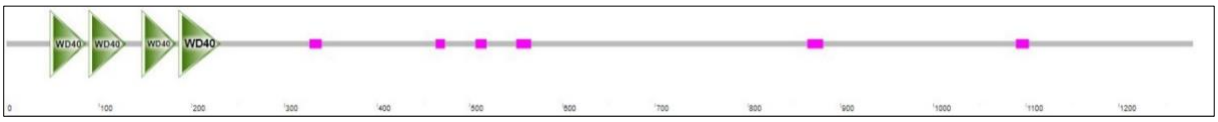

DRAM

DAP

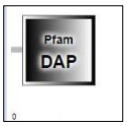

LC3.1

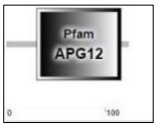

LC3.2

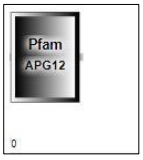

Figure 3.2: SMART analyses of amino acid sequence of the autophagy genes of *S. mansoni*. Accession numbers (Table 3.1) were confirmed the presence of conserved domains.

3.1.3 Identification of suitable reference gene for qRT-PCR analyses

As candidate reference gene for relative quantification of the qRT-qPCR data obtained in further experiments, Smletm1 (Smp_065110), encoding a LETM1 and EF hand domain-containing protein-1, was used (Haeberlein et al. 2019). Among four pre-selected candidate reference genes evaluated (Table 3.2), I found Sm*letm1* as the most stably expressed gene according to NormFinder analysis, which included male and female samples collected at different time points (t = d0, t = d1, t = d2, t = d4, t = d8, t = d12) during a 12 d *in vitro* culture period (Figure 3.3).

Table 3.2: List of four pre-selected candidate reference genes to analyze gene expression in *S. mansoni* males and females.

Gene	*Schistosoma mansoni* ID	Full name
Proteosome	Smp_073410	Proteosome subunit beta type 7
Phosphatase	Smp_166290	Serine/threonine-protein phosphatase 2A activator isoform b
Map3k9	Smp_176580	Mitogen-activated protein kinase kinase kinase 9
LETM1	Smp_065110	LETM1 and EF-hand domain-containing protein 1, mitochondrial

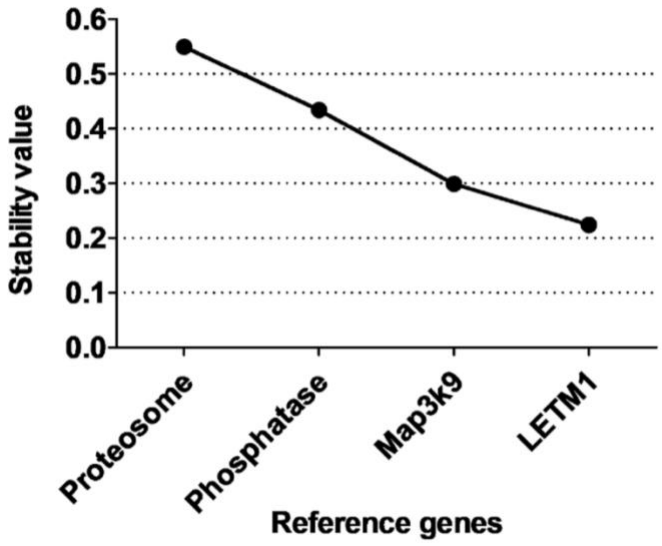

Figure 3.3: Ranking of expression stability values of four candidate reference genes between *S. mansoni* male and female worms. Stability values of gene expression were obtained by qRT-PCR and subsequent NormFinder analyses (Vandesompele et al. 2002). A low stability value of a candidate reference gene represents less variation and, therefore, indicates a more stable gene expression among *in vitro*-cultured male and female *S. mansoni*.

3.1.4 Sex-dependent transcription of autophagy genes

In order to address the question whether autophagy gene transcription differs among male and female worms, qRT-PCR analyses was performed. To this end, we compared the relative transcript levels of the selected genes between male and female worms at day 0, quickly

after perfusion from the final host. The majority of the seven autophagy genes showed similar transcription levels among males and females, except DAP1 and DRAM. DAP1 was significantly upregulated, while the opposite was true for DRAM, it showed significant downregulation in females compared to males (Figure 3.4).

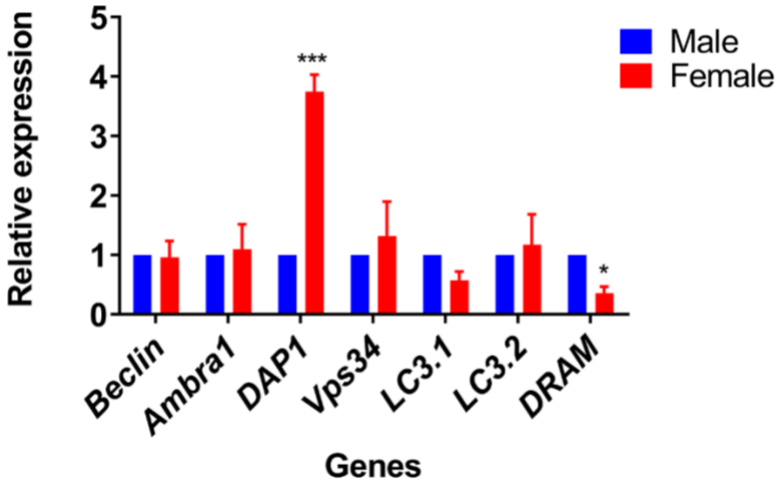

Figure 3.4: Relative transcript levels of autophagy genes in *S. mansoni* male and female worms collected immediately after perfusion. Data were normalized against Sm*letm1* as a reference gene, and expression levels were quantified relative to male samples by qRT-PCR analyzes. Error bars represent mean±SEM (n = 3; * = $p < 0.05$; *** = $p < 0.001$).

3.1.5 Effect of *in vitro* culture on transcript levels of autophagy-related genes

Modulation of the expression of autophagy-related genes is known to be influenced by stress and starvation (Karim et al. 2014). In my study, after perfusion the worms were transferred from the *in vivo* scenario (portal vein of the final host) to an artificial *in vitro* culture condition that could exert some influence on autophagy and its associated gene expression. Therefore, I analyzed the effect of the *in vitro* culture on the transcript levels of the seven selected autophagy genes. To this end, *S. mansoni* couples were cultured for up to 12 d. At different time points, couples were separated in male and female samples for qRT-PCR analyses (t = d 0, t = d 1, t = d 2, t = d 4, t = d 8, t = d 12). Overall, the transcript level of autophagy genes was similar in both sexes, with a common trend of decreased transcription for several genes after a prolonged *in vitro* culture of 12 d. Exceptionally, the transcript level of DAP1 in females showed a two-fold increase after 1 d, and then shifted to a continuously decreased level from d 4 on (Figure 3.5).

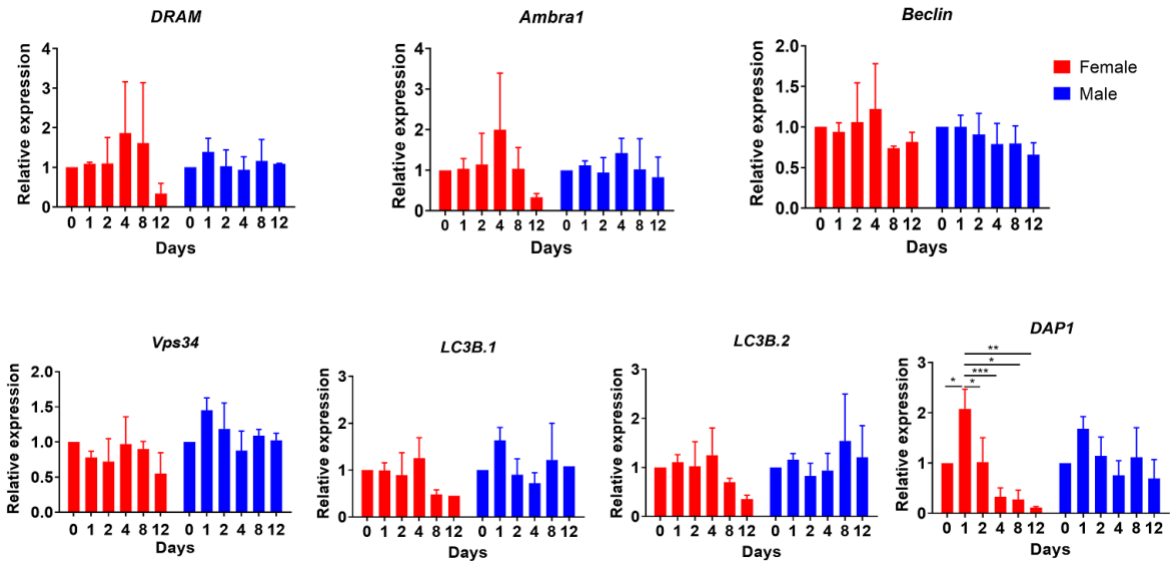

Figure 3.5: Influence of the *in vitro* culture on the relative transcript levels of autophagy genes in *S. mansoni* male and female worms. Relative expression of autophagy genes was determined for up to 12 d in *in vitro*-cultured male and female worms using qRT-PCR. Error bars represent mean±SEM (n = 3; * = $p < 0.05$; *** = $p < 0.001$).

3.1.6 Effect of the *in vitro* culture on protein expression of LC3

At the post-transcriptional level, I observed an effect of the *in vitro* culture on the modulation of autophagy by immunoblot analysis of LC3B, a key player for regulating autophagy. Following *in vitro* culture, protein samples of male and female worms were prepared at different time points (t = d 0, t = d 1, t = d 3). Compared to the constitutively and sex-independently expressed HSP70 protein I (Neumann et al. 1993; Lu et al. 2016), SmLC3B was found to be expressed in both sexes, but comparatively less in females compared to males (Figure 3.6). During active autophagy, the cytosolic form of LC3B (LC3B-I) is conjugated to phosphatidylethanolamine and thereby converted to LC3B-II, which is recruited to autophagosomal membranes (Tanida et al. 2008). Both, SmLC3B-I and SmLC3B-II protein levels decreased already after 1 d of *in vitro* culture compared to uncultured worms (d 0). This decrease was more pronounced in females compared to males, peaking in a barely detectable amount of both, the unconverted and converted LC3 form at day 3 (Figure 3.6).

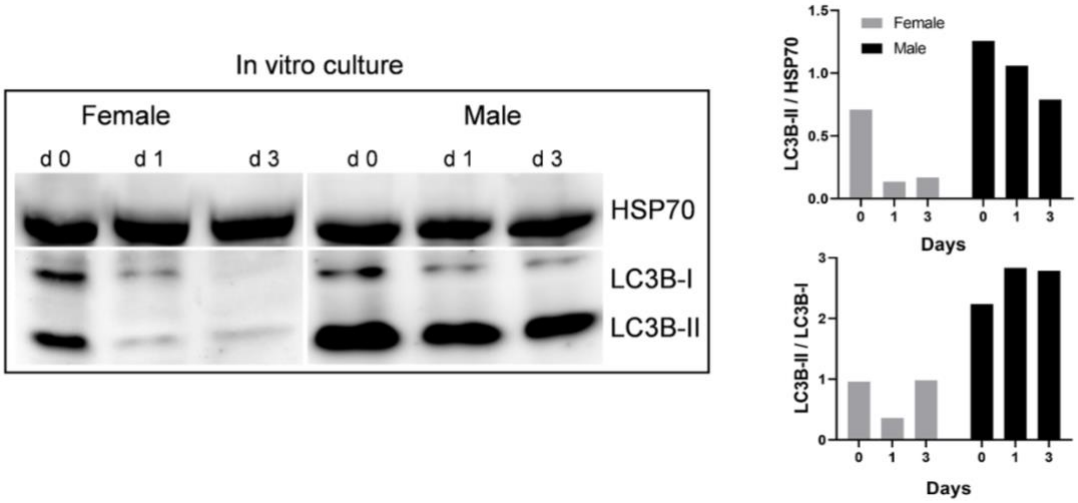

Figure 3.6: Influence of the *in vitro* culture on the modulation of autophagy protein LC3B. Male and female protein lysates targeting autophagy protein LC3B and a reference protein HSP70 were analysed by western blot. LC3B-I and its converted form LC3B-II can be distinguished as two separate bands. Graphs show the quantitative densitometric ratio of LC3B-II / HSP70 and LC3B-II / LC3B-I band intensities.

Taken together, the results showed that *in vitro* culture modulates the expression of autophagy genes in *S. mansoni* at the transcriptional as well as post-transcriptional levels.

3.1.7 Effect of chemical inhibitor and inducer on autophagy in *S. mansoni*

Next step, I investigated the modulation of autophagy in *S. mansoni* under the influence of chemical inducers or inhibitors of autophagy. Among these were BA1 (an autophagy inhibitor) and rapamycin (an autophagy inducer). *S. mansoni* couples were treated for 24 h with these chemical compounds, and after their separation protein collected from males and females for immunoblot analyses of LC3.

Rapamycin blocks the activation of the mammalian target of rapamycin (mTOR), which is an inhibitor of autophagy (Ravikumar et al. 2004). I observed a clear increase of LC3B expression in females treated with 1 µM rapamycin, based on the increased band intensities of both LC3B-I and LC3B-II compared to the untreated control. Interestingly, 5 µM of rapamycin increased only LC3B-II protein, but not LC3B-I. This may represent a complete conversion of LC3B-I into LC3B-II in females treated with 5 µM of rapamycin. Similarly for male worms treated with 5 µM of rapamycin, the ratio of LC3B-II/LC3B-I was higher compared to the control (untreated worms) (Figure 3.7).

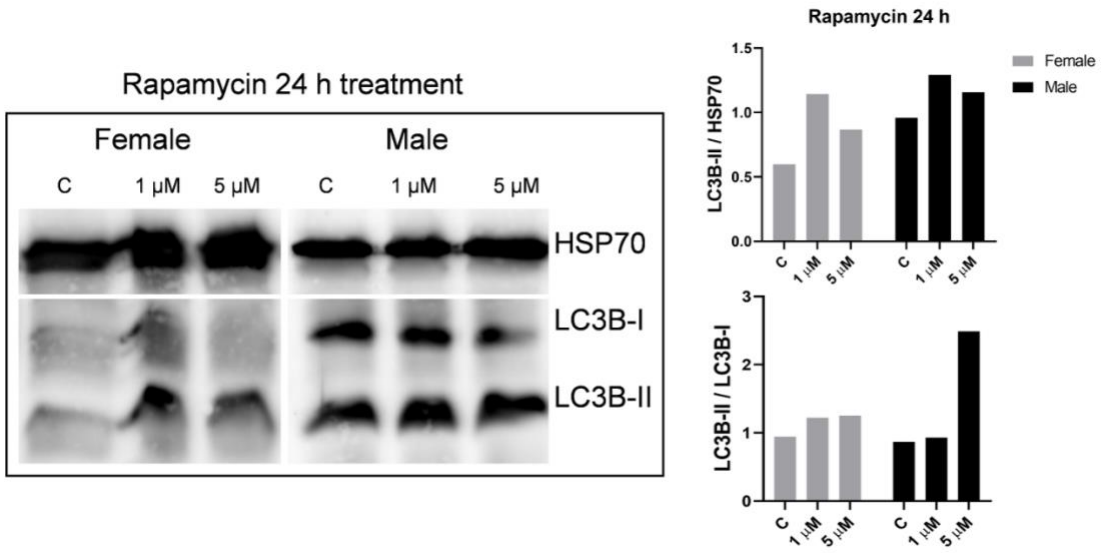

Figure 3.7: Immunoblot analyses of LC3B expression in rapamycin-treated *S. mansoni* male and female worms. Rapamycin at concentrations of 1 µM and 5 µM was used to treat worms *in vitro* for 24 h, and DMSO-treated worms served as control (C). HSP70 protein was used as loading control. LC3B-I and its converted form LC3B-II can be distinguished as two separate bands. Graphs show the quantitative densitometric ratio of LC3B-II / HSP70 and LC3B-II / LC3B-I band intensities.

BA1 is known to interfere with autophagy by inhibiting lysosome acidification and fusion of autophagosome and lysosome (Mauvezin and Neufeld 2015). At concentrations of 0.5 µM and 2.5 µM, the level of the LC3B-I form increased more than the LC3B-II level in both female and male samples compared to the untreated control (Figure 3.8).

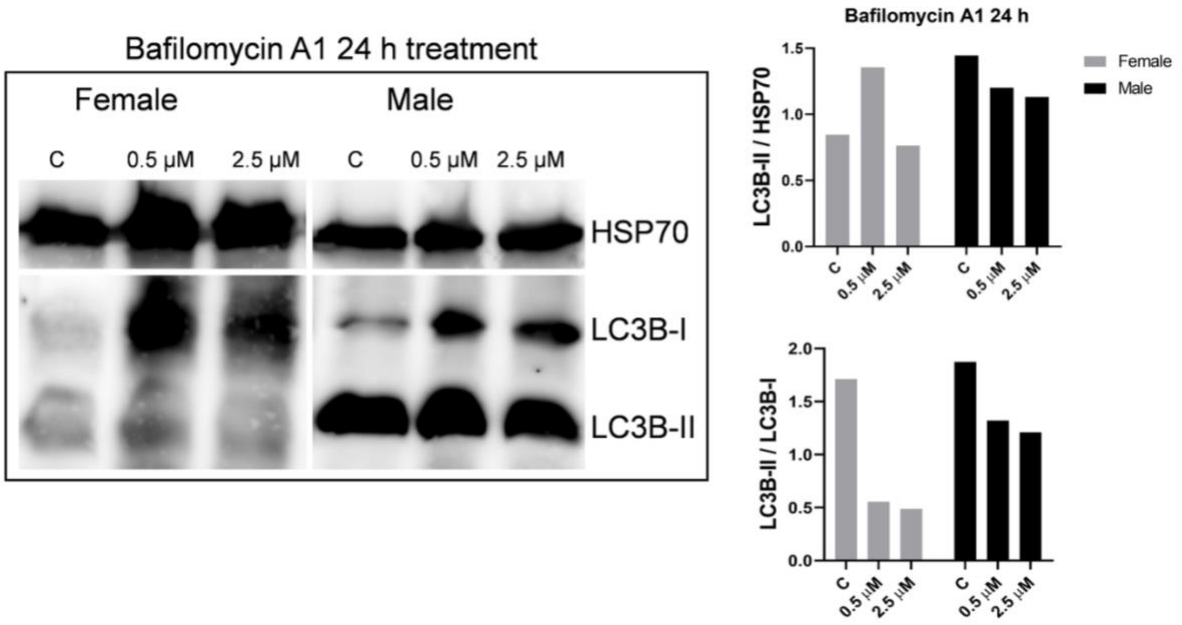

Figure 3.8: Immunoblot analyses of LC3B expression in bafilomycin A1-treated *S. mansoni* male and female worms. Bafilomycin A1 at concentrations of 0.5 µM and 2.5 µM was used to treat worms *in vitro* for 24 h, and DMSO-treated worms served as control (C). HSP70 protein was used as loading control. LC3B-I and its converted form LC3B-II can be distinguished as two separate bands. Graphs show the quantitative densitometric ratio of LC3B-II / HSP70 and LC3B-II / LC3B-I band intensities.

Overall, the results showed that autophagic flux depicted by LC3B protein levels in *S. mansoni* can be manipulated by chemical agents targeting autophagy. In general, female worms appeared to be more sensitive to chemical treatment as male worms.

3.1.8 Impairment of worm viability by autophagy inhibitors

As autophagy is vital for regulating cellular homeostasis in eukaryotes, I hypothesized that autophagy plays a similar role in *S. mansoni*. Therefore, treatment with autophagy inhibitors might influence worm viability and reproduction. In order to test this hypothesis, I treated *S. mansoni* couples with various concentrations of BA1 ranging from 0.1 to 2.5 µM *in vitro* for 72 h, and monitored effects on worm motility, pairing stability as well as egg production daily. My results showed dose-dependent effects of BA1 for all three parameters (Figure 3.9A-C). Pairing stability and worm motility drastically decreased after 24 h, and couples started to separate with reduced motility after treatment with 0.5 µM of BA1, while all couples were separated and egg production was stopped with 2.5 µM.

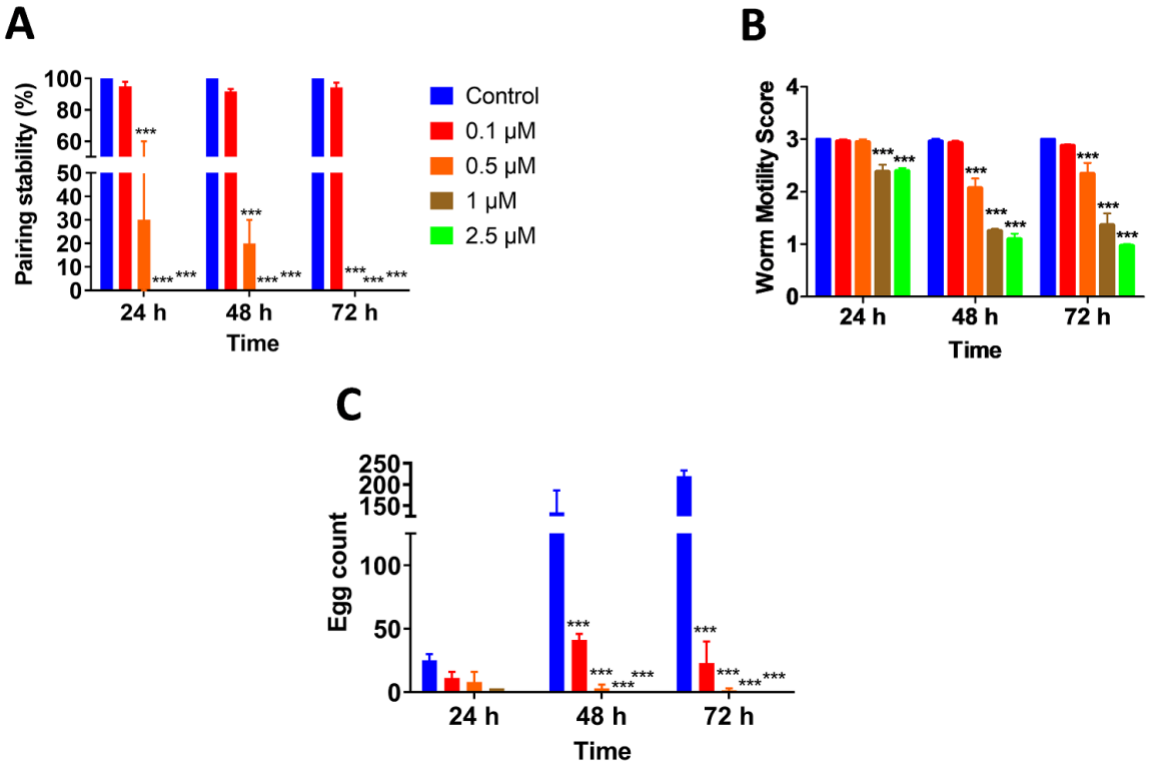

Figure 3.9: Influence of bafilomycin A1 on *S. mansoni* worm viability. Varying concentrations of bafilomycin A1 0.1-2.5 µM induced dose-dependent response of worms on pairing stability (A), worm motility score (B), and egg production (C) being examined at 24-72 h of treatment. Error bars represent mean±SEM (n = 3; *** = $p < 0.001$).

Phenotypically, bulb-like protrusions were eventually observed at the body surface of male worms, and body constriction were noticed in females after 72 h treatment with 0.5 µM BA1 (Figure 3.10B). At 2.5 µM, these phenotypic alterations were more obvious in male and female worms (Figure 3.10C). An analysis of dose-response curve to worm motility exhibited an IC50 of 0.8 µM (Figure 3.10D).

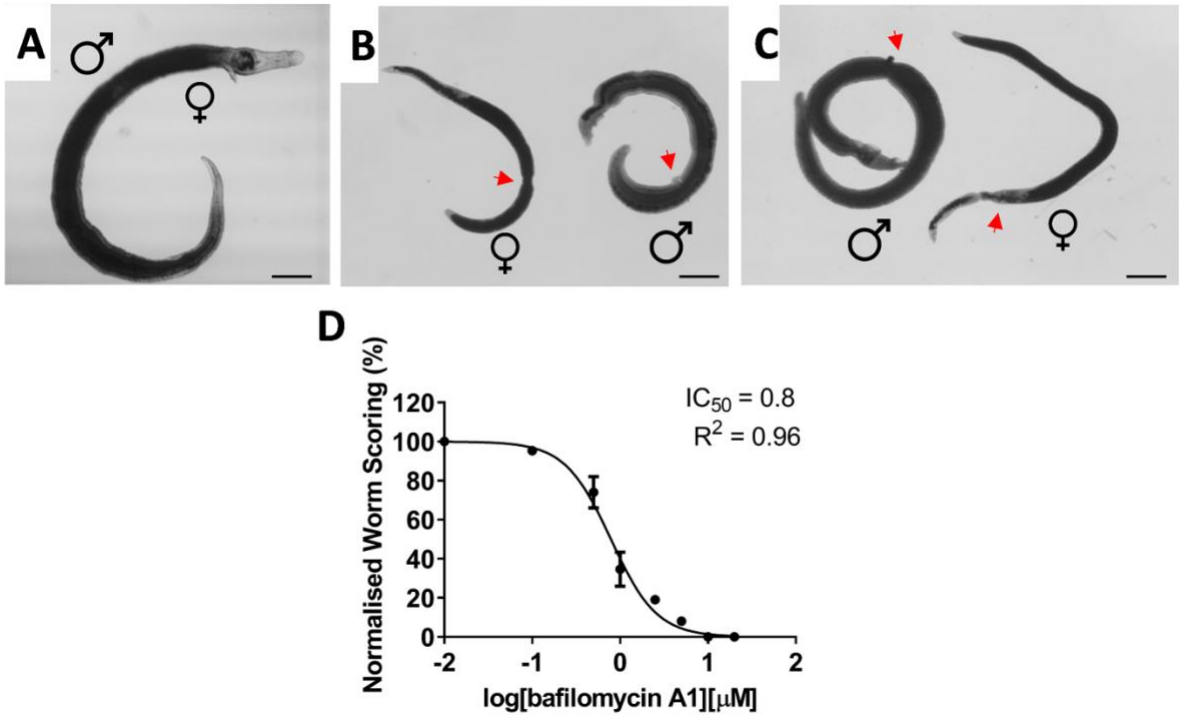

Figure 3.10: Phenotypic changes of adult *S. mansoni* worms under the influence of bafilomycin A1. Phenotypic changes of males and females treated for 72 h with 0.5 µM (B), 2.5 µM (C) of bafilomycin A1 and control group (A). Arrows represent the body protrusions in male worms and body constrictions in female worms. The graph shows the dose-dependent response curve (D) of worms treated with bafilomycin A1 for 72 h with calculated IC50 values. (n = 3; Scale bars = 100 µm)

In order to test another early phase inhibitor, wortmannin, I used concentrations ranging from 50 to 200 µM for 96 h *in vitro*. The effect of the two highest concentrations was drastic on all analyzed parameters, worm motility score, pairing stability, and egg production. However, an initial increase in worm motility was observed with the first 24 h of treatment with each wortmannin concentration (Figure 3.11A-C).

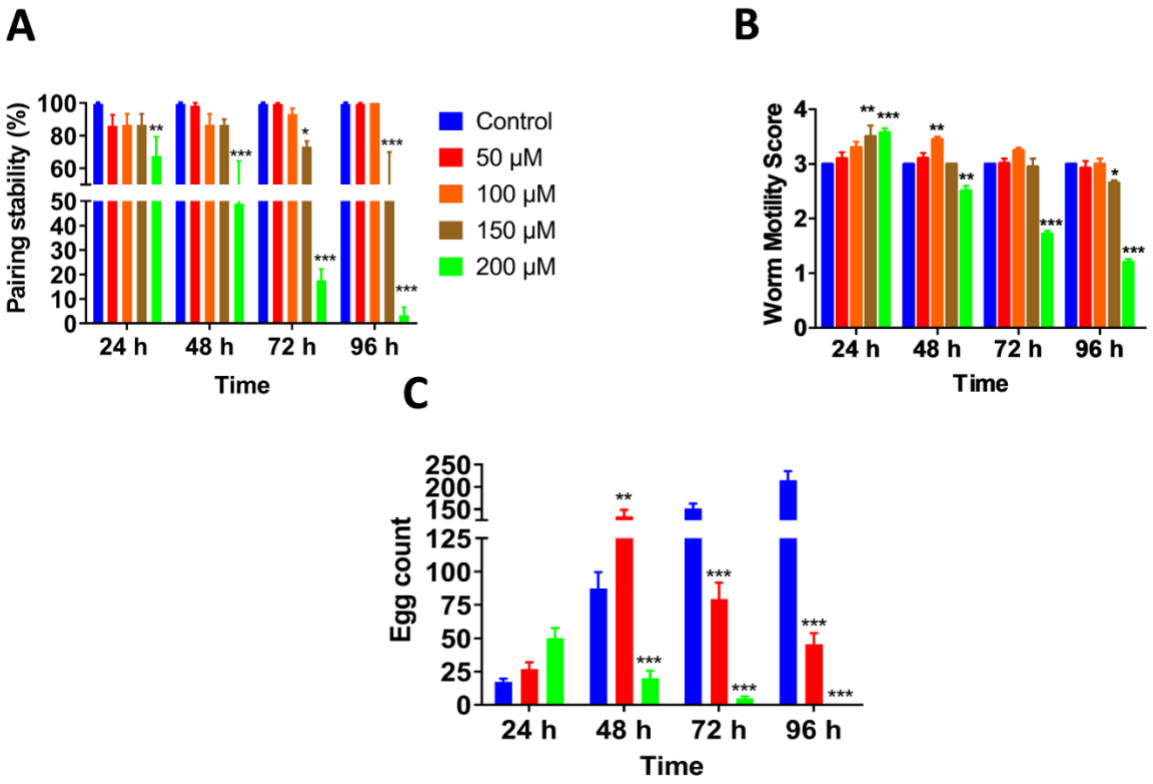

Figure 3.11: Influence of wortmannin on *S. mansoni* worm viability *in vitro*. Treatment of worms with varying concentrations of wortmannin ranging 50-200 µM induced drastic effects on pairing stability (A), worm motility score (B), and egg production (C) being examined at 24-96 h of treatment. Error bars represent mean±SEM (n = 3; * = $p < 0.05$; ** = $p < 0.01$; *** = $p < 0.001$).

Egg morphology was affected with obvious malformation of eggs showing reduced size and lack of vitelline cells and oocytes upon treatment with 50 µM (Figure 3.12B) wortmannin, while egg produced by control couples showed a normal morphology, as expected (Figure 3.12A). When couples were treated with 200 µM, I observed no eggs. Instead, cluster of vitellocytes and oocytes occurred in the culture medium (Figure 3.12C,D) which failed to fuse into well-formed eggs. Wortmannin induced a reduction in motility with an IC50 of 152.7 µM (Figure 3.12E).

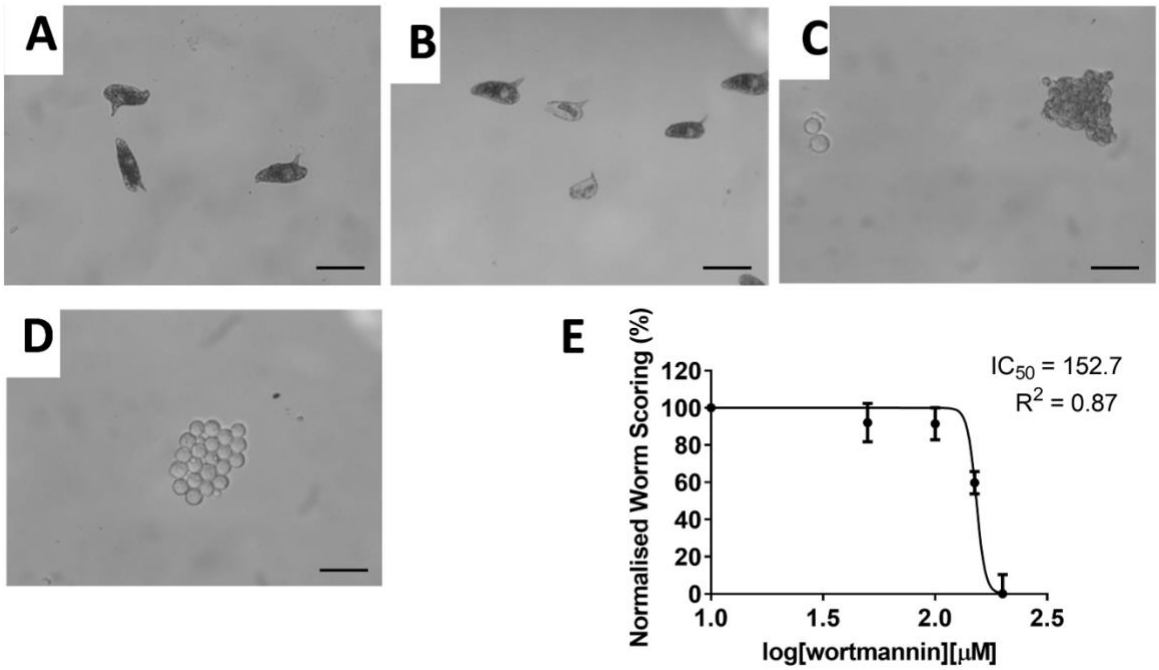

Figure 3.12: Phenotypic changes of *S. mansoni* eggs under the influence of wortmannin treatment *in vitro* for 96 h. Compared to normal eggs produced from control worms (A), eggs produced by treated couples (50 µM, B) showed reduced size. Accumulation of vitellocytes (C) and oocytes (D) was observed upon treatment of worms with 200 µM wortmannin for 96 h. The graph shows the dose-dependent response curve (E) of worms treated with wortmannin for 96 h with calculated IC50 values. Error bars represent mean±SEM (n = 3; Scale bars = 100 µm)

In order to study another early phase inhibitor of autophagy, spautin-1 was tested with different concentrations from 50 to 200 µM *in vitro* for 96 h. This treatment caused a complete loss of pairing stability and a significant reduction in worm motility and egg production (Figure 3.13A-C). Similar to wortmannin, also spautin-1 caused a slight increase in worm motility at all concentrations used during the first 24 h (Figure 3.13B).

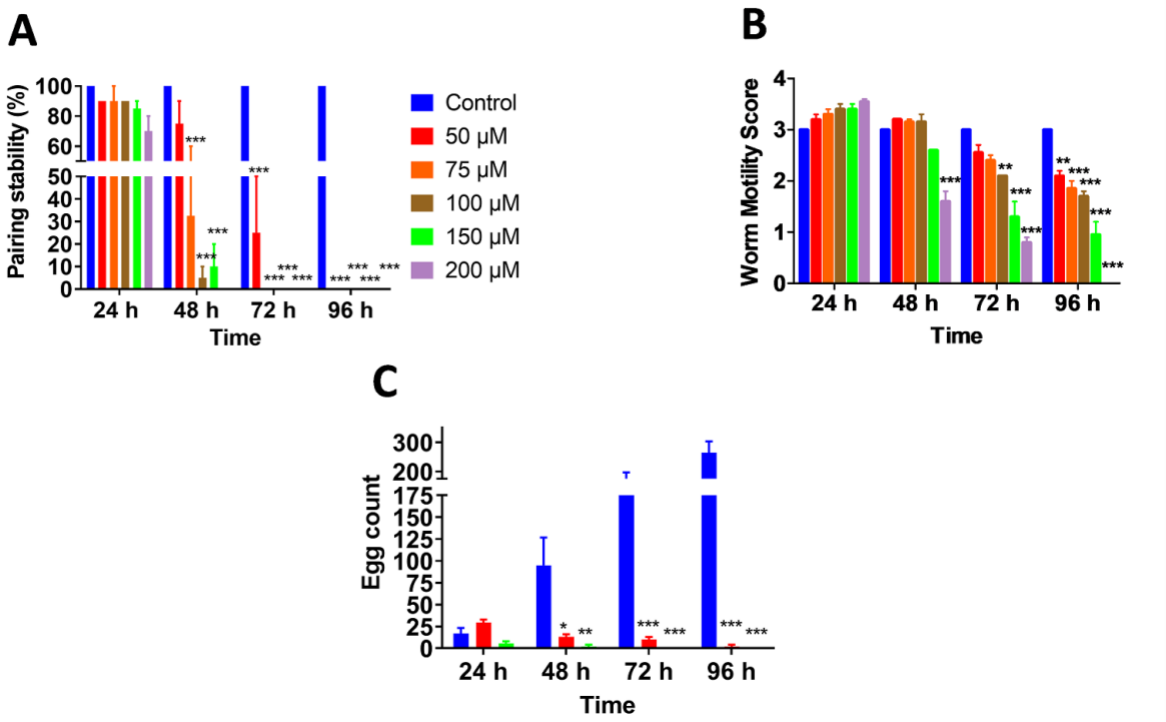

Figure 3.13: Influence of spatutin-1 on *S. mansoni* worm viability *in vitro*. Treatment of worms with different concentrations of spautin-1 (50 - 200 µM) for 96 h induced drastic effects on pairing stability (A), worm motility (B), and egg production (C). Error bars represent mean±SEM (n = 3; * = $p < 0.05$; ** = $p < 0.01$; *** = $p < 0.001$).

Phenotypically, bulges were observed at the body surface of male and female worms treated with 200 µM spautin-1 as compared to control worms (Figure 3.14A-C). With respect to worm motility, spautin-1 exhibited an IC50 of 94.9 µM (Figure 3.14D), and showed stronger effects on *S. mansoni* than wortmannin.

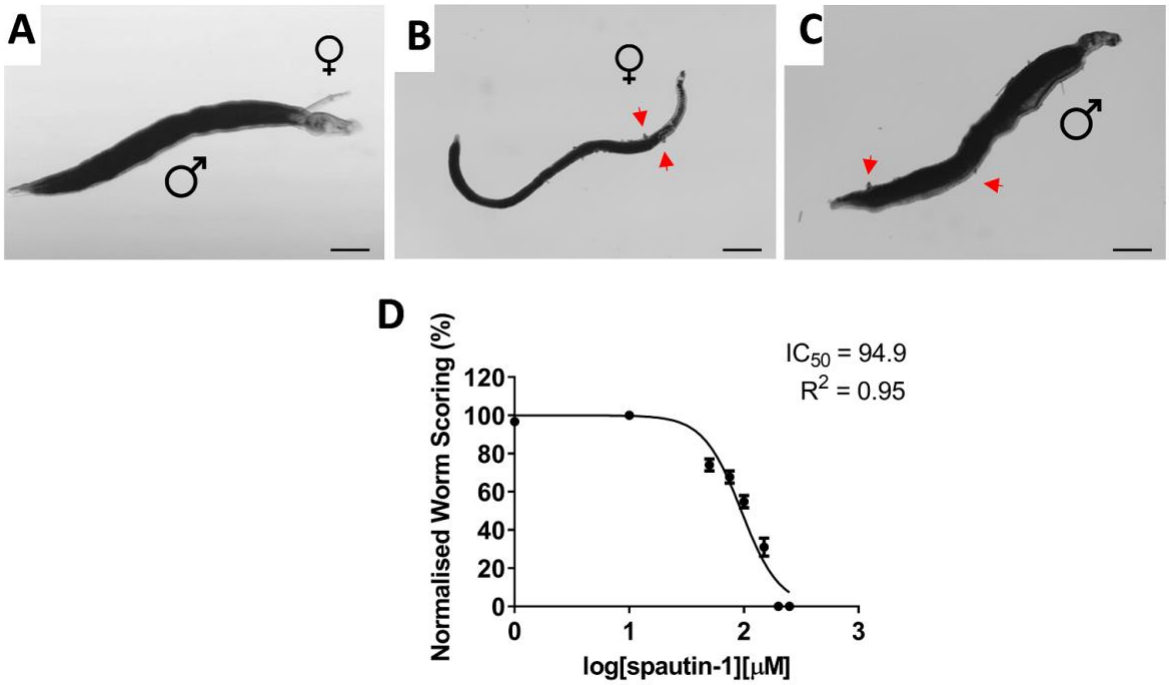

Figure 3.14: Phenotypic changes of *S. mansoni* worms under the influence of spautin-1 *in vitro* for 96 h. Compared to the control (A), bulges appeared along the tegumental surface of female (B) and male (C) worms after treatment with 200 µM of spautin-1 for 96 h. The graph shows the dose-dependent response curve (E) of worms treated with spautin-1 for 96 h with calculated IC50 values. Error bars represent mean±SEM (n = 3; Scale bars = 100 µm).

3.1.9 Autophagy inhibitors cause intestinal and gonadal change in *S. mansoni*

In order to investigate the morphological effects of modulating autophagy by inhibitors, I performed CLSM of *S. mansoni* couples treated with either BA1 (2.5 µM), wortmannin (200 µM), or spautin-1 (200 µM) for 72-96 h. BA1 and spautin-1 caused severe dilatations of the gut lumen (Figure 3.15) compared to control worms. Wortmannin caused the degradation of gastrodermis and the formation of tissue aggregates within gut lumen of females. These phenotypic changes were found only in female intestinal tissue, but not in males.

In addition to the intestinal morphology, gonads of the male (testes) and female (vitellarium and ovary) were also drastically affected by autophagy inhibitors. Compared to the vitellarium of control group females (untreated), fewer mature vitellocytes were found in the vitellarium of BA1-, wortmannin-, or spautin-1-treated females (Figure 3.15).

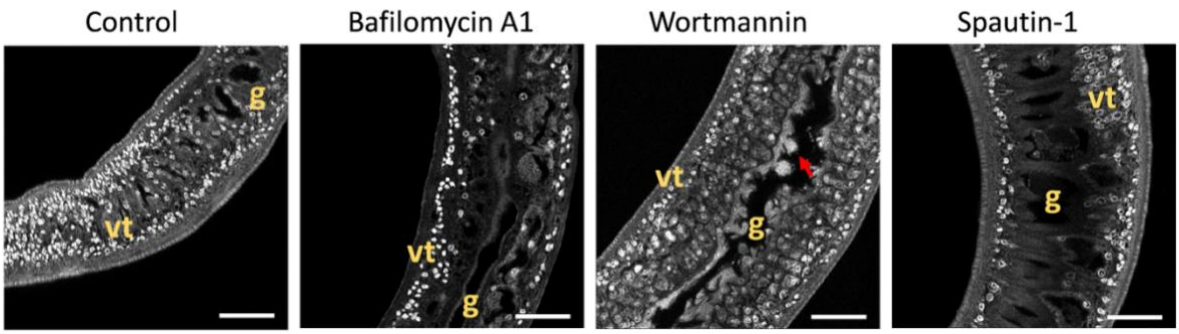

Figure 3.15: Morphologic changes in the female intestinal tract and the vitellarium following treatment with autophagy inhibitors. CLSM analyses of female worms treated with bafilomycin A1 (2.5 µM) for 72 h, and wortmannin (200 µM) or spautin-1 (200 µM) for 96 h. Red arrows indicate the presence of tissue aggregate in the gut lumen (g = gut; vt = vitellarium; Scale bars: 50 µm).

In control females, the ovary represents a typical oval structure containing small immature oocytes in the anterior part as well as large mature oocytes with a visible nucleolus in the posterior part. On the contrary, BA1-treated females exhibited partially degraded ovaries, and intact nucleoli were absent from mature oocytes, revealing intracellular degradation. Wortmannin treatment completely deformed the ovary structure and disorganized the distribution of immature and mature oocytes. Also, ovaries of spautin-1-treated females showed porous empty spaces within the ovary, a complete loss of immature oocytes, and a reduced number of mature oocytes (Figure 3.16).

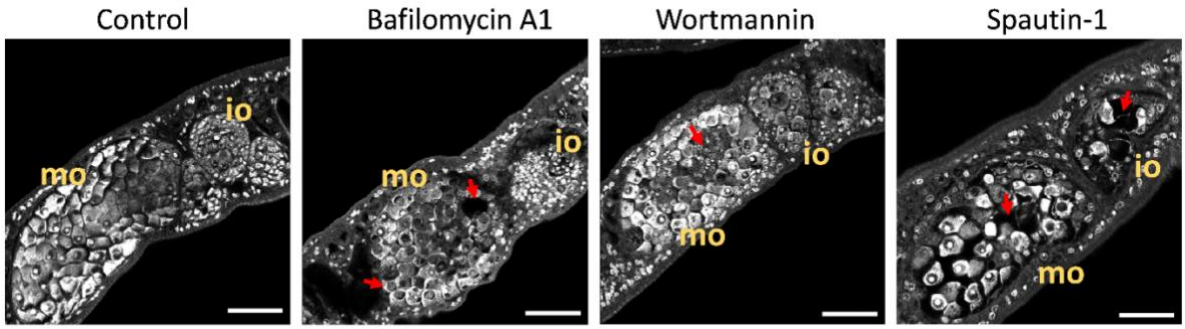

Figure 3.16: Morphologic changes in ovaries of *S. mansoni* females following treatment with autophagy inhibitors. CLSM analyses of female worms treated with bafilomycin A1 (2.5 µM) for 72 h, and wortmannin (200 µM) or spautin-1 (200 µM) for 96 h. Red arrows indicate the porous, disintegrated ovary area and the degradation of mature oocytes of bafilomycin A1-treated females. In wortmannin and spautin-1-treated females, the red arrow indicate porous

areas inside the ovary, and disintegrated, and disorganized oocytes compared to the normal ovary structure and normal oocytes of untreated females (control) (io = immature oocytes; mo = mature oocytes; Scale bars: 50 µm).

In untreated male worms, testes exhibit a typical lobular structure and an anterior seminal vesicle filled with mature spermatozoa. BA1-treated males exhibited disorganized testes lacking normal testicular lobes and with fewer spermatozoa in the seminal vesicle. Wortmannin caused an overall decrease in the number of testicular cells, disintegrated and porous testicular lobes, and few spermatozoa. Similar to ovaries, spautin-1 induced severe testicular disruption with empty spaces, reduced testicular cells and very few mature spermatozoa in the testes as well as empty seminal vesicles (Figure 3.17).

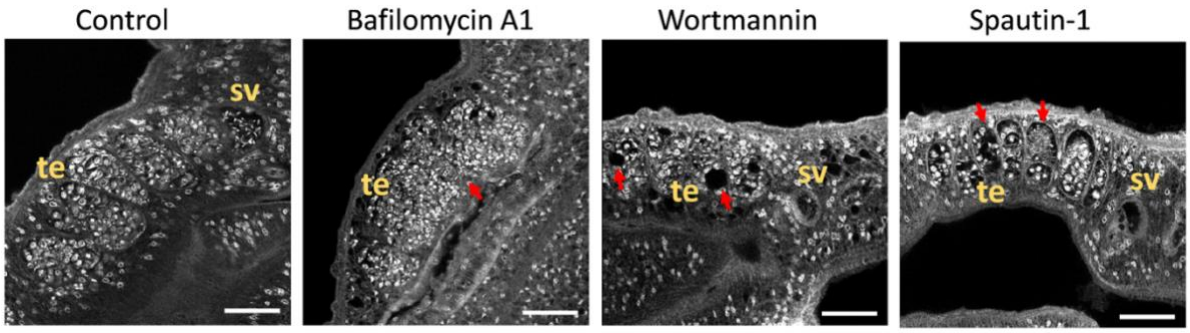

Figure 3.17: Morphologic changes in testes of *S. mansoni* males following treatment with autophagy inhibitors. CLSM analyses of male worms treated with bafilomycin A1 (2.5 µM) for 72 h, wortmannin (200 µM) and spautin-1 (200 µM) for 96 h. Red arrows indicate the disorganized testicular structure in bafilomycin A1-treated males and porous areas in tissues of wortmannin- and spautin-1-treated males compared to the normal testicular structure of untreated males (control) (sv = seminal vesical; te = testis; Scale bars: 50 µm).

3.2 Imatinib induces autophagy in *S. mansoni*

3.2.1 Effect of imatinib on LC3B

After the induction of autophagy, LC3B-I bound with phosphatidylethanolamine (PE) converts into LC3B-II and gets attach to the membranes of autophagosomes. Based on the LC3B immunoblotting assay, the amount of LC3B-II or the ratio between LC3B-II and LC3B-I usually correspond to the number of autophagosomes.

In order to determine the imatinib's response to modulation of autophagy, I analyzed the protein expression by LC3B immunoblotting after treatment of couples with 20 µM and 50 µM of imatinib for 24 h. My results of LC3B western blotting showed a clearly visible increase in LC3B expression in both sexes, can be seen as increased intensities of LC3B-I and LC3B-II bands as compared to control worms (Figure 3.18A).

Upon co-treatment of imatinib and BA1, the imatinib-induced LC3B protein expression was decreased by BA1 and showed LC3B protein expression level similar to that of control worms (Figure 3.18B). BA1, as a late phase autophagy inhibitor, is known to block the fusion process of autophagosomes and lysosomes. In principle, my results indicated that imatinib induce the autophagy marker LC3B, which was then blocked by the BA1.

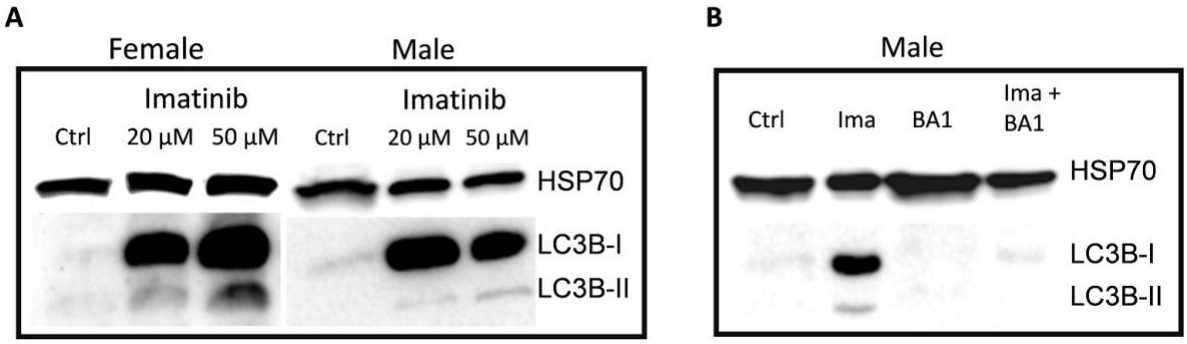

Figure 3.18: Influence of imatinib and/or bafilomycin A1 on the expression of LC3B protein in males and females of *S. mansoni*. After 24 h of drug treatment, protein lysates were used for immunoblotting of LC3B protein. HSP70 protein was used as loading control. LC3B-I and its converted form LC3B-II can be distinguished as two separate bands. LC3B-I and LC3B-II protein expression in males and females after 20 µM and 50 µM treatment of imatinib (A) compared to DMSO-treated worms as control group (Ctrl), and in males after 20 µM of imatinib (Ima), 0.1 µM of bafilomycin A1 (BA1) or co-treatment (Ima + BA1).

3.2.2 Phenotypic analyses of imatinib and/or BA1 treatment

As a next step, I investigated whether imatinib mediated induction of autophagy is needed for its anthelminthic efficacy. Towards this goal, I quantified the worm vitality, motility score and egg production after imatinib and/or BA1 single and double treatment.

Treatment of adult couples with 20 µM imatinib for 24 h caused 90% separation of couples and about 70% were detached from the petri dishes (Figure 3.19A,B). Despite significant decrease of pairing stability, egg production of imatinib-treated worms increased to three-fold as compared to control worms (Figure 3.19C). Couples treated with imatinib showed marked gut dilatations of female worms contrary to control worms (Figure 3.19D,E). After co-

treatment of 20 µM imatinib and 0.1 µM BA1 for 24 h, a similar extent of detachment of worms was noticed as for single imatinib treatment (Figure 2.19B). BA1 weakened the imatinib-caused phenotype in terms of pairing stability, egg production and gut dilatations. Upon co-treatment of imatinib and BA1, only 20% of the worm couples separated, imatinib-induced increase in egg production was less noticeable (Figure 3.19C) and significantly less number of females showed gut dilatations (Figure 3.19F,G).

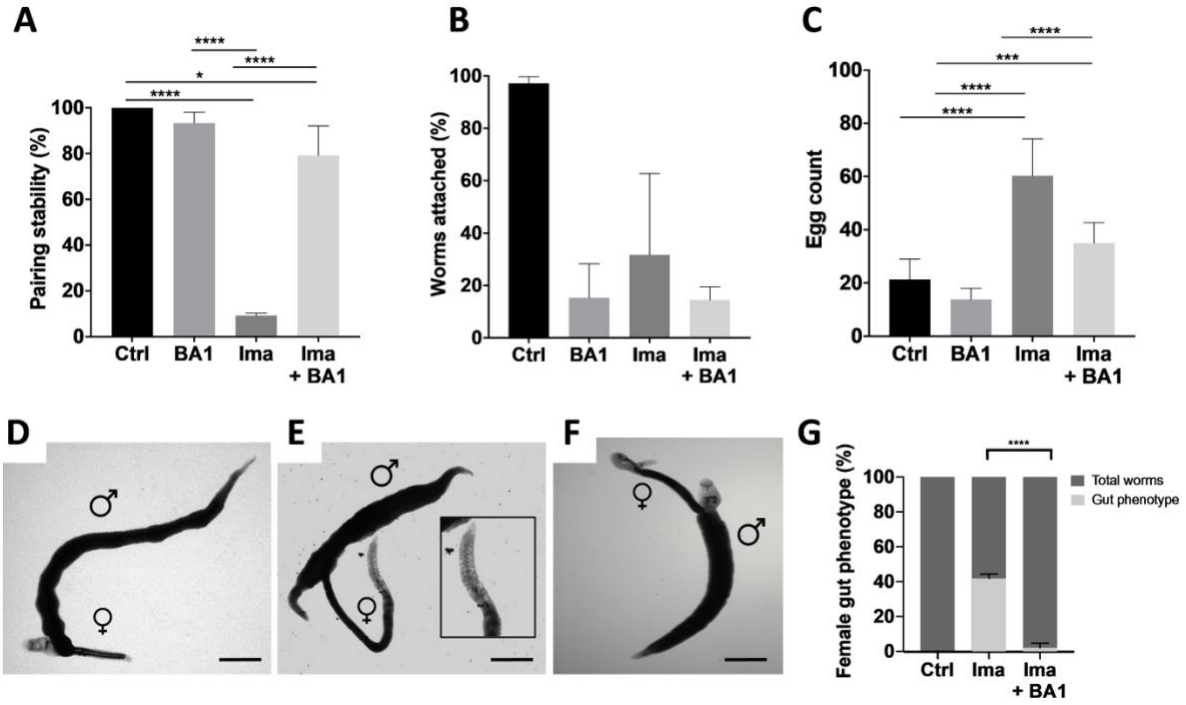

Figure 3.19: Influence of imatinib and/or bafilomycin A1 on the worm viability and reproduction of *S. mansoni*. Treatment of couples with either 20 µM of imatinib (Ima), 0.1 µM of bafilomycin A1 (BA1) or co-treatment (Ima + BA1). Co-treatment reversed the imatinib-caused effects on pairing stability (A), worm attachment (B) and egg production (C). Imatinib caused marked get dilatations in females (E) compared to DMSO-treated control group (D). Co-treatment prevented this phenotype of imatinib-induced gut dilatations (F) and graph represents the percentage of females observed with gut phenotype after imatinib and co-treatment and an un-paired t-test was used to analyze (G). Error bars represent mean±SEM (n = 3; * = $p < 0.05$; ** = $p < 0.01$; *** = $p < 0.001$; **** = $p < 0.001$; Scale bars: 100 µm).

3.2.3 CLSM analyses of intestinal morphology

To have detailed look at the intestinal phenotype, I analyzed the couples treated with imatinib, BA1, and imatinib and BA1 for 24 h by CLSM. The guts of DMSO-treated control exhibited a typical gastrodermis containing thick and continuous layer of syncytial cells

(Figure 3.20). Both male and female worms treated with 20 µM imatinib for 24 h showed extensive gut dilatations and gastrodermis appeared collapsed and disintegrated (Figure 3.20). More obviously in male worms, several disintegrated clusters of gastrodermal tissue were present within the gut lumen. Upon co-treatment of imatinib and BA1, the gut and gastrodermis didn't exhibit any changes which were caused by imatinib alone treatment, instead appeared similar to that of DMSO-treated control worms. The results of imatinib and BA1 co-treatment indicated that autophagy inhibition by BA1 diminished anti-schistosomal properties induced by imatinib.

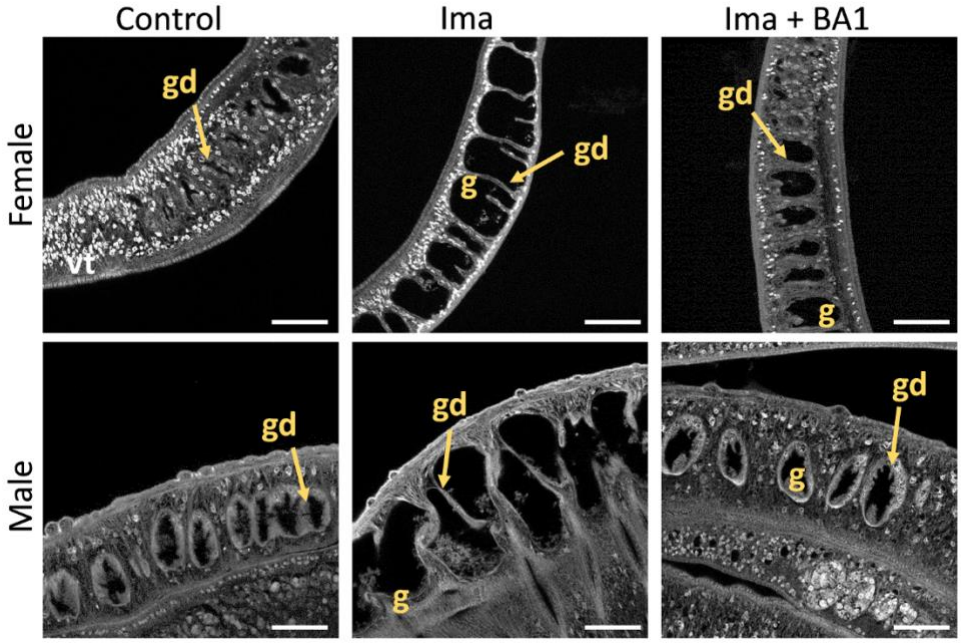

Figure 3.20: Confocal laser scanning microscopic analyses of Imatinib- and/or bafilomycin A1-treated *S. mansoni* on the intestinal morphology of males and females. Treatment of couples was performed for 24 h with either 20 µM of imatinib (Ima), 0.1 µM of bafilomycin A1 (BA1) or co-treatment (Ima + BA1). Co-treatment reversed the imatinib-induced effects marked get dilatations in males and females compared to DMSO-treated control group (g = gut; vt = vitellarium; Scale bars: 50 µm).

3.2.4 Expression of cathepsins after imatinib and/or BA1 treatment

In order to get functional understanding of imatinib caused effects, I investigated the role of cathepsins, since they are already well-known to play prominent roles in gut and gastrodermis of schistosomes (Wendt et al. 2020). Following single or double treatment of imatinib and BA1 for 24 h, I have not observed any significant modulation of cathepsin transcriptional levels of female worms. However, imatinib-treated male worms exhibited

significant downregulation of cathepsin transcript levels, particularly cathepsin B and cathepsin B1. Upon co-treatment of imatinib and BA1, this downregulation of cathepsin transcripts was impeded and the transcript level of cathepsin B (Smp_085180.1), cathepsin B1 (Smp_103610.1), cathepsin L (Smp_343260.1), cathepsin B-like peptidase (Smp_067060.1) appeared similar to that of DMSO-treated control male worms (Figure 3.21). Overall, I observed a diminishing influence of BA1 on imatinib-caused modulation of cathepsin transcript level as well as on the phenotypic effects.

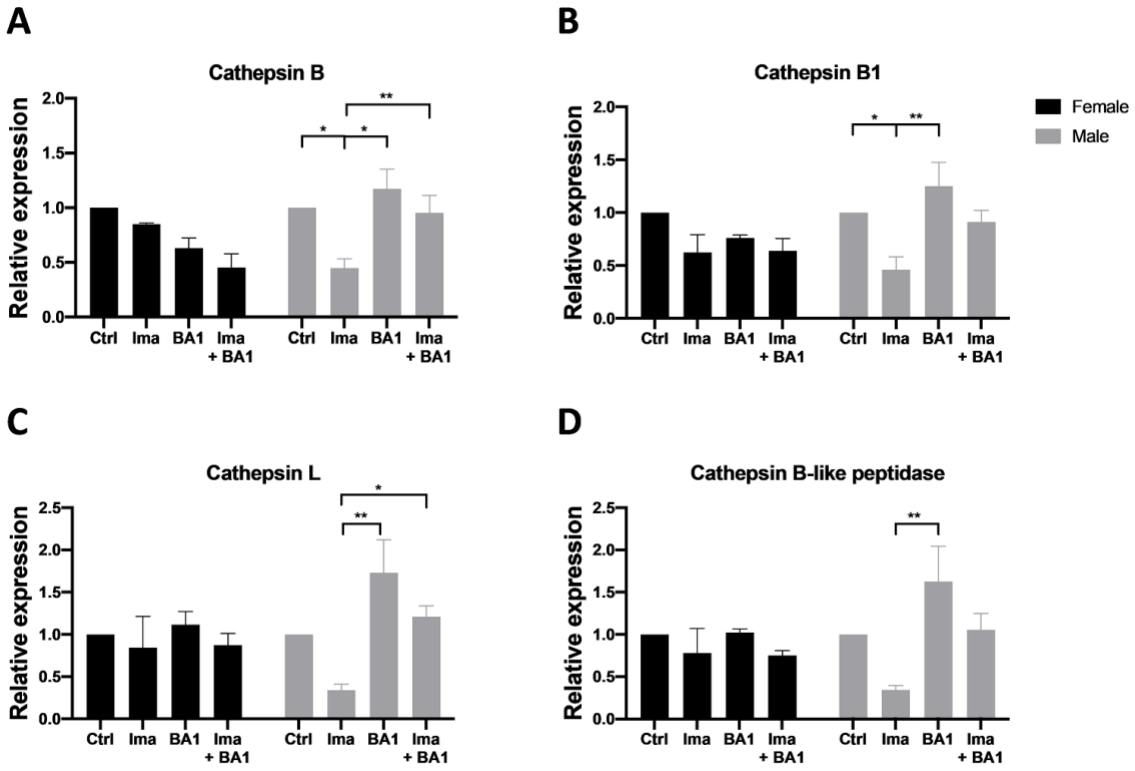

Figure 3.21: Influence of imatinib and/or bafilomycin A1 on the expression of cathepsin orthologs of *S. mansoni* males and females. Treatment of couples with either 20 µM of imatinib (Ima), 0.1 µM of bafilomycin A1 (BA1) or co-treatment (Ima + BA1). Co-treatment compensated the imatinib-caused reduction in transcriptional expression of cathepsin B (A), cathepsin B1 (B), cathepsin L (C) and cathepsin B-like peptidase (D). Relative expression of cathepsins were determined compared to control. Error bars represent mean±SEM (n = 3; * = $p < 0.05$; ** = $p < 0.01$).

4 UNPUBLISHED RESULTS

4.1 Comparison of RNA-Seq and qRT-PCR data

RNA-Seq is one of most reliable and robust techniques of next generation sequencing, however, exact copy numbers of specific mRNAs still need to be verified with a second method such as qRT-PCR (Coenye 2021). Therefore, transcriptomic data of *S. mansoni* independently obtained in other studies were validated for genes of interest by qRT-PCR. Among those bioinformatics data were RNA-Seq results of *S. mansoni,* which indicated that genes regulating several cellular pathways are expressed in sex-dependent and/or gonad-preferential patterns (Lu et al. 2016). During *in silico* analyses, I identified two orthologs of autophagy genes known from humans and model organisms that showed sex- or gonad-preferential expression in this transcriptomics data set. Among these genes is Sm*dap*1, which showed a sex-dependent expression pattern with higher expression in bisex (bs; pairing experienced) females (bF) as compared to bisex males (bM; pairing experienced) and single-sex (virgin-like/pairing-unexperienced) females (sF) (Figure 4.1). Another gene was Sm*ambra*1, one of the key players of Vps34 complex (Cianfanelli et al. 2015), which showed organ-preferential expression for the ovary of bF as compared to the ovary of sF. qRT-PCR results of Sm*ambra*1 showed a comparable transcript profile to the RNA-Seq data, except for the sample of single-sex ovary (sO; ovary of sF), which showed similar transcript levels in bO (ovary of bF) and sO (Fig. 4). Since qRT-PCR is more sensitive compared to RNA-seq (Costa et al. 2013), it appears more likely that there is no pairing-dependent effect on the transcript levels of this gene in ovaries of bF and sF. This is in sharp contrast to Sm*dap*1 for which a pairing-effect on gene expression in the ovaries was verified by qRT-PCR.

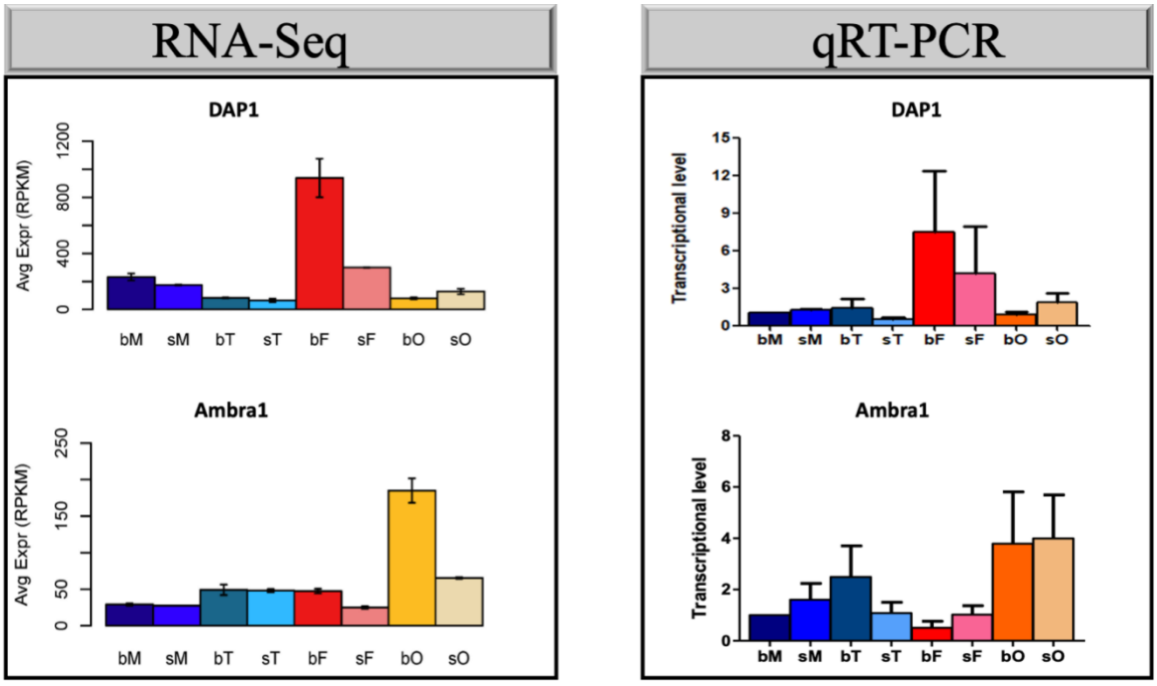

Figure 4.1: Comparison of RNA-Seq (left) and qRT-PCR data (right) to investigate the transcript levels of the autophagy genes Sm*dap1* (Smp_023840.1) and Sm*ambra1* (Smp_156350.1). Data represent the mean±SEM of three independent experiments and was normalized by using *Smletm1* (Smp_065110.1), a reference gene that was validated before transcription analyses of schistosomes *in vitro* for qRT-PCR (Haeberlein et al. 2019). The transcript levels of all samples were related to the bM sample. bM: males of bisex infections, sM: males of single-sex infections, bT: testes of bM, sT: testes of sM, bF: females of bisex infection, sF: females of single-sex infections, bO: ovaries of bF, sO: ovaries of sF. RNA-Seq data of selected genes were obtained from a previous study (Lu et al. 2016).

4.2 RNAi-mediated knock-down of autophagy genes

As a next step, I performed an approach to functionally characterize the autophagy genes by RNAi-mediated knock-down. To this end, schistosome couples were exposed to 2 µg/ml double stranded-(ds-)RNA (over a period of seven days with renewal of culture medium and dsRNA every 48 h) by the soaking method (Krautz-Peterson et al. 2010) *in vitro* to knock-down the target genes. The results indicated significant reductions in transcriptional levels detected by qRT-PCR analysis (Figure 4.2). However, morphologic analyses and egg count determination did not reveal significant differences between knock-down and control groups. Autophagy genes like Sm*beclin* and *SmVps34* showed 40-60% knock-down efficiency, while Sm*dram*, Sm*lc-I*, Sm*lc-II* and Sm*dap1* showed 70-90% knock-down efficiency. In general, knock-down efficiencies of autophagy genes were similar in male and female worms, except

for Sm*beclin*, where knock-down in male worms was 20% more efficient compared to female worms.

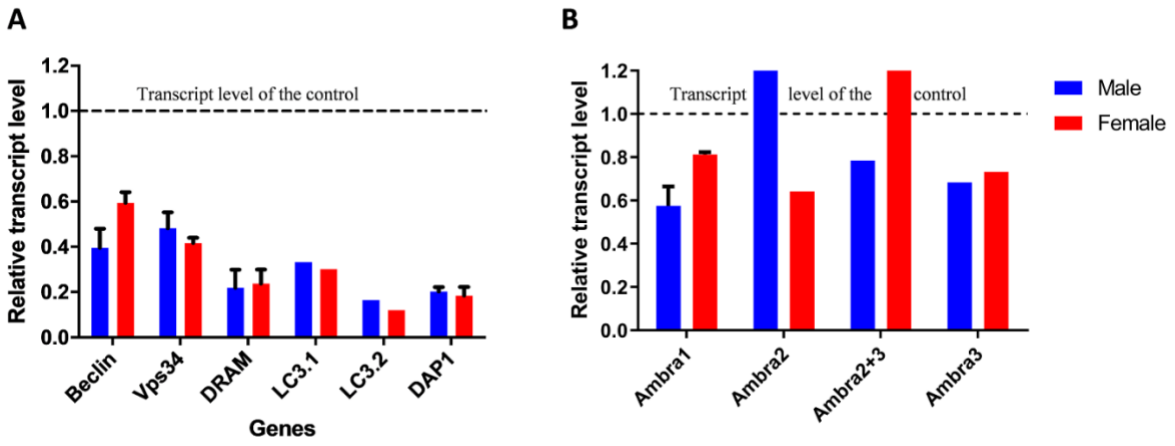

Figure 4.2: RNAi-mediated knock-down of autophagy genes in adult *S. mansoni*. qRT-PCR data were normalized compared to the transcript level of the control (untreated worms). Couples were treated with dsRNA for seven days. Medium and dsRNA were refreshed every 48 h. Subsequently, the transcript levels of specific genes were quantified separately for male and female worms (A). Different dsRNA templates were used to knock-down the transcript levels of Sm*ambra1* (B). Data represent the mean±SEM of three independent experiments, whereas the data without error bars represents only one experiment.

Because of the interesting pairing-dependent expression profile of Sm*dap1* in females (Figure 3.22) and in order to increase the efficiency of knock-down, an extended duration of treatment and more dsRNA was tested. For Sm*dap1* knock-down, schistosome couples were exposed to three times higher concentration of dsRNA (6 µg/ml) for up to 21 days by the soaking method, with renewal of culture medium and dsRNA every 48 h, as done previously. The results indicated significant reductions of transcriptional levels (67% in males, 70% in females) detected by qRT-PCR analysis (Figure 4.3). However, morphologic analyses and egg count determination did not reveal significant differences between knock-down and control groups. In addition, the morphology and cellular content of eggs laid by dsRNA-treated worms also did not reveal any significant differences as compared to control groups.

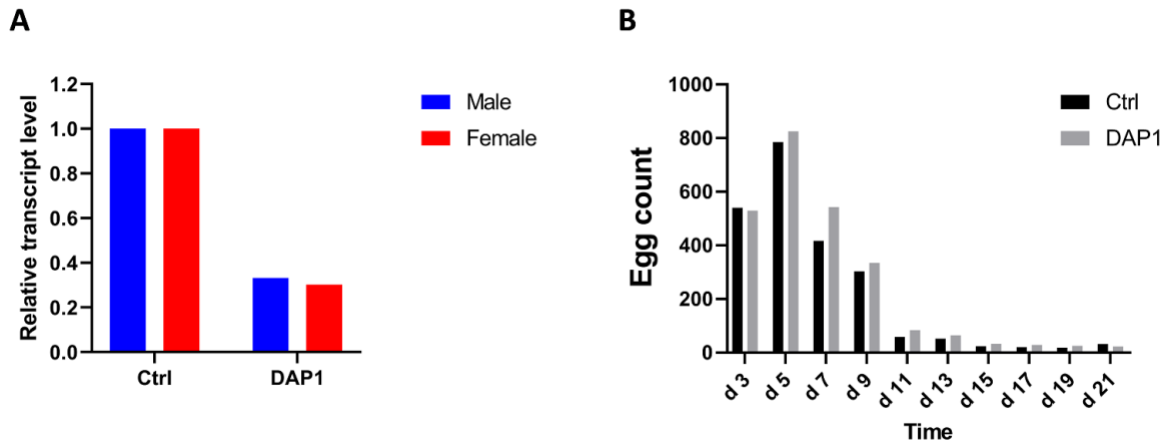

Figure 4.3: RNAi-mediated knock-down of Sm*dap1* in adult *S. mansoni*. The transcript level of Sm*dap1* was quantified separately for male and female worms after 21 d of culture (A), and the egg count of 10 couples each group was determined after every 48 h (B). qRT-PCR data were normalized compared to the transcript level of the control (untreated worms). Couples were treated with dsRNA for three weeks. Medium and dsRNA were refreshed every 48 h. Data represent only one experiment.

5 DISCUSSION AND OUTLOOK

5.1 Key findings

This thesis focused on the first exploration of the autophagy machinery in *S. mansoni*, characterized the role of autophagy modulation on the parasite's reproductive biology, and studied the effect of a known antischistosomal TK-inhibitor on autophagy. First, with an *in silico* approach, seven orthologs of autophagy-related proteins (Beclin, Vps34, Ambra1, DRAM, DAP1, LC3B.1, LC3B.2) were identified and characterized at the transcriptional and - with respect to LC3B - post-transcriptional levels in *S. mansoni*. The effect of *in vitro* culture on the expression of these autophagy genes was studied. The modulation of autophagy was studied using LC3B, a well-known autophagy marker, with the pharmacological activation (rapamycin treatment) and inhibition (BA1, spautin-1 and wortmannin treatment) of adult *S. mansoni* worms. Then, reproductive consequences in autophagy inhibitor-treated worms, like pairing stability, worm motility scoring, and egg production were determined by bright field microscopy and gonadal morphology was monitored by confocal laser scanning microscopy (CLSM) (Mughal et al. 2021b). Moreover, for the first time, I addressed the induction of autophagy in imatinib-treated *S. mansoni* using LC3B and cathepsins involvement. Furthermore, I used a co-treatment strategy (imatinib + BA1) to study the associated gut phenotype and modulation of autophagy (Mughal et al. 2021a).

For the first publication, I have identified several autophagy genes in *S. mansoni* and explored the transcriptional expression of these genes. Among others, I observed significant sex-dependent expression of DAP1, DRAM at the transcriptional level. Similarly, sex-dependent expression of LC3 was noticed but only at post-transcriptional level. I found that manipulation of autophagy by an inducer (rapamycin) and an inhibitor (BA1) regulated the LC3B protein expression, a marker for autophagy. I also found that the use of autophagy inhibitors negatively affected worm survival (worm vitality and intestinal morphology) and reproductive traits (pairing, egg production, and gonadal morphology). For the second publication, I found that the anticancer drug imatinib caused a significant increase of LC3B protein expression. This was reversed when worms were co-treated with BA1. Of note, I found that the drastic effects of imatinib on pairing stability, egg production, gut dilatations, and transcriptional expression of cathepsins were mitigated by BA1.

5.2 Exploration of the autophagy machinery in adult *S. mansoni* worms

Autophagy is a conserved catabolic process that maintains cellular homeostasis and cellular physiology under stress conditions (Cooper 2018). It counteracts infectious, carcinogenic, and starvation stresses to maintain the cellular homeostasis, and its dysregulation is known to cause various diseases in human (Yang and Klionsky 2010; Lee 2018). In much simpler organisms, such as *Saccharomyces cerevisiae*, *Dictyostelium discoideum*, and *Caenorhabditis elegans*, it is comparatively easy to study the functional involvement of autophagy in developmental processes (Di Bartolomeo et al. 2010). Similarly, the role of autophagic cell death has been implicated in various parasitic protozoan species like *Plasmodium falciparum, Toxoplasma gondii, Trypanosoma brucei, Trypanosoma cruzi* (Orvedahl and Levine 2009; Li et al. 2012; Sinai and Roepe 2012). This dynamic process is mainly divided into three discreet stages regulated by autophagy-related (Atg) proteins: (i) initiation of autophagy, (ii) autophagosome formation and elongation, (iii) autophagosome maturation and degradation. In model organisms, ULK1 (Atg 1) and Vps34-Beclin1 are considered to be essential induction complexes (Liang et al. 2006) and Atg12/Atg5 or LC3 (Atg8) conjugation as compulsory components of the autophagy machinery for autophagosome elongation and maturation (Kuma et al. 2002).

5.2.1 In silico analyses

As a first step, I identified seven orthologs of autophagy-related genes in *S. mansoni* (Beclin, Vps34, Ambra1, DRAM, DAP1, LC3B.1, LC3B.2), which are already known in humans and various model organisms. The results showed a high conservation among various organisms including schiostosomes. This suggested that the autophagy machinery in *S. mansoni* is comprised of a Vps34 core complex (formed by Beclin, Vps34 and Ambra1). Other members of the autophagy machinery found in *S. mansoni* included Dram (damage-regulated autophagy modulator), the autophagy marker LC3B, and DAP1 (death associated protein 1) as a negative regulator of autophagy. These autophagy-related proteins were also found to be evolutionary conserved in yeast and various mammals (Kawabata and Yoshimori 2020). As in many other organisms, essential components of the autophagy machinery seem to be evolutionary conserved in *S. mansoni* as well. However, an ULK1 ortholog was not found in *S. mansoni* by the *in silico* analyses. It appeared likely that *S. mansoni* lacks ULK1, but rather possesses all members of the Vps34-Beclin complex. Since Vps15, Atg101, and Atg13 are also close regulatory partners of Vps34-Beclin complex (Levine and Kroemer 2019), it

appeared likely that *S. mansoni* also possesses Vps15, Atg101, and Atg13 to facilitate the initiation of the autophagy process. Similarly, the presence of LC3 in *S. mansoni* indicated that another conjugation system, the Atg5-Atg16-Atg12 complex, is also present and might be evolutionary conserved. In addition, the conversion of LC3-I to LC3-II is mediated by Atg4, Atg3 and Atg7 in all model organisms (Levine and Kroemer 2019). Although I did not include these genes in my *in silico* investigation, it seems likely that these genes are also conserved in *S. mansoni*.

5.2.2 Relative autophagy gene expression in male and female *S. mansoni*

Transcriptomics data indicated that several signaling molecules of different cellular pathways show sex-dependent expression patterns in *S. mansoni* (Gobert et al. 2006; Cai et al. 2016; Lu et al. 2016, 2019; Wendt et al. 2020). Therefore, expression patterns of autophagy genes were explored separately in both males and females. The relative transcription of five protein orthologs (Beclin, Vps34, Ambra1, LC3B.1, LC3B.2) was found to be similar for both sexes, however two orthologs (DRAM, DAP1) were found to be differentially transcribed. DAP1 exhibited a higher transcriptional expression in bisex females compared to bisex males; a similar result was obtained in the previous transcriptomics approach (Lu et al. 2016). This suggested that DAP1 may be involved in regulating the proliferative activity in the female's gonads. DAP1 is a negative regulator or counterbalance of autophagy during metabolic stress, thus known to prevent the uncontrolled overstimulation of autophagic cell death (Koren et al. 2010). Studies in planarians found a dual role of DAP1 during body remodeling, i.e., promoting stem-cell proliferation as well as autophagic cell death. Moreover, DAP1 transcripts in planarians were found to be upregulated upon stress induction and highly expressed in gonads (González-Estévez et al. 2007; Koren et al. 2010). Since planarians are the closest free-living evolutionary relative of schistosomes, it might be possible that *Sm*DAP1 also plays a dual role.

In *S. mansoni*, DRAM also exhibited a sex-dependent expression pattern. Contrary to DAP1, its transcription level was higher in bisex males compared to bisex females. DRAM is also a highly conserved autophagy-related gene among various metazoan species including amphibians, fish, insects and worms, and is known to regulate autophagy via the p53 pathway (Crighton et al. 2007). I postulated that lower transcription of DRAM in females might be linked to a reduced p53-linked autophagy. Also, at the protein levels, LC3B expression suggested lower autophagic activity in females compared to males (Mughal et al. 2021b). In general, the fact that DAP1 (autophagy suppressor) expression is higher in females compared with males and DRAM (autophagy inducer) expression is lower in females compared with

males indicated a sex-dependent modulation of autophagic processes in *S. mansoni.* However, the significance and possible interaction of these two molecules for the regulation of autophagy have still to be determined.

5.3 Functional analyses and modulation of autophagy

5.3.1 Effect of the *in vitro* culture

The functional analysis of genes in *S. mansoni* by inhibitors or RNAi makes it necessary to culture worms for several days *in vitro*. The limitation is that culture media represent a fundamentally different environment to the worms compared to whole blood. Therefore, I investigated whether autophagy is modulated in the study organisms in response to the used *in vitro* culture environment, because stress and metabolic starvations are potential inducers of the onset of the autophagy machinery (Karim et al. 2014). Advanced schistosome media and culture conditions have been established, but they are still suboptimal compared to the *in vivo* conditions within the definitive host (Senft and Weller 1956; Cheever and Weller 1958). In theory, schistosome culture media could either induce starvation due to lack of red blood cells (leading to induce autophagy) or provide sufficient essential amino acids and nutrients (leading to inhibit autophagy). The results showed that the transcriptional level of six autophagy genes in *S. mansoni* remained similar during a 12 days *in vitro* culture period. However, the transcription of DAP1 protein increased at day 1 of the *in vitro* culture, but then showed a significant decrease until day 12, specifically in female worms. It is possible that the transcriptional upregulation of DAP1 protein immediately after the start of *in vitro* culture was due to its counter-regulatory effects on autophagy and thus prevented its overstimulation (Koren et al. 2010). Furthermore, I observed that the transcription level of LC3B was similar during 12 days of culture, however, LC3B protein decreased on day 1 in both male and female worms (Mughal et al. 2021b). This observation points towards the post-transcriptional modulation of this protein. Other studies on human and murine cell lines also showed decreased LC3B protein level after a few hours to three days of *in vitro* culture, while the mRNA expression remained unaltered during these times (Scherz-Shouval et al. 2010). In addition, there is evidence regarding the involvement of miRNAs during the post-transcriptional modulation of autophagy gene expression (Mikhaylova et al. 2012; Feng et al. 2015; Jia et al. 2019). Overall, the obtained results indicated a decrease in LC3B protein expression during *in vitro* culture of *S. mansoni*, and also that this decrease is not associated with changes in the transcriptional expression of LC3B as well as other autophagy genes.

5.3.2 Influence of autophagy inducer and inhibitor treatment on the LC3 protein

Apart from the commonly used strategy of inducing autophagy by starvation (Mizushima et al. 2010), this process can also be modulated by various chemical activators and inhibitors. Rapamycin, a potent inhibitor of mTOR (suppressor of autophagy), is a well-known autophagy inducer under *in vivo* and *in vitro* settings and has been tested in fly and mouse models (Ravikumar et al. 2004). The results showed that the expression of LC3B and its conversion to LC3B-II were increased after rapamycin treatment for 24 h only in *S. mansoni* females (Mughal et al. 2021b). In parallel to our result, the amount of LC3B-I was increased and its conversion to LC3B-II was enhanced in various cell lines, including neuroblastoma (Lin et al. 2018) and in mesenchymal stem cell (Molaei et al. 2015). Next to this, I also tested the effects of a vacuolar H^+ATPase (V-ATPase) autophagy inhibitor, BA1 (Yamamoto et al. 1998). Short-time exposure of *S. mansoni* to BA1 for 24 h increased the expression of LC3B-I in both males and females, however, the converted LC3B-II remained similar compared to control worms. Long-time exposure of 72 h showed increased conversion of LC3B-II in females (Mughal et al. 2021b). Similar results were also observed by BA1 treatment in various cell lines in which either LC3B-I was accumulated (Zhang et al. 2012), or the conversion of LC3B-II was increased (Fass et al. 2006; Kawai et al. 2007). In general, the exposure period of BA1 influences the expression profile of LC3B protein in such a way that a shorter exposure time increases LC3B-I levels, and a longer exposure time increases LC3B-II conversion relative to LC3B-I (Klionsky et al. 2008).

5.3.3 Effect of autophagy inhibitors on adult worms

Next, I extended the approach of testing autophagy inhibitors (BA1, wortmannin and spautin-1) to assess their antischistosomal activities. Classical studies have pointed to autophagic cell-death as a possible mechanism after treatment of schistosomes with various drugs and observed vacuolar changes within the gastrodermis (Clarkson and Erasmus 1984; Bogitsh 1985; Glaser et al. 2015). However, autophagy itself as the main target has not yet been considered. My results revealed that BA1 caused significant phenotypic alterations on pairing stability, worm motility, and egg production. This treatment also induced morphological changes in terms of cellular degradation of testes, ovaries and vitellarium (Mughal et al. 2021b). These findings are in concordance with already published studies of testicular and ovarian cell lines, where marked reduction in cellular proliferation and cellular homeostasis were observed upon BA1 treatment (Lu et al. 2015; Peng et al. 2017; Wang et al. 2018). Similarly, wortmannin (an early-stage inhibitor) exerted drastic effects on worm

motility, pairing stability, and egg production, as well as drastic egg mal-formation, and this in a dose-dependent manner. Couples treated with 200 μM of wortmannin released merely vitelline cells and oocytes, which appeared not to be packed in an eggshell, as it was found in control worms (Mughal et al. 2021b). Typically, the eggshell develops around 30-40 vitellocytes and one fertilized oocyte within the female ootype to synthesize an egg (Jurberg et al. 2009). Therefore, it may be possible that wortmannin inteferred with the early stages of zygotic formation and embryo development in *S. mansoni*, comparable to what was found in sea urchin eggs (De Nadai et al. 1998) and zebra fish embryos (Babic et al. 2018).

Furthermore, wortmannin also induced tissue degradation in *S. mansoni* male and female gonads, which appeared similar to the degradation found in granulosa cells of the mammalian ovary (Yan et al. 2009). Wortmannin also caused aggregate formation of tissue fragments in the intestine of *S. mansoni* females, a phenotype that resembled the observed gastrodermal degeneration after treatment with arylmethylamino steroids (Krieg et al. 2017). Another early-stage inhibitor, spautin-1, also demonstrated a drastic impact on all three noticed parameters (worm motility, pairing stability and egg production) and exerted small bulges on the worm's tegumental surface. In addition, spautin-1 caused a drastic reduction in testicular, ovarian, and vitelline cells. Notably, oogonia and immature ovarian cells were absent (Mughal et al. 2021b). Overall, the phenotypic changes caused by spautin-1 were more intense than for wortmannin. Similar to these results, a reduction of cellular viability was also found in osteosarcoma and ovarian cell lines (Liu et al. 2011; Vakifahmetoglu-Norberg et al. 2013; Schott et al. 2018). Taken together, the observed effects of three autophagy inhibitors suggested that autophagy plays a significant role for normal tissue homeostasis in *S. mansoni* gonads and the intestine. The use of relatively high concentrations of wortmannin and spautin-1 as compared to published cell culture studies can be explained by a possible variable uptake by the worms, chemical stability of inhibitors in culture medium and the worm body, and pharmacological distribution of inhibitors inside the worm body. Furthermore, higher inhibitor concentrations may be needed to observe effects in a multicellular organism with many membrane barriers to pass compared to a monolayer of cells in a typical cell-culture system.

5.3.4 Knock-down of autophagy-related genes by RNAi

In schistosomes, application of transgenesis techniques has been mainly made by knocking-down genes of interest using RNAi, especially after the exploration of genes, known as dicer and argonaute, related to the RNAi pathway in *S. mansoni* transcriptomics data (Verjovski-Almeida et al. 2003). My results of autophagy gene knock-down showed significant

reduction in the transcriptional level of specific autophagy genes *in vitro* during a dsRNA treatment period of 7 days (Fig. 5). However, the successful knock-down fail to show significant phenotypic effects in terms of worm viability and egg production as compared to control worms. In *S. mansoni*, several reports have attempted the specific gene knock-down in eggs (Rinaldi et al. 2009), schistosomula (Skelly et al. 2003; Correnti et al. 2005; Stefanić et al. 2010) and also in sporocysts (Boyle et al. 2003). More recently, RNAi has been carried out in adult *S. mansoni* at small-scale (Guidi et al. 2015) and large-scale (Wang et al. 2020) to uncover the potential therapeutic agents. Among several independent attempts of specific gene knock-down, some have failed to achieve a efficient reduction of transcript levels, some reported significant reduction of mRNA levels but without any significant phenotype (reviewed in (Geldhof et al. 2007; Beckmann et al. 2010b), while others reported off-target or other non-specific effects of dsRNA-mediated RNAi screening (Geldhof et al. 2007; Mourão et al. 2009). Genes for which RNAi induced phenotypes in adult worms are usually expressed either in gut or tegument, reason (Stefanić et al. 2010; Wang et al. 2020) which could be reached easily and early compared to other deeper body tissues. At the moment, half-life of autophagy protein in *S. mansoni* is completely unknown and in highly variable ranging from few minutes to years of duration in mammals (Zhang et al. 2016). If this is also true for autophagy proteins of schistosomes, it is highly likely that a 7 day knock-down period is insufficient to observe phenotypic effects. Another possibility could be the residual 30-35% of transcripts, since this level of knock-down was achieved using 2 - 6 µg/ml of dsRNA, therefore a higher concentration of dsRNA and knock-down for prolong period could address these two possibilities simultaneously. It is also likely that simultaneous knock-down approach of multiple genes should be preferred in complex and vital cellular processes where multiple genes form a complex to activate further downstream processes. One such example is presence of Vps34-complex and LC3B proteins regulating autophagy in my study.

5.4 Influence of imatinib on autophagy and its possible interaction

In the literature, some studies about autophagy inhibitors indicated that spautin-1 in combination with TK inhibitors exerted synergistic effects on autophagic cell death in cancer cell lines (Shao et al. 2014; Aveic et al. 2018; Ouchida et al. 2018). In order to explore imatinib action in *S. mansoni*, I investigated (i) whether imatinib can influence the expression level of autophagy genes, (ii) whether autophagy inhibition by BA1 may have either enhancing or weakening *in vitro* effects on imatinib's activity on *S. mansoni*, or (iii) whether cathepsins may play a functional role in imatinib's activity. In preliminary studies, imatinib had shown a drastic

impact on the viability and reproductive physiology of adult *S. mansoni* males and females (Beckmann and Grevelding 2010). Therefore, I also studied the cumulative effects of imatinib and the autophagy inhibitor BA1.

5.4.1 Co-treatment of imatinib and bafilomycin A1

Upon imatinib treatment, I detected a significant increase in LC3B expression, which was reversed when the worms were treated with the combination of imatinib and BA1 (Mughal et al. 2021a). The fact that BA1 attenuated imatinib-induced autophagy and mitigated the antischistosomal effects of imatinib possibly means that an autophagy inducer or a mTOR inhibitor might further deteriorate the imatinib-induced effects. In another study it was shown that rapamycin (inducer of autophagy) potentiated the effects of imatinib in resistant cancer lines (Tsurutani et al. 2005). Functional exploration detected an increased autophagosome formation upon co-treatment of rapamycin and imatinib compared to what was detected by imatinib treatment alone (Ertmer et al. 2007). It can be speculated that the PI3K/Akt/mTOR pathway is involved in the induction of autophagy following imatinib treatment and thus accompanied by autophagic cell death. Since c-Abl is the main molecular target of imatinib, it is also possible that c-Abl inhibition by imatinib may lead to autophagy induction. Also, imatinib interference with PI3K class II kinases could be involved in the autophagy regulating mechanism (Ertmer et al. 2007). Therefore, the potential of imatinib and its underlying mechanisms to induce autophagy in *S. mansoni* as well in other parasites should be further investigated.

5.4.2 Phenotypic changes and cathepsin transcription

Another aspect of co-treatment was that BA1 normalized the imatinib-caused phenotypic and molecular changes, and also reversed the imatinib-mediated down-regulation of cathepsin transcriptional levels (Mughal et al. 2021a). The cellular uptake of imatinib is regulated by cytoplasmic carrier proteins and diffusion processes (Zimmerman et al. 2013), and further lysosomal sequestration is governed by physiochemical properties and the pH difference between lysosome and cytosol (Burger et al. 2015). In this perspective, it has been proposed that cellular toxicity of imatinib is due to its accumulation in lysosomes (Burger et al. 2015). Another proposed mechanism of imatinib linked with autophagy is lysosomal dysfunction due to high intracellular imatinib concentration and thus cellular stress, which ultimately leads to autophagy activation (Hu et al. 2012). Since one of the main drastic effects of imatinib on *S. mansoni* is the development of profound gut dilatations (Beckmann and

Grevelding 2010), and since cathepsins are known to play a significant role in the schistosome gut (Sajid et al. 2003), we investigated whether transcriptional regulation of cathepsins is involved. The results showed that the BA1-induced upregulation of cathepsin transcripts compensated their downregulation caused by imatinib treatment alone. Similar to these results, another late-phase autophagy inhibitor, chloroquine, also increased the cathepsin transcription in CML cell lines (Carew et al. 2007). Based on the significance of cathepsins in schistosome biology (Caffrey et al. 2018) and the here observed down-regulation following imatinib treatment, it is tempting to speculate on an important role of cathepsin modulation in the antischistosomal activity of imatinib.

5.5 Implications of the results of this work and future studies

Briefly, the data of this work present the first comprehensive information on key autophagy genes in adult *S. mansoni*. Some identified autophagy genes showed sex-dependent transcriptional expression, which may indicate distinct roles in schistosome biology including the male-female interaction. Modulation of autophagy can be monitored using LC3B as an autophagy marker under the influence of autophagy inducer and inhibitors. In addition, manipulation of autophagy by autophagy-inhibitors caused significant negative effects on the vitality and the reproductive capacity, which included detrimental effects on gonads of both genders. Furthermore, as a second part of the project, I discovered the potential of imatinib to induce autophagy in adult *S. mansoni*. This finding provided a possible explanation for gut degeneration and dilatation caused by imatinib or the co-treatment of imatinib and BA1, respectively. The data also suggest that the antischistosomal property of imatinib might be further enhanced by impairment of cathepsins, but can be compensated by the autophagy inhibitor BA1. Therefore, I conclude that autophagy also in *S. mansoni* is a protective and homeostasis mechanism, and its dysregulation affects schistosome viability and reproduction. This finding may stimulate similar studies in further parasite models with veterinary and human health importance. Against this background, further research to identify antischistosomal targets within the autophagy machinery of *S. mansoni* and the combined use of imatinib with autophagy inducers might open new perspectives for controlling schistosomiasis and other neglected tropical diseases.

6 SUMMARY

Schistosomiasis is caused by dioecious schistosomes of the genus *Schistosoma* and is a neglected tropical disease of global importance for human and animal health. Praziquantel represents the only widely used drug to combat schistosomiasis. Due to concerns of developing drug resistance, the search for novel drug and vaccine candidates represents a feasible approach to fight schistosomiasis.

As a first part, my work focused on autophagy-related genes which, due to high evolutionary conservation, are potential regulators of autophagy. I identified seven autophagy genes (*Beclin*, *Ambra1*, *Vps34*, *LC3B*, *DRAM*, *DAP1*) in *S. mansoni* by *in silico* analyses and investigated the influence of *in vitro* culture conditions on the mRNA transcriptional level of these autophagy genes in male and female adult parasites based on quantitative real-time PCR. Among the autophagy-associated genes, some exhibited sex-dependent expression patterns. For example, the death-associated protein DAP1 in *S. mansoni* was found to be highly expressed in females compared to males. The opposite applied to the damage-regulated autophagy modulator DRAM. In addition, the effect of *in vitro* culture conditions significantly changed the mRNA expression level of DAP1 only in female *S. mansoni*. The conversion of LC3B-I into LC3B-II, a marker for autophagic flux, was increased by rapamycin and blocked by bafilomycin A1 (BA1) treatment of parasites as observed by western blot analyses. Furthermore, all tested autophagy inhibitors, BA1, wortmannin, and spautin-1 affected worm viability and egg production. All inhibitors drastically influenced the intestinal and gonadal morphology as shown by confocal laser scanning microscopy (CLSM).

As a second part, I observed an anticancer drug, imatinib drastically affected intestinal morphology and caused the death of adult worms at 50 μM or higher concentrations within 3-4 days *in vitro* (already published). Adult parasites were co-treated with imatinib and BA1. I identified a significant increase of LC3B protein following imatinib treatment. Of note, the drastic effects induced by imatinib on pairing stability, egg production, gut dilatation were mitigated by BA1. Furthermore, the mRNA levels of cathepsins, genes predominantly expressed in the schistosome gut, were reversed upon BA1 treatment in imatinib-treated male parasites. These results provided a possible explanation for the deleterious gut phenotype caused by imatinib, which might in part be explained by autophagy induction.

In general, my results indicated that autophagy regulation in *S. mansoni* represents not only a defense mechanism regulating cellular homeostasis, but when disrupted by chemical inhibition, can affect parasite viability and reproduction.

7 ZUSAMMENFASSUNG

Die Schistosomiasis wird durch Pärchenegel der Gattung *Schistosoma* verursacht und ist eine vernachlässigte Krankheit von globaler Bedeutung. Praziquantel ist das einzige zugelassene Medikament zur Bekämpfung der Schistosomiasis in endemischen Gebieten. Auf der Suche nach alternativen medizinischen Interventionen konzentrierte sich meine Arbeit daher auf die Charakterisierung eines für Zellen fundamentalen Mechanismus, der jedoch in Schistosomen bislang untererforscht war, die Autophagie.

Im ersten Teil meiner Arbeit konzentrierte ich mich auf verschiedene Gene, die mit der Autophagie in Zusammenhang stehen und die aufgrund ihrer hohen evolutionären Konserviertheit potenzielle Regulatoren der Autophagie-Mechanismen in *S. mansoni* sind. Ich identifizierte sieben Autophagie-Gene (Beclin, Ambra1, Vps34, LC3B, DRAM, DAP1) durch verschiedene *in silico*-Analysen und untersuchte den Einfluss der *in vitro*-Kulturbedingungen auf das mRNA-Transkriptionsniveau dieser Autophagie-Gene in männlichen und weiblichen adulten Parasiten mit Hilfe von quantitativer real-time PCR. Von diesen Autophagie-Genen wiesen einige ein geschlechtsabhängiges Expressionsmuster auf. So wurde beispielsweise DAP1 (Death-Associated Protein 1) in *S. mansoni* spezifisch bei Weibchen stärker exprimiert als bei Männchen, und das Gegenteil galt für DRAM (Damage-Regulated Autophagy Modulator). Darüber hinaus veränderte der Einfluss der *in vitro*-Kulturbedingungen die mRNA-Expressionsmenge von DAP1 nur bei weiblichen *S. mansoni*-Parasiten signifikant. Die Umwandlung von LC3B-I in LC3B-II, einem Marker für den Autophagiefluss, wurde durch den Autophagie-Aktivator Rapamycin erhöht und durch die Behandlung der Parasiten mit dem Autophagie-Inhibitor Bafilomycin A1 (BA1) blockiert, wie durch Western-Blot-Analysen festgestellt wurde. Darüber hinaus beeinträchtigten alle getesteten Autophagie-Inhibitoren namens BA1, Wortmannin und Spautin-1 die Lebensfähigkeit der Würmer, die Eiproduktion sowie die Morphologie des Darms und der Gonaden drastisch, wie konfokale Laser-Scanning-Mikroskopie (CLSM)-Analysen zeigten.

In einem zweiten Teil konnte ich bereits publizierte Daten bestätigen und zeigen, dass Imatinib, ein Abelson Protein-Tyrosinkinase-Inhibitor und Krebsmedikament, die Darmmorphologie der Parasiten ebenfalls drastisch beeinträchtigt und bei 50 µM oder höheren mikromolaren Konzentrationen innerhalb von 3-4 Tagen zum Tod führt. Darauf basierend wurden erwachsene Parasiten simultan mit der niedrigsten wirksamen Konzentration von Imatinib und BA1 behandelt. Nach der Behandlung mit Imatinib konnte ich einen signifikanten Anstieg des LC3B-Proteins feststellen. Interessanterweise wurden die drastischen

Auswirkungen von Imatinib auf die Paarungsstabilität, die Eiproduktion und die Darmdilatation durch BA1 abgeschwächt, wie die Ergebnisse aus Hellfeldmikroskopie und CLSM zeigten. Darüber hinaus wurde die mRNA-Expression von Cathepsinen (ein Gen, das hauptsächlich im Darm von Schistosomen lokalisiert ist) in mit Imatinib behandelten männlichen Parasiten durch die Behandlung mit BA1 umgekehrt. Meine Ergebnisse lieferten eine mögliche funktionelle Erklärung für die phänotypischen Effekte und die durch Imatinib ausgelöste Autophagie-Induktion.

Allgemein, bei *S. mansoni* erfüllt die Autophagie nicht nur einen Abwehrmechanismus, der die zelluläre Homöostase reguliert, sondern kann, wenn sie gestört ist, die Lebensfähigkeit und Reproduktionsfähigkeit des Parasiten beeinträchtigen. Darüber hinaus könnte die Imatinib-Behandlung in Kombination mit Autophagie-induzierenden Therapeutika neue Wege zur Bekämpfung von Schistosomen und anderen Parasiten eröffnen, die vernachlässigte Tropenkrankheiten verursachen.

8 LIST OF ABBREVIATIONS

Abbreviation	Full name
bM	Males of bisex infections
sM	Males of single-sex infections
bT	Testes of bM
sT	Testes of sM
bF	Females of bisex infections
sF	Females of single-sex infections
bO	Ovaries of bF
sO	Ovaries of sF
p.i.	Post infection
CLSM	Confocal laser scanning microscope
PCR	Polymerase chain reaction
qRT-PCR	Quantitative real-time PCR
dsRNA	Double stranded RNA
RNAi	RNA interference
SDS-PAGE	Sodium dodecyl sulphate–polyacrylamide gel electrophoresis
BSA	Bovine serum albumin
PVDF	Polyvinylidene fluoride
V	Volts
RT	Room temperature
°C	Degrees Celsius
mA	Milliampere
mm	Millimetre
ml	Millilitre
M	Molar
µM	Micromolar
µg	Microgram
h	Hour
d	Day
min	Minute

sec	Second
o/n	Overnight
CO_2	Carbon dioxide
AFA	Acidified formal alcohol
Ambra1	Autophagy and Beclin 1 regulator 1
DRAM	Damage-regulated autophagy modulator
DAP1	Death associated protein 1
LC3	Microtubule-associated protein 1A/1B-light chain 3
LC3.1	LC3 ortholog 1
LC3.2	LC3 ortholog 2
Vps34	Vacuolar sorting protein 34
Atg	Autophagy related
SNARE	Soluble N-ethylmaleimide-sensitive factor attachment protein receptor
LAMP	Lysosomal associated membrane protein
ULK1	Unc-51 like autophagy activating kinase 1
VAMP	Vesicle associated membrane protein
FIP200	FAK family-interacting protein of 200 kDa
PIK3	Phosphatidylinositol 3-kinase
PE	Phosphatidylethanolamine
TGF	Transforming growth factor
TRIKI	TGF beta receptor type I kinase inhibitor
GVBD	Germinal vesicle break down
mTOR	Mammalian target of rapamycin
mTORC1	Mammalian target of rapamycin complex 1
Abl	Abelson tyrosine
CML	Chronic myeloid leukemia
PTK	Protein tyrosine kinase
TK	Tyrosine kinase
CTK	Cytoplasmic tyrosine kinase
RTK	Receptor tyrosine kinase
BA1	Bafilomycin A1
Spautin-1	Specific and potent autophagy inhibitor-1
ß-Int1	Integrin beta 1

VKR	Venus kinase receptor
GPCR	G-protein-coupled receptor
ILK	Integrin-linked kinase
DMSO	Dimethyl sulfoxide
PINCH	Particularly interesting new cystein-histidine-rich protein
NCK-2	Non-catalytic region of tyrosine kinase adaptor protein
BCL-2	B cell lymphoma 2
BAX	BCL-2 assocaited X protein
BAK	BCL-2 antagonist killer 1
CQ	Chloroquine
HCQ	Hydroxychloroquine
LiCl	Lithium chloride
HCl	Hydrogen chloride
NH_4Cl	Ammonium chloride

9 LIST OF FIGURES AND TABLES

9.1 List of Figures

9.2 List of Tables

10 REFERENCES

Andrade LF, Nahum LA, Avelar LGA, et al (2011) Eukaryotic protein kinases (ePKs) of the helminth parasite *Schistosoma mansoni*. *BMC Genomics* 12:215. https://doi.org/10.1186/1471-2164-12-215

Armstrong JC (1965) Mating behavior and development of Schistosomes in the mouse. *J Parasitol* 51:605–616. https://doi.org/10.2307/3276242

Atkinson KH (1980) Chromosome analysis of *Schistosoma rodhaini* (Trematoda: Schistosomatidae). *Can J Genet Cytol* 22:143–147. https://doi.org/10.1139/g80-019

Aveic S, Pantile M, Polo P, et al (2018) Autophagy inhibition improves the cytotoxic effects of receptor tyrosine kinase inhibitors. *Cancer Cell Int* 18:1–12. https://doi.org/10.1186/s12935-018-0557-4

Avelar LGA, Nahum LA, Andrade LF, et al (2011) Functional diversity of the *Schistosoma mansoni* tyrosine kinases. *J Signal Transduct* 2011:603290. https://doi.org/10.1155/2011/603290

Babic T, Dinic J, Buric SS, et al (2018) Comparative toxicity evaluation of targeted anticancer therapeutics in embryonic zebrafish and sea urchin models. *Acta Biol Hung* 69:395–410. https://doi.org/10.1556/018.69.2018.4.3

Bahia D, Mortara RA, Kusel JR, et al (2007) *Schistosoma mansoni*: expression of Fes-like tyrosine kinase SmFes in the tegument and terebratorium suggests its involvement in host penetration. *Exp Parasitol* 116:225–232. https://doi.org/10.1016/j.exppara.2007.01.009

Barakat R, Morshedy H El (2011) Efficacy of two praziquantel treatments among primary school children in an area of high *Schistosoma mansoni* endemicity, Nile Delta, Egypt. *Parasitology* 138:440–446. https://doi.org/10.1017/S003118201000154X

Barone M V, Courtneidge SA (1995) Myc but not Fos rescue of PDGF signalling block caused by kinase-inactive Src. *Nature* 378:509–512. https://doi.org/10.1038/378509a0

Beckmann S, Buro C, Dissous C, et al (2010a) The Syk kinase SmTK4 of *Schistosoma mansoni* is involved in the regulation of spermatogenesis and oogenesis. *PLoS Pathog* 6:e1000769. https://doi.org/10.1371/journal.ppat.1000769

Beckmann S, Grevelding CG (2010) Imatinib has a fatal impact on morphology, pairing stability and survival of adult *Schistosoma mansoni in vitro*. *Int J Parasitol* 40:521–526. https://doi.org/10.1016/j.ijpara.2010.01.007

Beckmann S, Grevelding CG (2012) Paving the way for transgenic schistosomes.

Parasitology 139:651–668. https://doi.org/10.1017/S0031182011001466

Beckmann S, Hahnel S, Cailliau K, et al (2011) Characterization of the Src/Abl hybrid kinase SmTK6 of *Schistosoma mansoni*. *J Biol Chem* 286:42325–42336. https://doi.org/10.1074/jbc.M110.210336

Beckmann S, Quack T, Burmeister C, et al (2010b) *Schistosoma mansoni*: signal transduction processes during the development of the reproductive organs. *Parasitology* 137:497–520. https://doi.org/10.1017/S0031182010000053

Beckmann S, Quack T, Dissous C, et al (2012) Discovery of platyhelminth-specific α/β-integrin families and evidence for their role in reproduction in *Schistosoma mansoni*. *PLoS One* 7:e52519. https://doi.org/10.1371/journal.pone.0052519

Berriman M, Haas BJ, LoVerde PT, et al (2009) The genome of the blood fluke *Schistosoma mansoni*. *Nature* 460:352–8. https://doi.org/10.1038/nature08160

Bogitsh BJ (1985) *Schistosoma mansoni*: suramin and trypan blue *in vitro* and the ultrastructure of feeding schistosomules. *Exp Parasitol* 60:155–162. https://doi.org/10.1016/0014-4894(85)90018-9

Booth M, Mwatha JK, Joseph S, et al (2004) Periportal fibrosis in human *Schistosoma mansoni* infection is associated with low IL-10, low IFN-γ, high TNF-α, or low RANTES, depending on age and gender. *J Immunol* 172:1295–1303. https://doi.org/10.4049/jimmunol.172.2.1295

Bowman EJ, Siebers A, Altendorf K (1988) Bafilomycins: a class of inhibitors of membrane ATPases from microorganisms, animal cells, and plant cells. *Proc Natl Acad Sci U S A* 85:7972–7976. https://doi.org/10.1073/pnas.85.21.7972

Boyle JP, Wu X-J, Shoemaker CB, et al (2003) Using RNA interference to manipulate endogenous gene expression in *Schistosoma mansoni* sporocysts. *Mol Biochem Parasitol* 128:205–215. https://doi.org/10.1016/s0166-6851(03)00078-1

Braschi S, Wilson RA (2006) Proteins exposed at the adult schistosome surface revealed by biotinylation. *Mol Cell Proteomics* 5:347–356. https://doi.org/10.1074/mcp.M500287-MCP200

Burger H, Den Dekker AT, Segeletz S, et al (2015) Lysosomal sequestration determines intracellular imatinib levels. *Mol Pharmacol* 88:477–487. https://doi.org/10.1124/mol.114.097451

Buro C, Beckmann S, Oliveira KC, et al (2014) Imatinib treatment causes substantial transcriptional changes in adult *Schistosoma mansoni in vitro* exhibiting pleiotropic effects. *PLoS Negl Trop Dis* 8:e2923. https://doi.org/10.1371/journal.pntd.0002923

Buro C, Oliveira KC, Lu Z, et al (2013) Transcriptome analyses of inhibitor-treated schistosome females provide evidence for cooperating Src-kinase and TGFβ receptor pathways controlling mitosis and eggshell formation. *PLoS Pathog* 9:e1003448. https://doi.org/10.1371/journal.ppat.1003448

Caffrey CR, Goupil L, Rebello KM, et al (2018) Cysteine proteases as digestive enzymes in parasitic helminths. *PLoS Negl Trop Dis* 12:e0005840. https://doi.org/10.1371/journal.pntd.0005840

Cai P, Liu S, Piao X, et al (2016) Comprehensive transcriptome analysis of sex-biased expressed genes reveals discrete biological and physiological features of male and female *Schistosoma japonicum*. *PLoS Negl Trop Dis* 10:e0004684. https://doi.org/10.1371/journal.pntd.0004684

Carew JS, Nawrocki ST, Kahue CN, et al (2007) Targeting autophagy augments the anticancer activity of the histone deacetylase inhibitor SAHA to overcome Bcr-Abl–mediated drug resistance. *Blood* 110:313–322. https://doi.org/10.1182/blood-2006-10-050260

Chan MS, Guyatt HL, Bundy DA, et al (1996) Dynamic models of schistosomiasis morbidity. *Am J Trop Med Hyg* 55:52–62. https://doi.org/10.4269/ajtmh.1996.55.52

Cheever AW, Weller TH (1958) Observations on the growth and nutritional requirements of *Schistosoma mansoni in vitro*. *Am J Hyg* 68:322–339. https://doi.org/10.1093/oxfordjournals.aje.a119972

Cianfanelli V, Nazio F, Cecconi F (2015) Connecting autophagy: AMBRA1 and its network of regulation. *Mol Cell Oncol* 2:e970059. https://doi.org/10.4161/23723548.2014.970059

Clarkson J, Erasmus DA (1984) *Schistosoma mansoni*: An in vivo study of drug-induced autophagy in the gastrodermis. *J Helminthol* 58:59–68. https://doi.org/10.1017/S0022149X00028066

Coenye T (2021) Do results obtained with RNA-sequencing require independent verification? *Biofilm* 3:100043. https://doi.org/10.1016/j.bioflm.2021.100043

Cooper KF (2018) Till death do us part: The marriage of autophagy and apoptosis. *Oxid Med Cell Longev* 2018:4701275. https://doi.org/10.1155/2018/4701275

Correnti JM, Brindley PJ, Pearce EJ (2005) Long-term suppression of cathepsin B levels by RNA interference retards schistosome growth. *Mol Biochem Parasitol* 143:209–215. https://doi.org/10.1016/j.molbiopara.2005.06.007

Costa C, Giménez-Capitán A, Karachaliou N, et al (2013) Comprehensive molecular

screening: from the RT-PCR to the RNA-seq. *Transl lung cancer Res* 2:87–91. https://doi.org/10.3978/j.issn.2218-6751.2013.02.05

Crighton D, Wilkinson S, Ryan KM (2007) DRAM links autophagy to p53 and programmed cell death. *Autophagy* 3:72–4. https://doi.org/10.4161/auto.3438

De Bont J, Vercruysse J (1998) Schistosomiasis in cattle. *Adv Parasitol* 41:285–364. https://doi.org/10.1016/s0065-308x(08)60426-1

de Laval F, Savini H, Biance-Valero E, et al (2014) Human schistosomiasis: an emerging threat for Europe. *Lancet* 384:1094–1095. https://doi.org/10.1016/S0140-6736(14)61669-X

De Nadai C, Huitorel P, Chiri S, et al (1998) Effect of wortmannin, an inhibitor of phosphatidylinositol 3-kinase, on the first mitotic divisions of the fertilized sea urchin egg. *J Cell Sci* 111:2507–2518

Dessein AJ, Hillaire D, Elwali NE, et al (1999) Severe hepatic fibrosis in *Schistosoma mansoni* infection is controlled by a major locus that is closely linked to the interferon-gamma receptor gene. *Am J Hum Genet* 65:709–721. https://doi.org/10.1086/302526

Di Bartolomeo S, Nazio F, Cecconi F (2010) The role of autophagy during development in higher eukaryotes. *Traffic* 11:1280–1289. https://doi.org/10.1111/j.1600-0854.2010.01103.x

Dillon GP, Feltwell T, Skelton JP, et al (2006) Microarray analysis identifies genes preferentially expressed in the lung schistosomulum of *Schistosoma mansoni*. *Int J Parasitol* 36:1–8. https://doi.org/10.1016/j.ijpara.2005.10.008

Djouder N, Tuerk RD, Suter M, et al (2010) PKA phosphorylates and inactivates AMPKα to promote efficient lipolysis. *EMBO J* 29:469–481. https://doi.org/10.1038/emboj.2009.339

Doenhoff MJ, Cioli D, Utzinger J (2008) Praziquantel: mechanisms of action, resistance and new derivatives for schistosomiasis. *Curr Opin Infect Dis* 21:659–667. https://doi.org/10.1097/QCO.0b013e328318978f

Dorak M (2008) Real-time PCR; BIOS Advanced Methods. Taylor & Francis, Oxford.

Druker BJ, Tamura S, Buchdunger E, et al (1996) Effects of a selective inhibitor of the Ab1 tyrosine kinase on the growth of Bcr-Ab1 positive cells. *Nat Med* 2:561–566. https://doi.org/10.1038/nm0596-561

Duvall RH, DeWitt WB (1967) An improved perfusion technique for recovering adult schistosomes from laboratory animals. *Am J Trop Med Hyg* 16:483–486. https://doi.org/10.4269/ajtmh.1967.16.483

Egan DF, Shackelford DB, Mihaylova MM, et al (2011) Phosphorylation of ULK1 (hATG1) by AMP-activated protein kinase connects energy sensing to mitophagy. *Science* 331:456–461. https://doi.org/10.1126/science.1196371

El Ridi RAF, Tallima HA-M (2013) Novel therapeutic and prevention approaches for schistosomiasis: review. *J Adv Res* 4:467–478. https://doi.org/10.1016/j.jare.2012.05.002

Epple UD, Suriapranata I, Eskelinen EL, et al (2001) Aut5/Cvt17p, a putative lipase essential for disintegration of autophagic bodies inside the vacuole. *J Bacteriol* 183:5942–5955. https://doi.org/10.1128/JB.183.20.5942-5955.2001

Ertmer A, Huber V, Gilch S, et al (2007) The anticancer drug imatinib induces cellular autophagy. *Leukemia* 21:936–942. https://doi.org/10.1038/sj.leu.2404606

Eskelinen E-L (2005) Maturation of autophagic vacuoles in mammalian cells. *Autophagy* 1:1–10. https://doi.org/10.4161/auto.1.1.1270

Fader CM, Sánchez DG, Mestre MB, et al (2009) TI-VAMP/VAMP7 and VAMP3/cellubrevin: two v-SNARE proteins involved in specific steps of the autophagy/multivesicular body pathways. *Biochim Biophys Acta - Mol Cell Res* 1793:1901–1916. https://doi.org/10.1016/j.bbamcr.2009.09.011

Fass E, Shvets E, Degani I, et al (2006) Microtubules support production of starvation-induced autophagosomes but not their targeting and fusion with lysosomes. *J Biol Chem* 281:36303–36316. https://doi.org/10.1074/jbc.M607031200

Feng Y, Yao Z, Klionsky DJ (2015) How to control self-digestion: transcriptional, post-transcriptional, and post-translational regulation of autophagy. *Trends Cell Biol* 25:354–363. https://doi.org/10.1016/j.tcb.2015.02.002

Fitzpatrick JM, Hoffmann KF (2006) Dioecious *Schistosoma mansoni* express divergent gene repertoires regulated by pairing. *Int J Parasitol* 36:1081–1089. https://doi.org/10.1016/j.ijpara.2006.06.007

Fitzpatrick JM, Johansen MV, Johnston DA, et al (2004) Gender-associated gene expression in two related strains of *Schistosoma japonicum*. *Mol Biochem Parasitol* 136:191–209. https://doi.org/10.1016/j.molbiopara.2004.03.014

Frame MC (2002) Src in cancer: deregulation and consequences for cell behaviour. *Biochim Biophys Acta* 1602:114–130. https://doi.org/10.1016/s0304-419x(02)00040-9

French MD, Evans D, Fleming FM, et al (2018) Schistosomiasis in Africa: Improving strategies for long-term and sustainable morbidity control. *PLoS Negl Trop Dis* 12:e0006484. https://doi.org/10.1371/journal.pntd.0006484

Fukushige M, Chase-Topping M, Woolhouse MEJ, et al (2021) Efficacy of praziquantel has been maintained over four decades (from 1977 to 2018): A systematic review and meta-analysis of factors influence its efficacy. *PLoS Negl Trop Dis* 15:e0009189. https://doi.org/10.1371/journal.pntd.0009189

Furuta N, Fujita N, Noda T, et al (2010) Combinational soluble N-ethylmaleimide-sensitive factor attachment protein receptor proteins VAMP8 and Vti1b mediate fusion of antimicrobial and canonical autophagosomes with lysosomes. *Mol Biol Cell* 21:1001–1010. https://doi.org/10.1091/mbc.E09-08-0693

Gautret P, Mockenhaupt FP, Bottieau E, et al (2015) Schistosomiasis in Corsica and the pivotal role of travellers. *Lancet Infect Dis* 15:1378–1379. https://doi.org/10.1016/S1473-3099(15)00406-5

GBD 2016 DALYs and HALE Collaborators (2017) Global, regional, and national disability-adjusted life-years (DALYs) for 333 diseases and injuries and healthy life expectancy (HALE) for 195 countries and territories, 1990-2016: a systematic analysis for the Global Burden of Disease Study 2016. *Lancet* 390:1260–1344. https://doi.org/10.1016/S0140-6736(17)32130-X

Geldhof P, Visser A, Clark D, et al (2007) RNA interference in parasitic helminths: current situation, potential pitfalls and future prospects. *Parasitology* 134:609–619. https://doi.org/10.1017/S0031182006002071

Gelmedin V, Morel M, Hahnel S, et al (2017) Evidence for integrin - venus kinase receptor 1 alliance in the ovary of *Schistosoma mansoni* females controlling cell survival. *PLoS Pathog* 13:e1006147. https://doi.org/10.1371/journal.ppat.1006147

Geng J, Klionsky DJ (2008) The Atg8 and Atg12 ubiquitin-like conjugation systems in macroautophagy. *EMBO Rep* 9:859–864. https://doi.org/10.1038/embor.2008.163

Glaser J, Schurigt U, Suzuki BM, et al (2015) Anti-schistosomal activity of cinnamic acid esters: Eugenyl and thymyl cinnamate induce cytoplasmic vacuoles and death in schistosomula of *Schistosoma mansoni*. *Molecules* 20:10873–10883. https://doi.org/10.3390/molecules200610873

Gobert GN, McInnes R, Moertel L, et al (2006) Transcriptomics tool for the human Schistosoma blood flukes using microarray gene expression profiling. *Exp Parasitol* 114:160–172. https://doi.org/10.1016/j.exppara.2006.03.003

González-Estévez C, Felix DA, Aboobaker AA, et al (2007) Gtdap-1 promotes autophagy and is required for planarian remodeling during regeneration and starvation. *Proc Natl Acad Sci U S A* 104:13373–13378. https://doi.org/10.1073/pnas.0703588104

Gray DJ, Williams GM, Li Y, et al (2009) A cluster-randomised intervention trial against *Schistosoma japonicum* in the Peoples' Republic of China: bovine and human transmission. *PLoS One* 4:e5900. https://doi.org/10.1371/journal.pone.0005900

Grevelding CG (2004) Schistosoma. *Curr Biol* 14:R545. https://doi.org/10.1016/j.cub.2004.07.006

Grevelding CG (1995) The female-specific W1 sequence of the Puerto Rican strain of *Schistosoma mansoni* occurs in both genders of a Liberian strain. *Mol Biochem Parasitol* 71:269–272. https://doi.org/10.1016/0166-6851(94)00058-u

Grevelding CG (1999) Genomic instability in *Schistosoma mansoni*. *Mol Biochem Parasitol* 101:207–216. https://doi.org/10.1016/S0166-6851(99)00078-X

Grevelding CG, Sommer G, Kunz W (1997) Female-specific gene expression in *Schistosoma mansoni* is regulated by pairing. *Parasitology* 115:635–640. https://doi.org/10.1017/s0031182097001728

Gryseels B, Polman K, Clerinx J, et al (2006) Human schistosomiasis. *Lancet* 368:1106–1118. https://doi.org/10.1016/S0140-6736(06)69440-3

Guidi A, Mansour NR, Paveley RA, et al (2015) Application of RNAi to genomic drug target validation in Schistosomes. *PLoS Negl Trop Dis* 9:e0003801. https://doi.org/10.1371/journal.pntd.0003801

Gwinn DM, Shackelford DB, Egan DF, et al (2008) AMPK phosphorylation of raptor mediates a metabolic checkpoint. *Mol Cell* 30:214–226. https://doi.org/10.1016/j.molcel.2008.03.003

Haeberlein S, Angrisano A, Quack T, et al (2019) Identification of a new panel of reference genes to study pairing-dependent gene expression in *Schistosoma mansoni*. *Int J Parasitol* 49:615–624. https://doi.org/10.1016/j.ijpara.2019.01.006

Haeberlein S, Haas W (2008) Chemical attractants of human skin for swimming *Schistosoma mansoni* cercariae. *Parasitol Res* 102:657–662. https://doi.org/10.1007/s00436-007-0807-1

Hahnel S, Lu Z, Wilson RA, et al (2013) Whole-organ isolation approach as a basis for tissue-specific analyses in *Schistosoma mansoni*. *PLoS Negl Trop Dis* 7:e2336. https://doi.org/10.1371/journal.pntd.0002336

Hatz CFR (2006) Schistosomiasis: an underestimated problem in industrialized countries? *J Travel Med* 12:1–2. https://doi.org/10.2310/7060.2005.00001

He C, Klionsky DJ (2009) Regulation mechanisms and signaling pathways of autophagy. *Annu Rev Genet* 43:67–93. https://doi.org/10.1146/annurev-genet-102808-114910

Helgason GV, Karvela M, Holyoake TL (2011) Kill one bird with two stones: potential efficacy of BCR-ABL and autophagy inhibition in CML. *Blood* 118:2035–2043. https://doi.org/10.1182/blood-2011-01-330621

Henri S, Chevillard C, Mergani A, et al (2002) Cytokine regulation of periportal fibrosis in humans infected with *Schistosoma mansoni*: IFN-gamma is associated with protection against fibrosis and TNF-alpha with aggravation of disease. *J Immunol* 169:929–936. https://doi.org/10.4049/jimmunol.169.2.929

Hines-Kay J, Cupit PM, Sanchez MC, et al (2012) Transcriptional analysis of *Schistosoma mansoni* treated with praziquantel *in vitro*. *Mol Biochem Parasitol* 186:87–94. https://doi.org/10.1016/j.molbiopara.2012.09.006

Hoffmann KF, Wynn TA, Dunne DW (2002) Cytokine-mediated host responses during schistosome infections; walking the fine line between immunological control and immunopathology. *Adv Parasitol* 52:265–307. https://doi.org/10.1016/s0065-308x(02)52014-5

Hosokawa N, Hara T, Kaizuka T, et al (2009) Nutrient-dependent mTORC1 association with the ULK1-Atg13-FIP200 complex required for autophagy. *Mol Biol Cell* 20:1981–1991. https://doi.org/10.1091/mbc.e08-12-1248

Howe KL, Bolt BJ, Shafie M, et al (2017) WormBase ParaSite − a comprehensive resource for helminth genomics. *Mol Biochem Parasitol* 215:2–10. https://doi.org/10.1016/j.molbiopara.2016.11.005

Hu W, Lu S, McAlpine I, et al (2012) Mechanistic investigation of imatinib-induced cardiac toxicity and the involvement of c-Abl kinase. *Toxicol Sci* 129:188–199. https://doi.org/10.1093/toxsci/kfs192

Huang YX, Manderson L (2005) The social and economic context and determinants of schistosomiasis japonica. *Acta Trop* 96:223–231. https://doi.org/10.1016/j.actatropica.2005.07.015

Hubbard SR, Till JH (2000) Protein tyrosine kinase structure and function. *Annu Rev Biochem* 69:373–398. https://doi.org/10.1146/annurev.biochem.69.1.373

Inobaya MT, Olveda RM, Chau TN, et al (2014) Prevention and control of schistosomiasis: a current perspective. *Res Rep Trop Med* 2014:65–75. https://doi.org/10.2147/RRTM.S44274

Inoki K, Zhu T, Guan K-L (2003) TSC2 mediates cellular energy response to control cell growth and survival. *Cell* 115:577–590. https://doi.org/10.1016/s0092-8674(03)00929-2

Ishizawar R, Parsons SJ (2004) c-Src and cooperating partners in human cancer. *Cancer Cell*

6:209–214. https://doi.org/10.1016/j.ccr.2004.09.001

Itakura E, Kishi-Itakura C, Mizushima N (2012) The hairpin-type tail-anchored SNARE syntaxin 17 targets to autophagosomes for fusion with endosomes/lysosomes. *Cell* 151:1256–1269. https://doi.org/10.1016/j.cell.2012.11.001

Jia Y, Lin R, Jin H, et al (2019) MicroRNA-34 suppresses proliferation of human ovarian cancer cells by triggering autophagy and apoptosis and inhibits cell invasion by targeting Notch 1. *Biochimie* 160:193–199. https://doi.org/10.1016/j.biochi.2019.03.011

Jourdane J, Imbert-Establet D, Tchuenté LA (1995) Parthenogenesis in schistosomatidae. *Parasitol today* 11:427–430. https://doi.org/10.1016/0169-4758(95)80029-8

Jung CH, Jun CB, Ro SH, et al (2009) ULK-Atg13-FIP200 complexes mediate mTOR signaling to the autophagy machinery. *Mol Biol Cell* 20:1992–2003. https://doi.org/10.1091/mbc.E08-12-1249

Jurberg AD, Gonçalves T, Costa TA, et al (2009) The embryonic development of *Schistosoma mansoni* eggs: proposal for a new staging system. *Dev Genes Evol* 219:219–234. https://doi.org/10.1007/s00427-009-0285-9

Kabeya Y, Mizushima N, Ueno T, et al (2000) LC3, a mammalian homologue of yeast Apg8p, is localized in autophagosome membranes after processing. *EMBO J* 19:5720–5728. https://doi.org/10.1093/emboj/19.21.5720

Kapp K, Knobloch J, Schüssler P, et al (2004) The *Schistosoma mansoni* Src kinase TK3 is expressed in the gonads and likely involved in cytoskeletal organization. *Mol Biochem Parasitol* 138:171–182. https://doi.org/10.1016/j.molbiopara.2004.07.010

Kapp K, Schüssler P, Kunz W, et al (2001) Identification, isolation and characterization of a Fyn-like tyrosine kinase from *Schistosoma mansoni*. *Parasitology* 122:317–327. https://doi.org/10.1017/s0031182001007430

Karim MR, Kawanago H, Kadowaki M (2014) A quick signal of starvation induced autophagy: Transcription versus post-translational modification of LC3. *Anal Biochem* 465:28–34. https://doi.org/10.1016/j.ab.2014.07.007

Kawabata T, Yoshimori T (2020) Autophagosome biogenesis and human health. *Cell Discov* 6:33. https://doi.org/10.1038/s41421-020-0166-y

Kawai A, Uchiyama H, Takano S, et al (2007) Autophagosome-lysosome fusion depends on the pH in acidic compartments in CHO cells. *Autophagy* 3:154–157. https://doi.org/10.4161/auto.3634

Keiser J (2010) *In vitro* and *in vivo* trematode models for chemotherapeutic studies. *Parasitology* 137:589–603. https://doi.org/10.1017/S0031182009991739

Kim E, Goraksha-Hicks P, Li L, et al (2008) Regulation of TORC1 by Rag GTPases in nutrient response. *Nat Cell Biol* 10:935–945. https://doi.org/10.1038/ncb1753

Kim J, Kundu M, Viollet B, et al (2011) AMPK and mTOR regulate autophagy through direct phosphorylation of Ulk1. *Nat Cell Biol* 13:132–141. https://doi.org/10.1038/ncb2152

Klionsky DJ, Elazar Z, Seglen PO, et al (2008) Does bafilomycin A1 block the fusion of autophagosomes with lysosomes? *Autophagy* 4:849–850. https://doi.org/10.4161/auto.6845

Knobloch J, Beckmann S, Burmeister C, et al (2007) Tyrosine kinase and cooperative TGFbeta signaling in the reproductive organs of *Schistosoma mansoni*. *Exp Parasitol* 117:318–336. https://doi.org/10.1016/j.exppara.2007.04.006

Knobloch J, Kunz W, Grevelding CG (2006) Herbimycin A suppresses mitotic activity and egg production of female *Schistosoma mansoni*. *Int J Parasitol* 36:1261–1272. https://doi.org/10.1016/j.ijpara.2006.06.004

Knobloch J, Winnen R, Quack M, et al (2002) A novel Syk-family tyrosine kinase from *Schistosoma mansoni* which is preferentially transcribed in reproductive organs. *Gene* 294:87–97. https://doi.org/10.1016/s0378-1119(02)00760-6

Koren I, Reem E, Kimchi A (2010) DAP1, a novel substrate of mTOR, negatively regulates autophagy. *Curr Biol* 20:1093–1098. https://doi.org/10.1016/j.cub.2010.04.041

Krautz-Peterson G, Bhardwaj R, Faghiri Z, et al (2010) RNA interference in schistosomes: machinery and methodology. *Parasitology* 137:485–495. https://doi.org/10.1017/S0031182009991168

Krieg R, Jortzik E, Goetz A-A, et al (2017) Arylmethylamino steroids as antiparasitic agents. *Nat Commun* 8:14478. https://doi.org/10.1038/ncomms14478

Kuma A, Mizushima N, Ishihara N, et al (2002) Formation of the approximately 350-kDa Apg12-Apg5.Apg16 multimeric complex, mediated by Apg16 oligomerization, is essential for autophagy in yeast. *J Biol Chem* 277:18619–18625. https://doi.org/10.1074/jbc.M111889200

Kunz W (2001) Schistosome male–female interaction: induction of germ-cell differentiation. *Trends Parasitol* 17:227–231. https://doi.org/10.1016/S1471-4922(01)01893-1

Kunz W, Gohr L, Grevelding C, et al (1995) *Schistosoma mansoni*: control of female fertility by the male. *Mem Inst Oswaldo Cruz* 90:185–189. https://doi.org/10.1590/S0074-02761995000200010

Larson RA, Druker BJ, Guilhot F, et al (2008) Imatinib pharmacokinetics and its correlation

with response and safety in chronic-phase chronic myeloid leukemia: a subanalysis of the IRIS study. *Blood* 111:4022–4028. https://doi.org/10.1182/blood-2007-10-116475

Lee JW, Park S, Takahashi Y, et al (2010) The association of AMPK with ULK1 regulates autophagy. *PLoS One* 5:e15394. https://doi.org/10.1371/journal.pone.0015394

Lee M-S (2018) Overview of the minireviews on autophagy. *Mol Cells* 41:1–2. https://doi.org/10.14348/molcells.2018.0400

Levine B, Klionsky DJ (2004) Development by self-digestion: molecular mechanisms and biological functions of autophagy. *Dev Cell* 6:463–477. https://doi.org/10.1016/s1534-5807(04)00099-1

Levine B, Kroemer G (2019) Biological functions of autophagy genes: a disease perspective. *Cell* 176:11–42. https://doi.org/10.1016/j.cell.2018.09.048

Li F-J, Shen Q, Wang C, et al (2012) A role of autophagy in *Trypanosoma brucei* cell death. *Cell Microbiol* 14:1242–1256. https://doi.org/10.1111/j.1462-5822.2012.01795.x

Li X, Haeberlein S, Zhao L, et al (2019) The ABL kinase inhibitor imatinib causes phenotypic changes and lethality in adult *Schistosoma japonicum*. *Parasitol Res* 118:881–890. https://doi.org/10.1007/s00436-019-06224-x

Liang C, Feng P, Ku B, et al (2006) Autophagic and tumour suppressor activity of a novel Beclin1-binding protein UVRAG. *Nat Cell Biol* 8:688–698. https://doi.org/10.1038/ncb1426

Liang C, Lee JS, Inn KS, et al (2008) Beclin1-binding UVRAG targets the class C Vps complex to coordinate autophagosome maturation and endocytic trafficking. *Nat Cell Biol* 10:776–787. https://doi.org/10.1038/ncb1740

Liberatos JD, Short RB (1983) Identification of sex of schistosome larval stages. *J Parasitol* 69:1084–1089. https://doi.org/10.2307/3280870

Lin X, Han L, Weng J, et al (2018) Rapamycin inhibits proliferation and induces autophagy in human neuroblastoma cells. *Biosci Rep* 38:1–8. https://doi.org/10.1042/BSR20181822

Liu J, Xia H, Kim M, et al (2011) Beclin1 controls the levels of p53 by regulating the deubiquitination activity of USP10 and USP13. *Cell* 147:223–234. https://doi.org/10.1016/j.cell.2011.08.037

Logan-Klumpler FJ, De Silva N, Boehme U, et al (2012) GeneDB--an annotation database for pathogens. *Nucleic Acids Res* 40:D98-108. https://doi.org/10.1093/nar/gkr1032

LoVerde PT, Andrade LF, Oliveira G (2009) Signal transduction regulates schistosome reproductive biology. *Curr Opin Microbiol* 12:422–428.

https://doi.org/10.1016/j.mib.2009.06.005

LoVerde PT, Osman A, Hinck A (2007) *Schistosoma mansoni*: TGF-β signaling pathways. *Exp Parasitol* 117:304–317. https://doi.org/10.1016/j.exppara.2007.06.002

Lu X, Chen L, Chen Y, et al (2015) Bafilomycin A1 inhibits the growth and metastatic potential of the BEL-7402 liver cancer and HO-8910 ovarian cancer cell lines and induces alterations in their microRNA expression. *Exp Ther Med* 10:1829–1834. https://doi.org/10.3892/etm.2015.2758

Lu Z, Sessler F, Holroyd N, et al (2016) Schistosome sex matters: a deep view into gonad-specific and pairing-dependent transcriptomes reveals a complex gender interplay. *Sci Rep* 6:31150. https://doi.org/10.1038/srep31150

Lu Z, Spänig S, Weth O, et al (2019) Males, the wrongly neglected partners of the biologically unprecedented male–female interaction of schistosomes. *Front Genet* 10:796. https://doi.org/10.3389/fgene.2019.00796

Maiuri MC, Le Toumelin G, Criollo A, et al (2007) Functional and physical interaction between Bcl-X(L) and a BH3-like domain in Beclin-1. *EMBO J* 26:2527–2539. https://doi.org/10.1038/sj.emboj.7601689

Maniatis T, Fritsch EF, Sambrook J (1988) Molecular Cloning : a laboratory manual. 2nd edition. Cold Spring Harb ,New York

Manley PW, Cowan-Jacob SW, Buchdunger E, et al (2002) Imatinib: a selective tyrosine kinase inhibitor. *Eur J Cancer* 38:S19-27. https://doi.org/10.1016/s0959-8049(02)80599-8

Mauvezin C, Neufeld TP (2015) Bafilomycin A1 disrupts autophagic flux by inhibiting both V-ATPase-dependent acidification and Ca-P60A/SERCA-dependent autophagosome-lysosome fusion. *Autophagy* 11:1437–1438. https://doi.org/10.1080/15548627.2015.1066957

McManus DP, Bergquist R, Cai P, et al (2020) Schistosomiasis-from immunopathology to vaccines. *Semin Immunopathol* 42:355–371. https://doi.org/10.1007/s00281-020-00789-x

McManus DP, Dunne DW, Sacko M, et al (2018) Schistosomiasis. *Nat Rev Dis Prim* 4:13. https://doi.org/10.1038/s41572-018-0013-8

Mikhaylova O, Stratton Y, Hall D, et al (2012) VHL-regulated MiR-204 suppresses tumor growth through inhibition of LC3B-mediated autophagy in renal clear cell carcinoma. *Cancer Cell* 21:532–546. https://doi.org/10.1016/j.ccr.2012.02.019

Mizushima N (2007) Autophagy: process and function. *Genes Dev* 21:2861–2873.

https://doi.org/10.1101/gad.1599207

Mizushima N, Yoshimori T, Levine B (2010) Methods in mammalian autophagy research. *Cell* 140:313–326. https://doi.org/10.1016/j.cell.2010.01.028

Mohamed-Ali Q, Elwali NE, Abdelhameed AA, et al (1999) Susceptibility to periportal (Symmers) fibrosis in human *Schistosoma mansoni* infections: evidence that intensity and duration of infection, gender, and inherited factors are critical in disease progression. *J Infect Dis* 180:1298–1306. https://doi.org/10.1086/314999

Molaei S, Roudkenar MH, Amiri F, et al (2015) Down-regulation of the autophagy gene, ATG7 , protects bone marrow-derived mesenchymal stem cells from stressful conditions. *Blood Res* 50:80–86. https://doi.org/10.5045/br.2015.50.2.80

Monastyrska I, Rieter E, Klionsky DJ, et al (2009) Multiple roles of the cytoskeleton in autophagy. *Biol Rev* 84:431–448. https://doi.org/10.1111/j.1469-185X.2009.00082.x

Morel M, Vanderstraete M, Hahnel S, et al (2014) Receptor tyrosine kinases and schistosome reproduction: new targets for chemotherapy. *Front Genet* 5:238. https://doi.org/10.3389/fgene.2014.00238

Moriyasu Y, Ohsumi Y (1996) Autophagy in tobacco suspension-cultured cells in response to sucrose starvation. *Plant Physiol* 111:1233–1241. https://doi.org/10.1104/pp.111.4.1233

Mourão MM, de Moraes Mourão M, Dinguirard N, et al (2009) Phenotypic screen of early-developing larvae of the blood fluke, *Schistosoma mansoni*, using RNA interference. *PLoS Negl Trop Dis* 3:e502. https://doi.org/10.1371/journal.pntd.0000502

Mughal MN, Grevelding CG, Haeberlein S (2021a) The anticancer drug imatinib induces autophagy in *Schistosoma mansoni*. *Int J Parasitol* S0020-7519:Advance online publication. https://doi.org/10.1016/j.ijpara.2021.10.008

Mughal MN, Grevelding CG, Haeberlein S (2021b) First insights into the autophagy machinery of adult *Schistosoma mansoni*. *Int J Parasitol* 51:571–585. https://doi.org/10.1016/j.ijpara.2020.11.011

Mwatha JK, Jones FM, Mohamed G, et al (2003) Associations between anti-*Schistosoma mansoni* and anti-*Plasmodium falciparum* antibody responses and hepatosplenomegaly, in Kenyan schoolchildren. *J Infect Dis* 187:1337–1341. https://doi.org/10.1086/368362

Mwinzi PN, Karanja DM, Colley DG, et al (2001) Cellular immune responses of schistosomiasis patients are altered by human immunodeficiency virus type 1 coinfection. *J Infect Dis* 184:488–496. https://doi.org/10.1086/322783

Naus CWA, Jones FM, Satti MZ, et al (2003) Serological responses among individuals in areas where both schistosomiasis and malaria are endemic: cross-reactivity between

Schistosoma mansoni and *Plasmodium falciparum*. *J Infect Dis* 187:1272–1282. https://doi.org/10.1086/368361

Ndegwa D, Krautz-Peterson G, Skelly PJ (2007) Protocols for gene silencing in schistosomes. *Exp Parasitol* 117:284–291. https://doi.org/10.1016/j.exppara.2007.07.012

Neumann S, Ziv E, Lantner F, et al (1993) Regulation of HSP70 gene expression during the life cycle of the parasitic helminth *Schistosoma mansoni*. *Eur J Biochem* 212:589–596. https://doi.org/10.1111/j.1432-1033.1993.tb17697.x

Noda T, Ohsumi Y (1998) Tor, a phosphatidylinositol kinase homologue, controls autophagy in yeast. *J Biol Chem* 273:3963–3966. https://doi.org/10.1074/jbc.273.7.3963

Ohsumi Y (2001) Molecular dissection of autophagy: two ubiquitin-like systems. *Nat Rev Mol Cell Biol* 2:211–216. https://doi.org/10.1038/35056522

Olveda DU, Li Y, Olveda RM, et al (2014) Bilharzia in the Philippines: past, present, and future. *Int J Infect Dis* 18:52–56. https://doi.org/10.1016/j.ijid.2013.09.011

Orvedahl A, Levine B (2009) Eating the enemy within: autophagy in infectious diseases. *Cell Death Differ* 16:57–69. https://doi.org/10.1038/cdd.2008.130

Ouchida AT, Li Y, Geng J, et al (2018) Synergistic effect of a novel autophagy inhibitor and Quizartinib enhances cancer cell death. *Cell Death Differ* 9:138. https://doi.org/10.1038/s41419-017-0170-9

Pasquier B (2016) Autophagy inhibitors. *Cell Mol Life Sci* 73:985–1001. https://doi.org/10.1007/s00018-015-2104-y

Pattingre S, Tassa A, Qu X, et al (2005) Bcl-2 antiapoptotic proteins inhibit Beclin 1-dependent autophagy. *Cell* 122:927–939. https://doi.org/10.1016/j.cell.2005.07.002

Pearce EJ (2003) Progress towards a vaccine for schistosomiasis. *Acta Trop* 86:309–313. https://doi.org/10.1016/s0001-706x(03)00062-7

Pendergast AM (2002) The Abl family kinases: mechanisms of regulation and signaling. *Adv Cancer Res* 85:51–100. https://doi.org/10.1016/s0065-230x(02)85003-5

Peng Q, Qin J, Zhang Y, et al (2017) Autophagy maintains the stemness of ovarian cancer stem cells by FOXA2. *J Exp Clin Cancer Res* 36:1–12. https://doi.org/10.1186/s13046-017-0644-8

Platt TR, Brooks DR (1997) Evolution of the schistosomes (Digenea: Schistosomatoidea): the origin of dioecy and colonization of the venous system. *J Parasitol* 83:1035–1044. https://doi.org/10.2307/3284358

Popiel I, Basch PF (1984) Reproductive development of female *Schistosoma mansoni*

(Digenea: Schistosomatidae) following bisexual pairing of worms and worm segments. *J Exp Zool* 232:141–150. https://doi.org/10.1002/jez.1402320117

Powis G, Bonjouklian R, Berggren MM, et al (1994) Wortmannin, a potent and selective inhibitor of phosphatidylinositol-3-kinase. *Cancer Res* 54:2419–2423

Ramirez B, Bickle Q, Yousif F, et al (2007) Schistosomes: challenges in compound screening. *Expert Opin Drug Discov* 2:S53–S61. https://doi.org/10.1517/17460441.2.S1.S53

Ravikumar B, Vacher C, Berger Z, et al (2004) Inhibition of mTOR induces autophagy and reduces toxicity of polyglutamine expansions in fly and mouse models of Huntington disease. *Nat Genet* 36:585–595. https://doi.org/10.1038/ng1362

Reimers N, Homann A, Höschler B, et al (2015) Drug-induced exposure of *Schistosoma mansoni* antigens SmCD59a and SmKK7. *PLoS Negl Trop Dis* 9:e0003593. https://doi.org/10.1371/journal.pntd.0003593

Rinaldi G, Morales ME, Alrefaei YN, et al (2009) RNA interference targeting leucine aminopeptidase blocks hatching of *Schistosoma mansoni* eggs. *Mol Biochem Parasitol* 167:118–126. https://doi.org/10.1016/j.molbiopara.2009.05.002

Rodrigues V, Piper K, Couissinier-Paris P, et al (1999) Genetic control of schistosome infections by the SM1 locus of the 5q31-q33 region is linked to differentiation of type 2 helper T lymphocytes. *Infect Immun* 67:4689–4692. https://doi.org/10.1128/IAI.67.9.4689-4692.1999

Ross AGP, Bartley PB, Sleigh AC, et al (2002) Schistosomiasis. *N Engl J Med* 346:1212–1220. https://doi.org/10.1056/NEJMra012396

Sajid M, McKerrow JH, Hansell E, et al (2003) Functional expression and characterization of *Schistosoma mansoni* cathepsin B and its trans-activation by an endogenous asparaginyl endopeptidase. *Mol Biochem Parasitol* 131:65–75. https://doi.org/10.1016/s0166-6851(03)00194-4

Salas-Coronas J, Bargues MD, Lozano-Serrano AB, et al (2021) Evidence of autochthonous transmission of urinary schistosomiasis in Almeria (southeast Spain): An outbreak analysis. *Travel Med Infect Dis* 44:102165. https://doi.org/10.1016/j.tmaid.2021.102165

Sancak Y, Peterson TR, Shaul YD, et al (2008) The rag GTPases bind raptor and mediate amino acid signaling to mTORC1. *Science* 320:1496–1501. https://doi.org/10.1126/science.1157535

Scherz-Shouval R, Weidberg H, Gonen C, et al (2010) p53-dependent regulation of autophagy protein LC3 supports cancer cell survival under prolonged starvation. *Proc*

Natl Acad Sci 107:18511–18516. https://doi.org/10.1073/pnas.1006124107

Schneider CA, Rasband WS, Eliceiri KW (2012) NIH Image to ImageJ: 25 years of image analysis. *Nat Methods* 9:671–675. https://doi.org/10.1038/NMETH.2089

Schott CR, Ludwig L, Mutsaers AJ, et al (2018) The autophagy inhibitor spautin-1, either alone or combined with doxorubicin, decreases cell survival and colony formation in canine appendicular osteosarcoma cells. *PLoS One* 13:7–10. https://doi.org/10.1371/journal.pone.0206427

Senft AW, Weller TH (1956) Growth and regeneration of *Schistosotna mansoni in vitro*. *Exp Biol Med* 93:16–19. https://doi.org/10.3181/00379727-93-22649

Shang L, Chen S, Du F, et al (2011) Nutrient starvation elicits an acute autophagic response mediated by Ulk1 dephosphorylation and its subsequent dissociation from AMPK. *Proc Natl Acad Sci U S A* 108:4788–4793. https://doi.org/10.1073/pnas.1100844108

Shao S, Li S, Qin Y, et al (2014) Spautin-1, a novel autophagy inhibitor, enhances imatinib-induced apoptosis in chronic myeloid leukemia. *Int J Oncol* 44:1661–1668. https://doi.org/10.3892/ijo.2014.2313

Sinai AP, Roepe PD (2012) Autophagy in Apicomplexa: a life sustaining death mechanism? *Trends Parasitol* 28:358–364. https://doi.org/10.1016/j.pt.2012.06.006

Skelly PJ, Da'dara A, Harn DA (2003) Suppression of cathepsin B expression in *Schistosoma mansoni* by RNA interference. *Int J Parasitol* 33:363–369. https://doi.org/10.1016/s0020-7519(03)00030-4

Skendros P, Mitroulis I, Ritis K (2018) Autophagy in neutrophils: from granulopoiesis to neutrophil extracellular traps. *Front Cell Dev Biol* 6:109. https://doi.org/10.3389/fcell.2018.00109

Smithers SR, Terry RJ (1965) The infection of laboratory hosts with cercariae of *Schistosoma mansoni* and the recovery of the adult worms. *Parasitology* 55:695–700. https://doi.org/10.1017/s0031182000086248

Song LG, Wu XY, Sacko M, et al (2016) History of schistosomiasis epidemiology, current status, and challenges in China: on the road to schistosomiasis elimination. *Parasitol Res* 115:4071–4081. https://doi.org/10.1007/s00436-016-5253-5

Staskiewicz L, Thorburn J, Morgan MJ, et al (2013) Inhibiting autophagy by shRNA knockdown cautions and recommendations. *Autophagy* 9:1449–1450. https://doi.org/10.4161/auto.24895

Stefanić S, Dvořák J, Horn M, et al (2010) RNA interference in *Schistosoma mansoni* schistosomula: selectivity, sensitivity and operation for larger-scale screening. *PLoS*

Negl Trop Dis 4:e850. https://doi.org/10.1371/journal.pntd.0000850

Stephan JS, Yeh YY, Vidhya Ramachandran V, et al (2010) The Tor and cAMP-dependent protein kinase signaling pathways coordinately control autophagy in *Saccharomyces cerevisiae*. *Autophagy* 6:294–295. https://doi.org/10.4161/auto.6.2.11129

Takeshige K, Baba M, Tsuboi S, et al (1992) Autophagy in yeast demonstrated with proteinase-deficient mutants and conditions for its induction. *J Cell Biol* 119:301–311. https://doi.org/10.1083/jcb.119.2.301

Tanida I, Minematsu-Ikeguchi N, Ueno T, et al (2005) Lysosomal turnover, but not a cellular level, of endogenous LC3 is a marker for autophagy. *Autophagy* 1:84–91. https://doi.org/10.4161/auto.1.2.1697

Tanida I, Ueno T, Kominami E (2008) LC3 and autophagy. *Methods Mol Biol* 445:77–88. https://doi.org/10.1007/978-1-59745-157-4_4

Tatosyan AG, Mizenina OA (2000) Kinases of the Src family: structure and functions. *Biochemistry (Mosc)* 65:49–58

Teter SA, Eggerton KP, Scott S V., et al (2001) Degradation of lipid vesicles in the yeast vacuole requires function of Cvt17, a putative lipase. *J Biol Chem* 276:2083–2087. https://doi.org/10.1074/jbc.C000739200

Thelen M, Wymann MP, Langen H (1994) Wortmannin binds specifically to 1-phosphatidylinositol 3-kinase while inhibiting guanine nucleotide-binding protein-coupled receptor signaling in neutrophil leukocytes. *Proc Natl Acad Sci U S A* 91:4960–4964. https://doi.org/10.1073/pnas.91.11.4960

Thomas SM, Brugge JS (1997) Cellular functions regulated by Src family kinases. *Annu Rev Cell Dev Biol* 13:513–609. https://doi.org/10.1146/annurev.cellbio.13.1.513

Tsurutani J, West KA, Sayyah J, et al (2005) Inhibition of the phosphatidylinositol 3-kinase/Akt/mammalian target of rapamycin pathway but not the MEK/ERK pathway attenuates laminin-mediated small cell lung cancer cellular survival and resistance to imatinib mesylate or chemotherapy. *Cancer Res* 65:8423–8432. https://doi.org/10.1158/0008-5472.CAN-05-0058

Vakifahmetoglu-Norberg H, Kim M, Xia H guang, et al (2013) Chaperone-mediated autophagy degrades mutant p53. *Genes Dev* 27:1718–1730. https://doi.org/10.1101/gad.220897.113

Vanderstraete M, Gouignard N, Cailliau K, et al (2014) Venus kinase receptors control reproduction in the platyhelminth parasite *Schistosoma mansoni*. *PLoS Pathog* 10:e1004138. https://doi.org/10.1371/journal.ppat.1004138

Vandesompele J, De Preter K, Pattyn F, et al (2002) Accurate normalization of real-time quantitative RT-PCR data by geometric averaging of multiple internal control genes. *Genome Biol* 3:RESEARCH0034. https://doi.org/10.1186/gb-2002-3-7-research0034

Verjee MA (2020) Schistosomiasis: Still a cause of significant morbidity and mortality. *Res Rep Trop Med* 10:153–163. https://doi.org/10.2147/RRTM.S204345

Verjovski-Almeida S, DeMarco R, Martins EAL, et al (2003) Transcriptome analysis of the acoelomate human parasite *Schistosoma mansoni*. *Nat Genet* 35:148–157. https://doi.org/10.1038/ng1237

Vermeire JJ, Taft AS, Hoffmann KF, et al (2006) *Schistosoma mansoni*: DNA microarray gene expression profiling during the miracidium-to-mother sporocyst transformation. *Mol Biochem Parasitol* 147:39–47. https://doi.org/10.1016/j.molbiopara.2006.01.006

Wang L De, Chen HG, Guo JG, et al (2009) A strategy to control transmission of *Schistosoma japonicum* in China. *N Engl J Med* 360:121–128. https://doi.org/10.1056/NEJMoa0800135

Wang J, Paz C, Padalino G, et al (2020) Large-scale RNAi screening uncovers therapeutic targets in the parasite *Schistosoma mansoni*. *Science* 369:1649–1653. https://doi.org/10.1126/science.abb7699

Wang Q, Bu S, Xin D, et al (2018) Autophagy is indispensable for the self-renewal and quiescence of ovarian cancer spheroid cells with stem cell-like properties. *Oxid Med Cell Longev* 2018:1–15. https://doi.org/10.1155/2018/7010472

Wang SF, Oh S, Si YX, et al (2012) Computational prediction of protein-protein interactions of human tyrosinase. *Enzyme Res* 2012:192867. https://doi.org/10.1155/2012/192867

Wendt G, Zhao L, Chen R, et al (2020) A single-cell RNA-seq atlas of *Schistosoma mansoni* identifies a key regulator of blood feeding. *Science* 369:1644–1649. https://doi.org/10.1126/science.abb7709

WHO (2020) WHO reveals leading causes of death and disability worldwide: 2000-2019. World Heal Organ. https://doi.org/https://www.who.int/data/gho/data/themes/mortality-and-global-health-estimates

Wiesinger D, Gubler HU, Haefliger W, et al (1974) Antiinflammatory activity of the new mould metabolite 11-desacetoxy-wortmannin and of some of its derivatives. *Experientia* 30:135–136. https://doi.org/10.1007/BF01927691

Wilson RA (2012) The cell biology of schistosomes: a window on the evolution of the early metazoa. *Protoplasma* 249:503–518. https://doi.org/10.1007/s00709-011-0326-x

Yamamoto A, Tagawa Y, Yoshimori T, et al (1998) Bafilomycin A1 prevents maturation of

autophagic vacuoles by inhibiting fusion between autophagosomes and lysosomes in rat hepatoma cell line, H-4-II-E cells. *Cell Struct Funct* 23:33–42. https://doi.org/10.1247/csf.23.33

Yan M, Wang J, Wu X, et al (2009) Induction of insulin resistance by phosphatidylinositol-3-kinase inhibitor in porcine granulosa cells. *Fertil Steril* 92:2119–2121. https://doi.org/10.1016/j.fertnstert.2009.06.019

Yang Z, Klionsky DJ (2010) Mammalian autophagy: core molecular machinery and signaling regulation. *Curr Opin Cell Biol* 22:124–131. https://doi.org/10.1016/j.ceb.2009.11.014

Yoshimoto K, Hanaoka H, Sato S, et al (2004) Processing of ATG8s, ubiquitin-like proteins, and their deconjugation by ATG4s are essential for plant autophagy. *Plant Cell* 16:2967–2983. https://doi.org/10.1105/tpc.104.025395

You H, McManus DP, Hu W, et al (2013) Transcriptional responses of in vivo praziquantel exposure in schistosomes identifies a functional role for calcium signalling pathway member CamKII. *PLoS Pathog* 9:e1003254. https://doi.org/10.1371/journal.ppat.1003254

Zhang T, Shen S, Qu J, et al (2016) Global analysis of cellular protein flux quantifies the selectivity of basal autophagy. *Cell Rep* 14:2426–2439. https://doi.org/10.1016/j.celrep.2016.02.040

Zhang X, Garbett K, Veeraraghavalu K, et al (2012) A role for presenilins in autophagy revisited: normal acidification of lysosomes in cells lacking PSEN1 and PSEN2. *J Neurosci* 32:8633–8648. https://doi.org/10.1523/JNEUROSCI.0556-12.2012

Zimmerman EI, Hu S, Roberts JL, et al (2013) Contribution of OATP1B1 and OATP1B3 to the disposition of sorafenib and sorafenib-glucuronide. *Clin Cancer Res* 19:1458–1466. https://doi.org/10.1158/1078-0432.CCR-12-3306

11 SUPPLEMENTARY DATA

Beclin

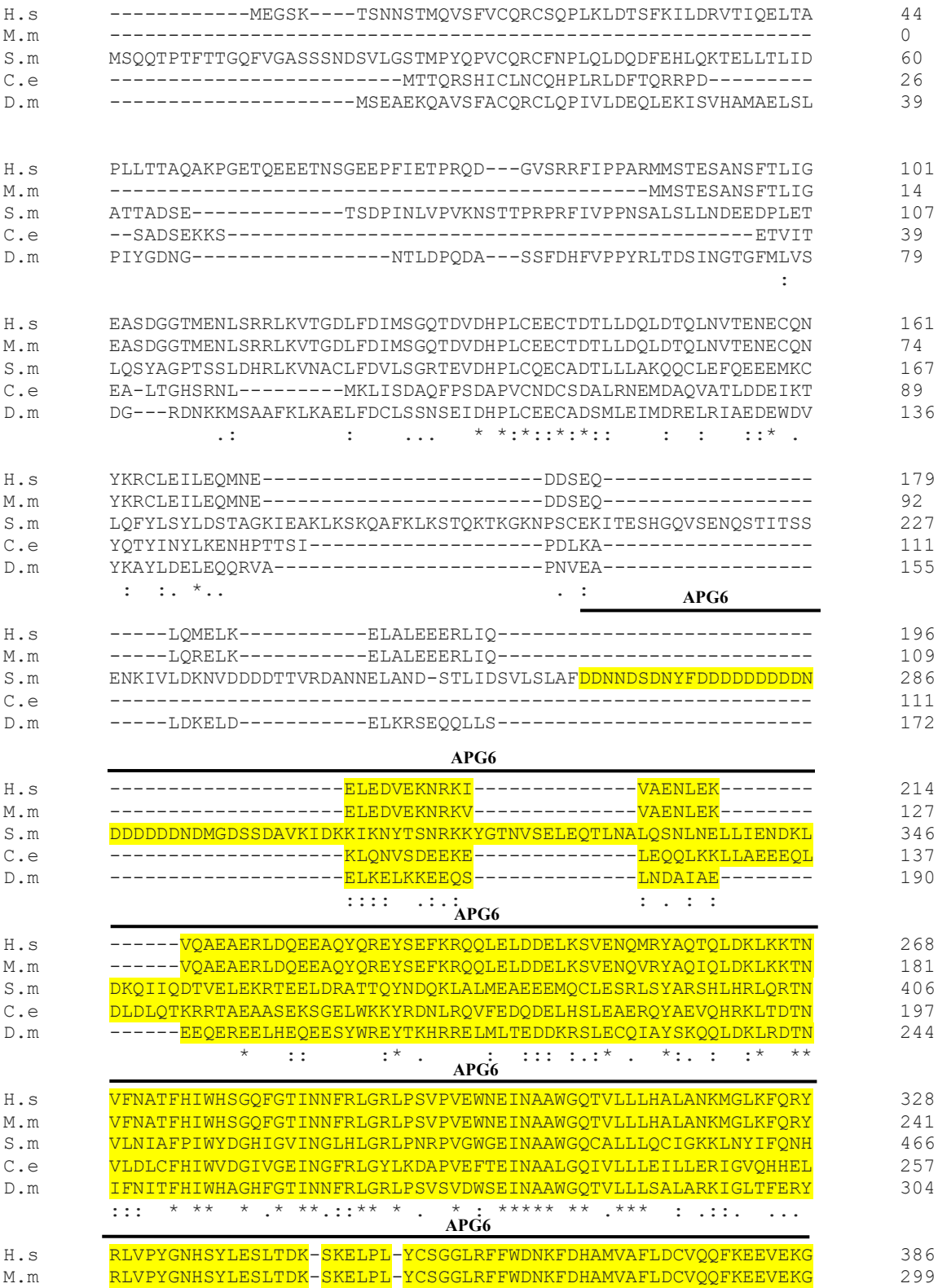

```
S.m      RIVPMGSQSKMVQLS-I-SKEFPLYYTTGGMRLLSAGKFDTAMINFLDCLNQAQQIIEHT      524
C.e      MPVAMGSHSYIKLRRNGIDMETYALYG-QGTPLSGSSGIDPGIRRFLQLLEFLLKELKDR      316
D.m      RVVPFGNHSYVEVLG-E-NRELPL-YGSGGFKFFWDTKFDAAMVAFLDCLTQFQKEVEKR      361
           *  *.:* :       . *    *   *  :     :* .:  **: :    : ::.
                                    APG6
H.s      ETRFCLPYRMDVEKGKIEDTGGSGGSYSIKTQFNSEEQWTKALKFMLTNLKWGLAWVSSQ      446
M.m      ETRFCLPYRMDVEKGKIEDTGGSGGSYSIKTQFNSEEQWTKALKFMLTNLKWGLAWVSSQ      359
S.m      -SYMQLPFRIK-DKGKLQD--PDGQIYSIKWNGNSEENWTKALKMMLINMKWIIAALSTK      580
C.e      NKNFKPPYQIHAD--SLV---DNGVKYNAVMTLNTDVRWTRAMALMLTDLKAACAQCDAL      371
D.m      DTEFLLPYKMEK--GKIID-PSTGNSYSIKIQFNSEEQWTKALKFMLTNLKWGLAWVSSQ      418
          . :  *:::.    .:      *  *.     *:: .**:*: :** ::*   *  .:

H.s      FYNK-------------       450
M.m      FYNK-------------       363
S.m      KNKKAINIQSTLSTMDK       597
C.e      RSPI-------------       375
D.m      FVSP-------------       422
```

Vps34

```
H.s      -MGEAEKFHYIYSCDLDINVQLK-------------------------------------       22
M.m      -MGEAEKFHYIYSCDLDINVQLKIGSLEGKREQKSYKAVLEDPMLK---FSGLYQETCS-      55
S.m      --MGSLSLGYYPSCDVATATS-------GLASTDDRQSTLIYPCIKIMNITGFDAERYKV      51
C.e      ------------------------------------------------------------       0
D.m      MDQPDDHFRYIHSSSLHERVQIKVGTLEGKKRQPDYEKLLEDPILR---FSGLYSEEHP-      56

H.s      ---------------------------------------------IWNEWLKLPVKYPDL       37
M.m      --DLYVTCQVFAE-GKPLALPVRTSY--KAFSTRW----------NWNEWLKLPVKYPDL      100
S.m      IKGEYTPLACYGELRINYCITRDIPFLSNSFITNWSQTQVNLDRQLFNEAFDLPLPYNAL      111
C.e      ------------------------------------------------------------       0
D.m      --SFQVRLQVFNQ-GRPYCLPVTSSY--KAFGKRW----------SWNEWVTLPLQFSDL      101

H.s      PRNAQVALTIWDVY---GPGKAVPVGGTTVSLFGKYGMFRQGMHDLKVWPNVEA------      88
M.m      PRNAQVALTIWDVY---GPGSAVPVGGTTVSLFGKYGMFRQGMHDLKVWPNVEA------      151
S.m      YDYNGICFVLSSTYTDKKGMHEQLIAGANMKLYNSKKVFRQGIYELELHPLEPLGVYRLE      171
C.e      ------------------------------------------------------------       0
D.m      PRSAMLVLTILDCS---GAGQTTVIGGTSISMFGKDGMFRQGMYDLRVWLGVEG------      152

H.s      DGSEPTKTPGRTSSTLSEDQMSRLAKLTKAHRQGHMVKVDWLDRLTFREIEMINESEKRS      148
M.m      DGSEPTRTPGRTSSTLSEDQMSRLAKLTKAHRQGHMVKVDWLDRLTFREIEMINESEKRS      211
S.m      DVEKLVREPTFDSKPSNMDTMNQILKTSRKHLRNELLE-TPLDRHCMPDVEHAVDEAKRA      230
C.e      ------------------------------------------------------------       0
D.m      DGNFPSRTPGKGKE-SSKSQMQRLGKLAKKHRNGQVQKVDWLDRLTFREIEVINEREKRM      211

H.s      SNFMYLMVEFRCVKCDD-KEYGIVYYEKDGDESSPILTSFELVKVPDPQMSMENLVESKH      207
M.m      SNFMYLMVEFRCVKCDD-KEYGIVYYEKDGDESSPILTSFELVKVPDPQMSMENLVESKH      270
S.m      SGRLFLSVKFEFSRSHPSVYMPVIFQRPFLPE-----------QSELRADRWNPVDEKY      278
C.e      ----------------------MRVSTSVNGGVGIVSACTRYCVADPELLLESLAEVKH      37
D.m      SDYMFLMIEFPAIVVDDMYNYAVVYFEPEGDVKYKLPAKPKLVSVPDSEIQMENLVERKH      271
                               :                      : .    . .: *:
                                        PI3Ka
H.s      HKLARSLRSGP--SDHDLKPNAATRDQLNI-IVSYPPTKQLTYEEQDLVWKFRYYLTNQ-      263
M.m      HKLARSLRSGP--SDHDLKPNATTRDQLNI-IVSYPPTKQLTYEEQDLVWKFRYYLTNQ-      326
S.m      FKMTRNARTAD--VDRARKPNKDILDRLKL-VLDLPPGLNISESDGDLIWKYRFYLADKF      335
C.e      SAMTRRIRDVEDERHRQVKPNKQAKDRLET-IVNLPSSQVLTREQRDLVWKFRHYLRQF-      95
D.m      HRLARSERSGI--SDRDAKPTASIRDQLHTIVYRYPPTYVLSSEEQDLVWKFRFYLSSH-      328
           ::*  *      .:  **.    *:*.  :   *    :: .: **:**:*.** .
                                    PI3Ka
H.s      -EKALTKFLKCVNWDLPQEAKQALELLGKWKPMDVEDSLELLSSHYTNPTVRRYAVARLR      322
```


M.m -EKALTKFLKCVNWDLPQEAKQALELLGKWKPMDVEDSLELLSSHYTNPTVRRYAVARLR 385
S.m PETSLAKFILSVRWEYTEQVNQAVELLKQWPTIAPEHVLELFTRQFLHPAGRRFAVHRLE 395
C.e -PKALNKYLRSVNWVHPQEVKTALALMNDWELIEAEDALELLSSAFTHPAVRAYSVSRLL 154
D.m -KKALTKFLKCINWKLEDEVTQALWMLANWAPMDVEDALELLSPTFTHPQVRKYAVSRLA 387
PI3Ka
H.s QA-DDEDLLMYLLQLVQALKYENFDDIKNG---LEPTKKDS-------Q---------- 360
M.m QA-DDEDLLMYLLQLVQALKYENFDDIKNG---LEPTKKDS-------Q---------- 423
S.m AA-SDEELILYLYQLVQALRYENWHDIFSVR----PKRNDRTSKRNVSDVIKEGNSEEVK 450
C.e EAASPEQVLLYLPQLVQALKYEQGQQLPEEGNPV-P-------------VVSEEEG---- 196
D.m QA-PDEDLLLYLLQLVQALKYEDPRHIVHLHGCIFPERDVV-------RSILDDNGSLLD 439
PI3Ka
H.s -SSVS-ENVSNSGINSAEIDS----------SQIITSPLPS 389
M.m -TSAS-ESLSNSGVSSGDIDS----------SQIITNPLPP 452
S.m STN---------LTSNRKIPSSF----------R--TGRGGA--LS----- 473
C.e ----------KI---------- 200
D.m QSSLSDLSATSSGLHGSVIPANQRAASVLAAIKSDKSVSPGSAGGSGSGGQGSVALPNPS 499
PI3Ka
H.s VSSPPP------ASKT--KEVP---DGENLEQDLCTFLISRACKNSTLANYLYWYVIVEC 438
M.m VASPPP------ASKA--KEVS---DGENLEQDLCTFLISRACKNSTLANYLYWYVIVEC 501
S.m ----------NIERSREELIGWHSDLKKEWKEDLASFLIRRAQLNFRIANYLYWFLRLEA 523
C.e VATTPTEELE----GRDMTVVTKKEARKAASGDLATFLIDYALASPKVSNYLYWHLKTEI 256
D.m APATPGSSSLPCDSNSNALMLAEGISFGSVPANLCTFLIQRACTNATLANYFYWYLSIEV 559
PI3Ka
H.s EDQDT--------QQRDPKTHEMYLNVMRRFSQALLKGDKSVRVMRSLLAAQQTFVDRLV 490
M.m EDQDT--------QQRDPKTHEMYLNVMRRFSQALLKGDKSVRVMRSLLAAQQTFVDRLV 553
S.m NSNDGEDDFSEQDTVNSPDTQKMYKHVLNRLLHAFDAGSPTCQKWNIELLQQTQFIQDLC 583
C.e ESTKE----------SKEEHSKMYQNIQDRLMEALVKRP-DTRAQVDSLHQQQIFVEDLI 305
D.m EEVESV-------RKQDERAHDMYAMVLKMFLKVLENGNFNLRGIFYNLRKQRRFIDELV 612
H.s HLMKAVQRESGNRKK-KNERLQALLGDNE--KMNLSDVELIPLPLEPQVKIRGIIPETAT 547
M.m HLMKAVQRESGNRKK-KNERLQALLGDNE--KMNLSDVELIPLPLEPQVKIRGIIPETAT 610
S.m RLLKSVTNDLGNRSRKVIQFYVSKLD-SEEYAHIRHIDKPFPLPLNPDIIVCGVQSSTAT 642
C.e ILMNEAKARGGRLNESKSAEFRTMLSRA----KHMLDLKGVHLPLDPSFRLSSVIPDTAS 361
D.m KLVKLVAKEPGNRNK-KTEKFQKLLAEQDMFKVNFTNFEPIPFPLDPEIYITKIVPMRTS 671
PI3Kc
H.s LFKSALMPAQLFFKTE-D--------GGKYPVIFKHGDDLRQDQLILQIISLMDKLLRKE 598
M.m LFKSALMPAQLFFKTE-D--------GGKYPVIFKHGDDLRQDQLILQIISLMDKLLRKE 661
S.m LFKSFQRPALLTFIQPN---------GDTYRAILKHGDDLRQDQLVLQMIELMDVILRKE 693
C.e FFKSEMMPAKISFKVLQPNGKADRNIPEEYTVIFKTGDDLRQDQLIQQMVRLIDIILKKG 421
D.m LFKSALMPAKLTFVTSIA--------HHEYAAIFKHGDDLRQDQLILQMITLMDKLLRRE 723
PI3Kc
H.s NLDLKLTPYKVLATSTKHGFMQFIQSVPVAEVLDTEG-----SIQNFFRKYAPSENGPNG 653
M.m NLDLKLTPYKVLATSTKHGFMQFIQSVPVAEVLDTEG-----SIQNFFRKYAPSETGPYG 716
S.m NFDLRLTPYKVLATSNRLGLVQFVESISLADILHRST------LLAYLQLKAPSPNSPMG 747
C.e QLDLKLTPYLVLSTGVGQGFVQCIKSKPLRAIQEQYKAHKMDCIREAMK-ELRPGDGPFG 480
D.m NLDLKLTPYKVLATSSKHGFLQYVDSCTVAEVLAREG-----NIHNFFRKHHPCDNGPYG 778
PI3Kc
H.s ISAEVMDTYVKSCAGYCVITYILGVGDRHLDNLLLTKTGKLFHIDFGYILGRDPKPLPPP 713
M.m ISAEVMDTYVKSCAGYCVITYILGVGDRHLDNLLLTKTGKLFHIDFGYILGRDPKPLPPP 776
S.m VQKDVMETYIRSCAGYCVITYLLGVGDRHMENLLLTADGHLFHIDFSFILGADPKPMAPE 807
C.e IEPNVIDNYVRSLAGYSVIMYILGLGDRHLDNLLLCENGKLFHVDFGFILGRDPKPMPPP 540
D.m ISAEVMDTYIKSCAGYCVITYLLGVGDRHLDNLLLTTNGKLFHIDFGYILGRDPKPMPPP 838
PI3Kc
H.s MKLNKEMVEGMGGTQSEQYQEFRKQCYTAFLHLRRYSNLILNLFSLMVDANIPDIALEPD 773
M.m MKLNKEMVEGMGGTQSEQYQEFRKQCYTAFLHLRRYSNLILNLFSLMVDANIPDIALEPD 836
S.m VRLTRAMIDGMGGPNSNQFNEFWKITFTAFLILRRHANLFLTLFSLMSNTGIQSFNGQQN 867
C.e MKLTSEMVQVMGGVKSKQFLEFVQHVDSAYRILRRHSNVLLNLFSLMLDAGIPDIAAEPD 600
D.m MKLSKEMVEAMGGISSEHHHEFRKQCYTAYLHLRRHANVMLNLFSLMVDATVPDIALEPD 898

```
          ::*.  *:: *** .*::. ** :   :*:  ***::*::*.***** :: : .:  : :
                                  PI3Kc
H.s       KTVKKVQDKFRLDLSDEEAVHYMQSLIDESVHALFAAVVEQIHKFAQYWRK        824
M.m       KTVKKVQDKFRLDLSDEEAVHYMQSLIDESVHALFAAVVEQIHKFAQYWRK        887
S.m       NASEFLKEHFCVHQSEEKAVSRLANRMTESIKAIVPDIMERIHTIVQYMRN        918
C.e       KAIFKIEQRLRLDLSDEAATKHIFTQIESSLNAKMAMISDIIHAYKQNLM-        650
D.m       KAVKKVEENLQLGLTDEEAVQHLQSLLDVSITAVMPALVEQIHRFTQYWRK        949
          ::   :::.: :  ::* *.  : . :  *: * .  : : **   *
```

Dram

```
                                  Frag1
H.s       MLCF-L--RGMAFVPFLLVTWSSAAFIISYVVAVLSGHVNPFLPYISDTGTTPPESGIFG  57
M.m       MLCF-L--RGMAFVPFLLVTWSSAAFIISYVVAVLSGHVNPFLPYISDTGTTPPESGIFG  57
S.m       -----MASFAVHYFVIGLILAIVGTFSISYLISTSDHHASVIFPYISDTGALPPESCVFG  55
C.e       -MCVGLSKLGFGPLPVLIALIFFVQSFFVYTIAVLKHDVDPIFPYLSSAADKRPQSCIFA  59
D.m       -----M--SQVYLLPVLTFLIFQVTFLGTYIFAVLEGHVVPTVPYISDAATYSPESCVFG  53
               :    .  . .              * .:. . ..   .**:*.:.   *:* :*.
                                  Frag1
H.s       FMINFSAFLGAATMYTRYKIVQKQNQT---CYFSTPVFNLVSLVLGLVGCFGMGIVANFQ  114
M.m       FMINFSAFLGAATMYTRYKIVEKQNET---CYFSTPVFNLVSLALGLVGCIGMGIVANFQ  114
S.m       QLLNICSFLSFVCIYCWYLHECNVMYTLQ-GPNSHIVFARLTCIIGCLSALGMSIVANFQ  114
C.e       IGANISSVLLALVVFVRYRQLRGIFAFYDEA--NLQAWNWRQKWFGYIAALGLFFVANVQ  117
D.m       QLINIGSVLLGITIYVRYRQVLQLYEHHPDLDGSVLRQNRLALWFGLVSCLGISFVGNFQ  113
             *: :.*    ::  *                .              :* :..:*: :*.*.*
                                  Frag1
H.s       ELAVPVVHDGGALLAFVCGVVYTLLQSIISYKSCPQWNSLSTCHIRMVISA-----VSCA  169
M.m       ELAVPVVHDGGALLAFVCGVVYTLLQSIISYKSCPQWNSLTTCHVRMAISA-----VSCA  169
S.m       EASLIVVHLIGAMMTFGLGVVFSALVTYSTRKH---------LEYNFKIYVFRLILTICG  165
C.e       ETAIIPVHMSSAVASFGGFSIYMIFQCYLTHRVTPTITLRTVFYYRVIFTIFSVICFCCS  177
D.m       ETNVRIVHFIGAFCCFGCGTLYFWMQALISYLIFPMSGTRINAHLRLGMSV-----VCTI  168
          *  :  **  .*.  *    ::  :    :              .. :
                                  Frag1
H.s       AVIPMIV-------CASLISITKLEWNPR--EKDYVYHVVSAICEWTVAFGFIFYFLTFI  220
M.m       AVVPMIA-------CASLISITKLEWNPK--EKDYIYHVVSAICEWTVAFGFIFYFLTFI  220
S.m       FLANLGVFIFGH-LSGEIHGPFPRKWDPS--ETGFKYHVMSSFCEWLMSFTFLLFFASMI  222
C.e       FGFGIAA--SKIFHKTYPDLPTPRPWSRRIYQPGYELHQISALAEWGCAISQIFFIQSFG  235
D.m       LFILLAV--TGVMSHILFKGQNPRKWYPS--DGGWYFHVVSSISEWVIATVFSFFILSFT  224
             : .                 *     : .:  * :*::.**  :    ::: ::
          Frag1
H.s       QDFQSVTLRISTEINGDI------------------      238
M.m       QDFQSVTLRISTEINDDF------------------      238
S.m       FELRNYELESVKIRRIVIAPENNEQ--APLLA----      252
C.e       PEFEDISLDYYLKSHYVPRGALEQEEYENEYQGYGI      271
D.m       NEFRDVSLSHPQIALMSYSTTI--------------      246
           ::..  *
```

LC3-B.1

```
                                                  APG1
H.s       MPSEKTFKQRRTFEQRVEDVRLIREQHPTKIPVIIERYKGEKQLPVLDKTKFLVPDHVNM  60
M.m       MPSEKTFKQRRSFEQRVEDVRLIREQHPTKIPVIIERYKGEKQLPVLDKTKFLVPDHVNM  60
S.m       --MKFQYKEDRPFEKRLEEGQNIRKKYPSSVPVIVEKSPR-ARVGNLEKNKYLVPSDLTV  57
C.e       --MKWAYKEENNFEKRRAEGDKIRRKYPDRIPVIVEKAPK-SKLHDLDKKKYLVPSDLTV  57
D.m       --MKFQYKEEHAFEKRRAEGDKIRRKYPDRVPVIVEKAPK-ARIGDLDKKKYLVPSDLTV  57
             :  :*: . **:*  :   **.::*  :***:*:     ::  *:*.*:***..:.:
                                  APG1
H.s       SELIKIIRRRLQLNANQAFFLLVNGHSMVSVSTPISEVYESEKDEDGFLYMVYASQETFG  120
M.m       SELIKIIRRRLQLNANQAFFLLVNGHSMVSVSTPISEVYESERDEDGFLYMVYASQETFG  120
S.m       GQFYFLIRKKIQLNPEEALFFFVKDI-IPPTSATMGALYQEHHDRDLFLYIAYSDESIYG  116
C.e       GQFYFLIRKRIQLRPEDALFFFVNNV-IPQTMTTMGQLYQDHHEEDLFLYIAYSDESVYG  116
```

```
D.m      GQFYFLIRKRIHLRPEDALFFFVNNV-IPPTSATMGSLYQEHHEEDYFLYIAYSDENVYG      116
         .::  :**::::*. ::*:*::*:.  :  . : :. :*:..::.* ***:.*:.:. :*

H.s      MKLSV---          125
M.m      TAMAV---          125
S.m      SVEDCTSS          124
C.e      GEVEKKE-          123
D.m      MAKIN---          121
```

LC3-B.2

```
H.s      MPSEKTFKQRRTFEQRVEDVRLIREQHPTKIPVIIERYKGEKQLPVLDKTKFLVPDHVNM      60
M.m      MPSEKTFKQRRSFEQRVEDVRLIREQHPTKIPVIIERYKGEKQLPVLDKTKFLVPDHVNM      60
S.m      ------------------------------------------------------------      0
C.e      --MKWAYKEENNFEKRRAEGDKIRRKYPDRIPVIVEKAPK-SKLHDLDKKKYLVPSDLTV      57
D.m      --MKFQYKEEHAFEKRRAEGDKIRRKYPDRVPVIVEKAPK-ARIGDLDKKKYLVPSDLTV      57
                                      APG1
H.s      SELIKIIRRRLQLNANQAFFLLVNGHSMVSVSTPISEVYESEKDEDGFLYMVYASQETFG      120
M.m      SELIKIIRRRLQLNANQAFFLLVNGHSMVSVSTPISEVYESERDEDGFLYMVYASQETFG      120
S.m      ---MWIIRKRIDISSEKALFLFVEKN-MPQTSATIGQLYHNFHDDDGFLYISYSGENSFG      56
C.e      GQFYFLIRKRIQLRPEDALFFFVNNV-IPQTMTTMGQLYQDHHEEDLFLYIAYSDESVYG      116
D.m      GQFYFLIRKRIHLRPEDALFFFVNNV-IPPTSATMGSLYQEHHEEDYFLYIAYSDENVYG      116
              :**:*:.:  :.*:*::*:   :  . : :..:*.. :::* ***: *:.:. :*

H.s      MKLSV-- 125
M.m      TAMAV-- 125
S.m      SGSCTSS 63
C.e      GEVEKKE 123
D.m      MAKIN-- 121
```

DAP1

```
                                  DAP
H.s      MANEVQDLLSPRKGGHPPAVKAGGMRISKKQEIG---TLERHTKKTGFEKTSAIANVAKI      57
M.m      -MSSPPEGKLETKAGHPPAVKAGGMRIVQKHPHTGDGKEERDKDDQEWESTSPPKPTVFI      59
S.m      ---MMDGTSDTTNISHPPAVKAGKMRIVKHVKHDATVEVRCEEDSP---------------      43
C.e      -MMDNNITETEMKVGHPPANKVGGRRVVNRKDRKNSDSND----NANSEGSDEVVR----      51
D.m      ----MADEQPNLVAGHPPALKAGGMRIVQHKAPTAERAPKDAEDCTGL-TQPIAVNSGSV      55
                     .**** *.*  *: ::
                          DAP
H.s      QTLDALNDALEKLNYKF-PATVHMAHQKPTPALEKVVPL---KRIYIIQQPRKC--   107
M.m      ------SGVIARGDKDFPPAAAQVAHQKPHASMDKHVS----PRTQHIQQPRK---   102
S.m      ------HELLTKEELEYHDRCIKAYHDKPMPTVTKPHND---NTKRIIQQPLK---   87
C.e      --EIIDYDLPAKMERSYPTEAVKKVHEKPMPAIQPVHINRDANSGVHRFQPRKQTH   105
D.m      ------SGAPVKGNTDFTPASAQVAHSPKPPAAV--QQ----KPQIHIQQPRK---   96
                    : : .:     :  *.    :                 ** *
```

Supplementary Figure S1: Multiple sequence alignment of amino acid sequences of autophagy genes identified for *S. mansoni* (S.m) with orthologues from *Homo sapiens* (H.s), *Mus musculus* (M.m), *Caenorhabditis elegans* (C.e), and *Drosophila melanogaster* (D.m). Conserved protein domains are highlighted. * indicates identical amino acids. (For accession numbers, see Table 3.1).

12 PUBLICATIONS AND CONFERENCE CONTRIBUTIONS

12.1 Original papers

Mughal, M. N., Grevelding, C. G., & Haeberlein, S. (2021). First insights into the autophagy machinery of adult *Schistosoma mansoni*. *International Journal for Parasitology*, *51*(7), 571–585. https://doi.org/10.1016/j.ijpara.2020.11.011

Mughal, M. N., Grevelding, C. G., & Haeberlein, S. (2021). The anticancer drug imatinib induces autophagy in *Schistosoma mansoni*. *International Journal for Parasitology*, S0020-7519(21)00312-X. Advance online publication. https://doi.org/10.1016/j.ijpara.2021.10.008

12.2 Conference contributions

- **Mughal, M. N.**, Grevelding, C. G., & Haeberlein, S. (2021) First insights into the autophagy machinery of adult *Schistosoma mansoni. 14. GGL-Jahrestagung 2021,* 29.-30. September.

- **Mughal, M. N.**, Grevelding, C. G., & Haeberlein, S. (2021) First insights into the autophagy machinery of adult *Schistosoma mansoni. 29. Jahrestagung der Deutschen Gesellschaft für Parasitologie,* 15.-17. März.

- **Mughal, M. N.**, Grevelding, C. G., & Haeberlein, S. (2020) Towards understanding the autophagy machinery of adult *Schistosoma mansoni. Erste digitale GGL-Jahrestagung 2020,* 29.-30. September.

- Poster: **Mughal, M. N.**, Grevelding, C. G., & Haeberlein, S. (2019) Preliminary data on the autophagy machinery of adult *Schistosoma mansoni. 12. GGL-Jahrestagung 2019,* 4.-5. September.

- Poster: **Mughal, M. N.**, Grevelding, C. G., & Haeberlein, S. (2018) The role of autophagy in reproductive biology of *Schistosoma mansoni. 11. GGL-Jahrestagung 2018,* 19.-20. September

13 DECLARATION

I declare that I have completed this dissertation single-handedly without the unauthorized help of a second party and only with the assistance acknowledged therein. I have appropriately acknowledged and referenced all text passages that are derived literally from or are based on the content of published or unpublished work of others, and all information that relates to verbal communications. I have abided by the principles of good scientific conduct laid down in the charter of the Justus Liebig University of Giessen in carrying out the investigations described in the dissertation.

Ich erkläre: Ich habe die vorgelegte Dissertation selbständig, ohne unerlaubte fremde Hilfe und nur mit den Hilfen angefertigt, die ich in der Dissertation angegeben habe. Alle Textstellen, die wörtlich oder sinngemäß aus veröffentlichten oder nicht veröffentlichten Schriften entnommen sind, und alle Angaben, die auf mündlichen Auskünften beruhen, sind als solche kenntlich gemacht. Bei den von mir durchgeführten und in der Dissertation erwähnten Untersuchungen habe ich die Grundsätze guter wissenschaftlicher Praxis, wie sie in der Satzung der Justus-Liebig-Universität Gießen zur Sicherung guter wissenschaftlicher Praxis niedergelegt sind, eingehalten.

Gießen, 24. January 2022

Mudassar Niaz Mughal

14 ACKNOWLEDGEMENT

Spiritually, I humbly bend myself before Almighty ALLAH of the worlds, the greatest Beneficient, the most Merciful and thank HIM for everything I have been blessed with in my entire life. Peace and blessing of ALLAH be upon the last messenger MUHAMMAD (PBHU), the greatest social reformer and the best of human being.

Worldly, first of all, I express my deepest gratitude for their extreme patience, continuous encouragement and generous support during the course of this project to my supervisors Prof. Dr. Christoph Grevelding and PD. Dr. Simone Häberlein. Especially I thank PD. Dr. Simone Häberlein for valuable suggestions and guiding me to kick-start my life in Germany. Her broad knowledge in various aspects of parasitology benefits me at both experimental and theoretical concepts directing me on the way to be a good researcher.

I would like to thank Prof. Dr. Andreas Meinhardt for his willingness to be my supervisor and to review my thesis.

My deep sense of gratitude for Dr. Thomas Quack and Dr. Oliver Weth for their keen interest, constructive comments, auspicious guidance and boosting up my morale during discussions regarding research work. A big gratitude gesture for my ex- and present labmates of AG Grevelding, Parasitologie, for their technical guidance and needful assistance during this study period: Oliver Puckelwaldt, Mandy Beutler, Josina Kellershohn, Maria Stitz, Martin Haimann, Max Möscheid, Monique Überall. I am feeling dearth of words to express my gratitude to colleague and friends: Ershun Zhou, Xuesong Li, Hicham Houhou and Hang Yan for their scholarly criticism, important suggestions and absolute friendly atmosphere during this project. It is my pleasure acknowledging earnest devotion and excellent work of Christina Scheld, Bianca Kulik and Geogette Stovall for maintaining schistosome life-cycle.

This work was intellectually supported by GGL (Giessen Graduate for Life Sciences) by their diverse courses and wide-range of workshops, and financially supported by the DAAD Research Grant # 57381412 (German Academic Exchange Service) to the author.

With deep emotions of benevolence, I am earnestly indebted to my Mother, Father, family members who have given their unequivocal support (also to those who taunted me, given me names and left me with their harsh words) and friends who have always wished to see me glittering high on the skies of the success.

Der Lebenslauf wurde aus der elektronischen Version der Arbeit entfernt.

The curriculum vitae was removed from the electronic version of the paper.